

# Noncovalent Immobilization of Enantioselective Catalysts

José M. Fraile,\* José I. García, and José A. Mayoral

Departamento de Química Orgánica, Instituto de Ciencia de Materiales de Aragón, and Instituto Universitario de Catálisis Homogénea, Facultad de Ciencias, Universidad de Zaragoza - C.S.I.C., E-50009 Zaragoza, Spain

Received May 20, 2008

## Contents

1. Introduction and Scope	360
2. Electrostatic Methods	361
2.1. Immobilization on Clays and Other Noncrystalline Inorganic Materials	362
2.2. Immobilization on Polymers and Related Hybrid Materials	369
2.3. Immobilization on Zeolites and Mesoporous Crystalline Materials	371
2.4. Immobilization on Organically Modified Inorganic Supports	375
2.5. Immobilization on Cationic Supports	377
3. Coordinative Methods	382
3.1. Unmodified Supports as Ligands	382
3.2. Metal–Organic Frameworks	386
3.3. Modified Supports as Ligands	391
4. Adsorption Methods	394
4.1. Immobilization by Physisorption	394
4.2. Immobilization by Hydrogen Bonding with the Support	400
4.3. Supported Liquid Phases	404
4.4. Nanoparticles as Supports for Chiral Catalysts	406
5. Entrapment Methods	407
5.1. Entrapment into Flexible Matrixes	407
5.2. Entrapment into Rigid Supports	409
6. Concluding Remarks	414
7. Acknowledgments	414
8. References	414

## 1. Introduction and Scope

Among the different methods to obtain enantiomerically pure compounds, namely, resolution, diastereomeric synthesis, and enantioselective catalysis, the use of chiral catalysts<sup>1</sup> is probably the most attractive system due to the phenomenon of the multiplication of chirality. However, enantioselective catalysis is seldom used in industrial processes<sup>2–4</sup> due to a variety of factors, among them the difficulty of catalyst separation from the reaction medium, which increases the high cost of the chiral catalyst and provokes contamination problems in the final product. One possible solution for those problems is the use of heterogeneous chiral catalysts that would help to easily separate and reuse the catalyst. The most convenient strategy to prepare chiral heterogeneous catalysts is the immobilization of chiral homogeneous catalysts,<sup>5</sup> and the most used method to immobilize chiral complexes is without doubt the formation of a covalent bond between the

solid support and the chiral ligand. One important drawback of this method is the need for an additional functionalization of the chiral ligand with two negative consequences, the rise in the catalyst preparation cost and the possible modification of the conformational preferences of the supported complex, leading to unpredictable and, in many occasions, negative effects on the enantioselectivity.

The objective of this review is to bring together, in a critical view, all the knowledge about methods of immobilization applied to enantioselective catalysts that do not require the covalent link of the chiral ligand to a solid support, either organic (polymeric) or inorganic. These methods are quite underestimated, because the link between catalytic complex and support is sometimes not too strong, but they offer new possibilities for immobilization. One practical advantage is that many of them do not require modification of the known, commercially available chiral ligands used in solution chemistry. Another important advantage is that many of these methods are simple and efficient, precluding any important supplementary cost, which is very attractive for potential industrial applications. Finally, there exist possibilities to control the stereochemical outcome of the catalytic process due to the relative position of the complex with respect to the support, although this is a field that is just starting to show its potential.

In precedent reviews about immobilization of chiral catalysts, the focus was put on the last general achievements regarding either one particular type of catalyst to be immobilized<sup>6–10</sup> or one type of reaction to be carried out.<sup>11–13</sup> In other cases, the focus was directed to the type of support,<sup>14–20</sup> or even the reviews were devoted to immobilization in general,<sup>21–23</sup> but in all cases, they were classified according to catalysts or reactions, that is, the final application of the catalyst. In this review, we want to stress on the noncovalent immobilization methods, showing the advantages and limitations of each one, including the applicability to different catalytic complexes and, of course, different catalyzed reactions. The immobilization methods have been classified, depending on the system used to keep the complex linked to the support, into four categories (Figure 1): electrostatic, coordinative, adsorptive, and entrapment methods.

This classification is quite different from those reported in previous papers, mainly regarding the distinction between coordinative and adsorptive methods. We have tried to distinguish between specific coordinative support–catalyst interactions, that is, the participation of the support either modified or not in the coordination sphere of the metal, and mere adsorption of the complex onto a support through nonspecific weak interactions, such as van der Waals or

\* To whom correspondence should be addressed. Phone: 0034 976762272. Fax: 0034 976762077. E-mail: jmfraile@unizar.es.



José M. Fraile received a Ph. D. degree from the University of Zaragoza in 1992. After a postdoctoral stage in the Ecole Nationale Supérieure de Chimie de Montpellier (1993–1994) and a period as Assistant Professor in the University of Zaragoza, he joined the C.S.I.C. (Spanish Council for Scientific Research) in the Instituto de Ciencia de Materiales de Aragón as Tenured Scientist, and in 2008, he has been promoted to a Research Scientist position. His research interests focus on the preparation and application of heterogeneous catalysts on selective organic synthesis, mainly chiral catalysts for enantioselective processes.



José A. Mayoral received his Ph.D. (1983) from the University of Zaragoza and joined this university in 1983 as assistant professor. He became Senior Lecturer in 1986 and full Professor in Organic Chemistry in 2004. His research interests pointed to asymmetric syntheses, since he developed his Ph.D. in the obtaining of new chiral amino acids by asymmetric hydrogenation with chiral rhodium complexes. Afterwards he worked in asymmetric syntheses using traditional methodologies such as Diels–Alder reactions. Nowadays his interests are focused on uncommon aspects of the application of solid catalysts to organic synthesis, the immobilization of chiral catalysts, and the study of mechanistic aspects of organic reactions.



José I. García received a Ph.D. degree from the University of Zaragoza in 1986 (Ph.D. Thesis Award). After a postdoctoral stage in the “Institut de Topologie et de Dynamique des Systèmes” at CNRS-Université de Paris VII, in 1990 he obtained a position of Tenured Scientist in the CSIC, with the subject “Modeling of Chemical Phenomena”. In 2002, he was promoted to a position of CSIC Research Scientist, and in 2007 to CSIC Research Professor. His main research interests are the application of heterogeneous catalysts to selective organic syntheses, especially to asymmetric syntheses, and particularly the mechanistic and molecular modeling aspects. He has also worked in the modeling of solvent effects on organic reactivity, from both the experimental and theoretical viewpoint, as well as in the application of statistical experimental designs to chemical problems.

hydrogen bonding with any part of the complex, including ligands and counterion.

Sometimes the separation between methods is not clear, for example, the transition from a purely ionic (electrostatic) to a covalent (coordinative) metal–support bond or the existence of electrostatic metal–support interactions in a entrapped catalyst.

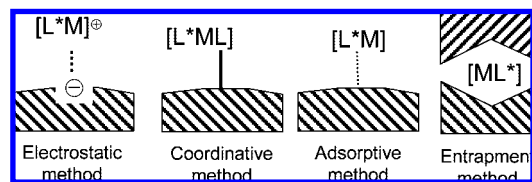
This review is devoted to immobilized catalysts, considering them as organometallic (or metal–organic) complexes or more generally single-site catalysts, and hence we have avoided any reference to modified heterogeneous catalysts<sup>24</sup> (typical examples are Raney-Ni modified with tartaric acid and Pt/alumina modified with cinchona alkaloids), despite the fact that the chiral modifier is not covalently bonded to the solid support.

In each section, the most commonly used supports will be presented, together with the immobilization methodology.

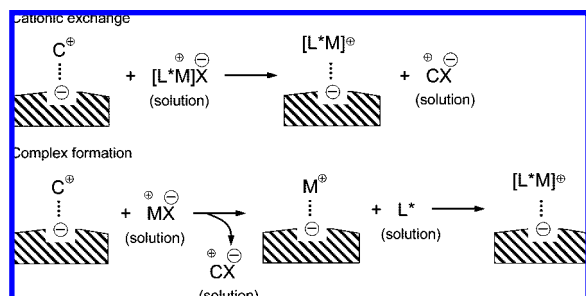
## 2. Electrostatic Methods

Cationic complexes need the presence of a counterion, typically  $\text{PF}_6^-$ ,  $\text{BF}_4^-$ , or another weakly coordinating anion. This anion can be exchanged by a solid with a negative charge that will act as the counterion of the complex, immobilizing it on the surface of the solid through an electrostatic interaction, provided that the chiral catalytic complex remains charged all along the catalytic cycle. The use of an anionic support to immobilize a positively charged chiral catalytic complex was probably the first noncovalent immobilization method described in the literature. Two main general methods can be envisaged to carry out this type of immobilization (Figure 2): the direct cationic exchange of the complex performed in solution and the formation of the complex on a pre-exchanged metal center. In the first case, the out-coming salt, formed by the compensating cation of the solid ( $\text{C}^+$ ) and the counteranion of the complex ( $\text{X}^-$ ), will be eliminated to the solution or will remain on the solid depending on the solvent used in the exchange process. Both methods have theoretical advantages and disadvantages. The direct exchange, by far the most frequently employed method, allows the formation of a well-characterized complex in solution, which is exchanged on the solid unaltered if it is stable enough. The addition of the ligand on the pre-exchanged metal allows forcing the complex formation with an excess of ligand, but it may find problems due to the possible exchange of the smaller metal salt in sites inaccessible for the bulkier complex. Factors such as the exchange solvent, which must facilitate the ion mobility, are important to achieve the best exchange ratios and hence the best immobilized catalysts.

The first type of support used was clay minerals, but afterward supports of different natures (organic, inorganic, hybrid) have been used. In this part of the review, the contributions are organized by the type of support, because



**Figure 1.** Classification of noncovalent methods of immobilization.



**Figure 2.** Methodologies to perform the immobilization through electrostatic interactions.

immobilization and catalytic results are greatly conditioned by its choice.

## 2.1. Immobilization on Clays and Other Noncrystalline Inorganic Materials

Clays (both natural and synthetic) are well-known inorganic cation exchangers. Clays are aluminosilicates or magnesiumsilicates with a lamellar (two-dimensionally ordered) structure. Each clay sheet is typically formed by three layers, two tetrahedral  $\text{SiO}_2$  layers with an octahedral  $\text{Al}_2\text{O}_3$  or  $\text{MgO}$  layer between them. A typical structure is shown in Figure 3. The exchange capacity is mainly determined by isomorphous substitutions in the crystalline structure of these solids. Aluminum by silicon, magnesium by aluminum, or lithium by magnesium isomorphous substitutions can generate charge defaults in the structure, which are usually counterbalanced by inclusion of hydrated monovalent cations (lithium or sodium, but also ammonium) into the interlamellar spaces, and confer cation exchange ability to these materials.

The first noncovalent immobilization described in the literature was the electrostatic immobilization of  $[(\text{PNNP})\text{Rh}(\text{cod})]^+$  ( $\text{cod} = \text{cyclooctadiene}$ ) complex (Figure 4) on different clays (hectorite, bentonite, nontronite, and halloysite).<sup>25</sup> The direct exchange of the perchlorate complex was carried out in anhydrous methanol, and a prehydrogenation step of the complex (not possible in solution due to the formation of metallic Rh) was necessary to reach optimal results.

The solid catalysts were tested in the hydrogenation of several amino acid precursors (Scheme 1). The type of clay was crucial for the catalytic performance, mainly in the case of bulky cinnamic substrates, with hectorite as the best support and halloysite as the worst one.  $[(\text{PNNP})\text{Rh}(\text{cod})]$ -hectorite was very active for the hydrogenation of 2-acetamidoacrylic acid, and it was recoverable for 5 runs with the same enantioselectivity (72%, 72%, 75%, 70% and 69% ee). However the recoverability was not so good in the case of cinnamic substrates, with enantioselectivities decreasing from 49% ee in the first run to 24% ee in the third one for (*Z*)-2-acetamidocinnamic acid, and from 72% to 47% ee for (*Z*)-2-acetamido-3-(4-acetoxy-3-methoxyphenyl)-acrylic acid. This

was really a pioneering work that showed the feasibility of this kind of immobilization, having to wait for several years to find new papers on electrostatic immobilization of chiral catalysts.

Sixteen years after the first paper on this subject, Shimazu and co-workers described the second example of electrostatic immobilization of Rh complexes on clays.<sup>26</sup> In this case, the support was a synthetic hectorite and the supported complexes were  $[(\text{BINAP})\text{Rh}(\text{cod})]^+$  and  $[(\text{BPPFA})\text{Rh}(\text{cod})]^+$  ( $\text{BINAP} = 2,2'$ -bis(diphenylphosphino)-1,1'-binaphthyl,  $\text{BPPFA} = N,N$ -dimethyl-1-[1',2-bis(diphenylphosphino)ferrocenyl] ethylamine; Figure 5), directly exchanged from the perchlorate precursor in water/acetonitrile mixture. Exchange was confirmed by disappearance of the IR bands of the starting  $\text{ClO}_4^-$ , and intercalation of complexes between the clay sheets was proposed, even with preferred orientations, from the basal spacing data obtained from XRD pattern.

The supported complexes were tested in the hydrogenation reactions of different itaconate, citraconate, and mesaconate esters to obtain the corresponding succinate (Scheme 2). The effect of solvent and type of substrate was studied in depth (Table 1).

In the case of  $[(\text{BINAP})\text{Rh}(\text{cod})]$ hectorite, results were highly dependent on both parameters and in a different way than the parameters affect the homogeneous reaction. Diethyl and dimethyl itaconates gave poor enantioselectivity in all cases; only dibutyl itaconate led to significant enantiomeric excesses. The use of solvents with low dielectric constant was detrimental for catalytic activity, but increased the enantioselectivity. However, cyclohexane was necessary to get significant asymmetric induction with the supported catalyst. At high cyclohexane content, enantioselectivity was even higher than that in solution (66% vs 55% ee). A possible explanation for both the lower activity and the higher selectivity is the isomerization of itaconate to mesaconate, detected as an intermediate in the heterogeneous reaction. BPPF was a more efficient ligand regarding enantioselectivity (up to 88% ee), although the reaction rate was much slower. Spatial restrictions between the clay layers were invoked to explain this effect, although the effect of clay on isomerization was not considered. Recovery and reuse of the supported catalysts were not described.

The same group described the immobilization of  $[(\text{DIO-P})\text{Rh}(\text{cod})]^+$  ( $\text{DIO-P} = (2,2\text{-dimethyl-1,3-dioxolane-4,5-diyl-bis-methylene})\text{bis(diphenylphosphine)}$ ) by direct cationic exchange in methanol/water mixture on the same type of hectorite clay<sup>27</sup> and on a hectorite pre-exchanged with large dimethyldioctadecylammonium cations<sup>28</sup> (Figure 6).

The authors claimed the intercalation of the complex between the clay layers from XRD data (Figure 7). However, partial delamination of clay, with loss of the stacking order of clay layers, seems a more accurate description due to the drop in intensity of the (001) diffraction line, in agreement with our own findings.

Results from itaconate hydrogenation were only modest, up to 20% ee for diethyl itaconate and no improvement with higher esters. The presence of an additional ammonium cation showed some positive effects on activity and selectivity but only for diastereoselective hydrogenations.

Margalef-Català et al. reported the immobilization of  $[(\text{BDPP})\text{Ir}(\text{cod})]\text{PF}_6$  ( $\text{BDPP} = 2,4\text{-bis(diphenylphosphino)pentane}$ ; Figure 8) on K10 montmorillonite by adsorption from a dichloromethane solution.<sup>29</sup> Despite not being a truly

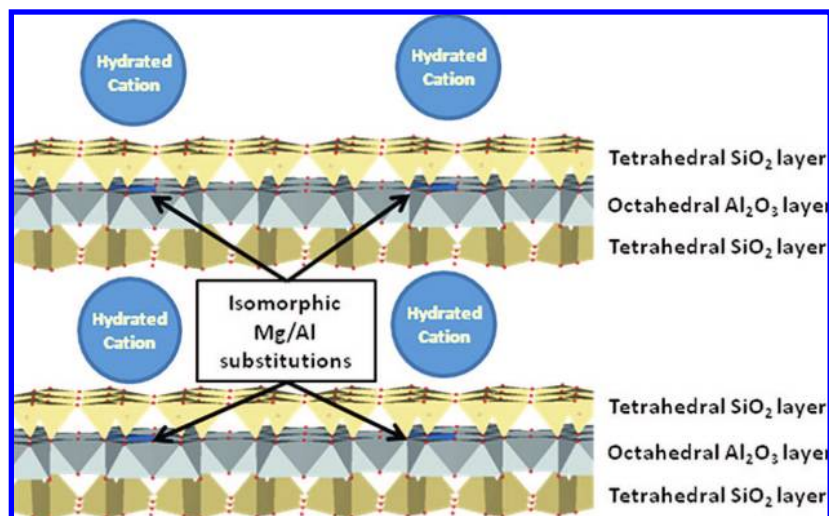


Figure 3. Typical smectite clay layered structure.

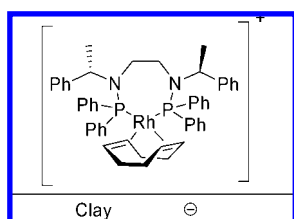


Figure 4. [(PNNP)Rh(cod)]clay.

Scheme 1

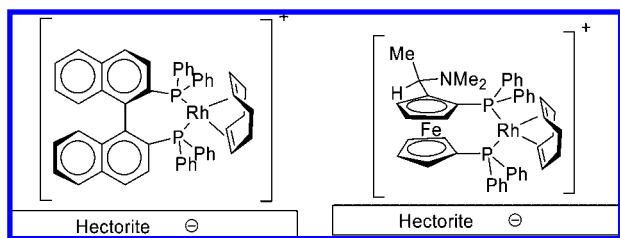
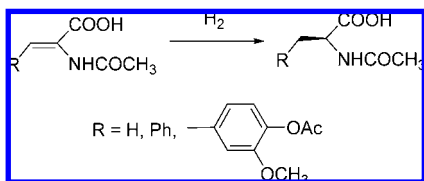


Figure 5. [(BINAP)Rh(cod)]hectorite and [(BPPFA)Rh(cod)]hectorite.

cationic exchange (the out-coming salt was not washed), the main catalyst–support interaction should be electrostatic, and hence this example and the following ones coming from the same group have been included in this section.

The homogeneous catalyst showed a high activity for the hydrogenation of imines (Scheme 3) but without enantioselectivity. However the supported catalyst showed a similar activity with 18% ee, which was increased upon recovery to 23%, 48%, and 59% ee in successive runs, although with significantly reduced activity. Oxygen seemed to be responsible for this effect, because pretreatment under O<sub>2</sub> atmosphere increased the enantioselectivity values of the two first runs to 40% and 53% ee, respectively. This is only possible with the supported complex, because the same treatment of the homogeneous catalyst led to no enantiomeric excess. Leaching of inactive iridium species was detected.

Scheme 2

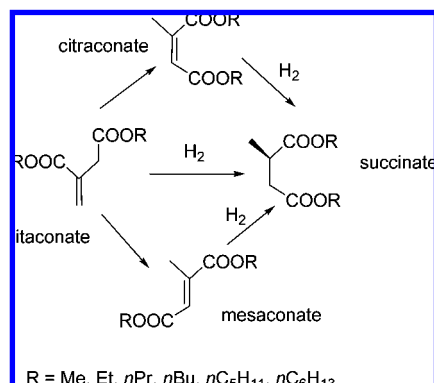


Table 1. Results from Hydrogenation of Dibutyl Itaconate with Hectorite-Supported Rh Catalysts<sup>a</sup>

ligand	solvent	ClO <sub>4</sub> <sup>-</sup>		hectorite	
		conversion, % (time, h)	% ee	conversion, % (time, h)	% ee
BINAP	MeOH	93 (12)	2	98 (24)	3
	EtOH	100 (2)	38	100 (46)	8
	1-PrOH	100 (4)	38	100 (96)	4
	EtOH/Cy (5:1)	100 (2)	41	93 (47)	43
	EtOH/Cy (2:1)	100 (3)	58	100 (144)	58
	EtOH/Cy (1:2)	90 (18)	55	96 (360)	66
BPPFA	EtOH/Cy (2:1) <sup>b</sup>	100 (74) <sup>b</sup>	81 <sup>b</sup>	100 (312) <sup>b</sup>	84 <sup>b</sup>
	MeOH	100 (40)	15	92 (408)	64
	EtOH	100 (118)	32	100 (720)	88
	1-PrOH	100 (118)	56	100 (552)	84

<sup>a</sup> Data from ref 26. <sup>b</sup> Hydrogenation of dibutyl mesaconate.

The same group described the immobilization of several Rh complexes, [(BINAP)Rh(cod)]<sup>+</sup>, [(QUINAP)Rh(cod)]<sup>+</sup> (QUINAP = 1-(2-diphenylphosphino-1-naphthyl)isoquinoline), and [(BDPP)Rh(cod)]<sup>+</sup> (Figure 9) by the same method on different supports, mainly K10 montmorillonite and bentonite clays. Both cation and anion (BF<sub>4</sub><sup>-</sup>) of the complex were adsorbed on K10, as detected by <sup>19</sup>F and <sup>31</sup>P NMR of the remaining solution.

With both BINAP and QUINAP ligands, it was possible to reproduce the excellent results obtained in solution for the asymmetric hydroboration of styrene (Scheme 4): 96% yield, 97% selectivity to branched product, 55% ee with BINAP (recoverable once) and 98% yield, 97% selectivity to branched product, 88% ee with QUINAP (recoverable

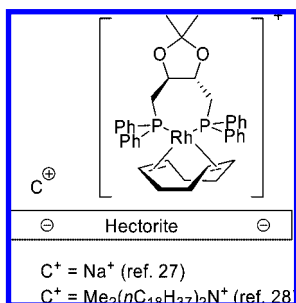


Figure 6. [(DIOP)Rh(cod)]hectorite.

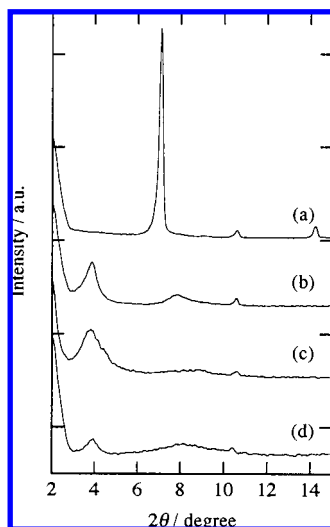


Figure 7. XRD diffraction patterns of sodium hectorite (a) and [(DIOP)Rh(cod)]hectorite as-prepared (b), after reaction (c), and swollen with 1-propanol (d). Reprinted by permission of Elsevier (Copyright 1999) from ref 27.

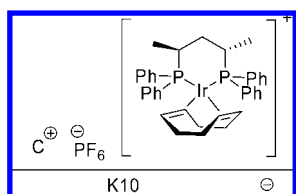
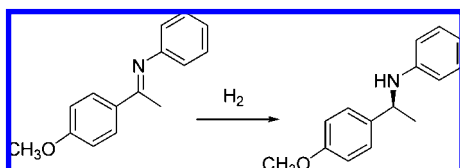


Figure 8. [(BDPP)Ir(cod)]K10.

### Scheme 3



three times).<sup>30</sup> The main advantage of this methodology is the separation of the immobilized catalyst before the oxidation step, allowing in this way the successful recovery of the catalyst.

In the case of catalysts supported on bentonites, the immobilization process of [(QUINAP)Rh(cod)]<sup>+</sup> was ascribed to truly cationic exchange by conductometric measurement of the washings.<sup>31</sup> In depth studies on the nature of the catalyst–support interaction were described,<sup>32</sup> showing that a neutral species (BINAP) was not adsorbed on clays, whereas cationic species with anions unable to form hydrogen bonds (BPh<sub>4</sub><sup>−</sup>) were easily adsorbed. This seems to confirm the electrostatic nature of this interaction. Excellent

results (Table 2) were described for the enantioselective hydroboration of several alkenes (Scheme 4) with both types of clays. However, in many cases an induction period was observed, and the maximum catalytic performance was obtained in the second or even in the third run.

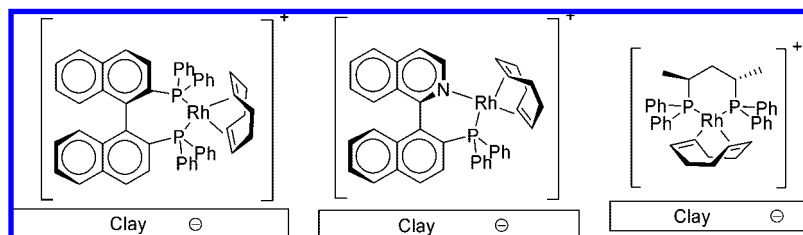
Chiral bis(oxazoline)–copper (Box–Cu) complexes have been extensively immobilized on clays and, to a much lesser extent, other noncrystalline inorganic solids, following this cation-exchange strategy. The resulting immobilized complexes have been used as catalysts in a variety of organic reactions, particularly in carbene-transfer reactions. Cyclopropanation reaction of styrene with diazocompounds (mainly ethyl diazoacetate) (Scheme 5) has been the benchmark reaction used to test these catalysts. This benchmark reaction has the advantage of requiring a small proportion of catalyst and providing different selectivities (chemoselectivity, given by the cyclopropanes/fumarate+maleate ratio, diastereoselectivity, given by the *trans/cis* cyclopropanes ratio, and, of course, enantioselectivities in *trans*- and *cis*-cyclopropanes). In this way, much information concerning immobilization effects on the reaction course can be extracted from a single experiment. Mechanistic studies point to a common copper–carbene intermediate as the key species in determining all the reaction selectivities, simplifying the interpretation of the results.<sup>33</sup>

Historically, immobilization of cationic Box–Cu complexes through ionic exchange on anionic supports, and particularly on clays, was the first example of this strategy described and has been thoroughly explored by Mayoral and co-workers since 1997.

The immobilization of PhBox–CuCl<sub>2</sub> and BnBox–CuCl<sub>2</sub> complexes by cationic exchange onto clays (laponite and bentonite, Figure 10) and their use in the benchmark reaction was the first case described for these systems.<sup>34</sup>

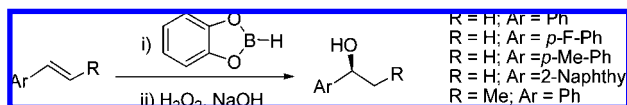
The chemical integrity of the supported complex is an important issue to correctly interpret the results, so it was studied by different spectroscopic techniques, such as FT-IR, EPR, and EXAFS, comparing solution, solid, and clay-supported complexes. These experiments demonstrated that the whole complex was supported and kept its chemical nature upon immobilization and that the starting chloride counteranion was lost during the exchange process, so that the catalytic complex was firmly bound to the anionic support through electrostatic interactions.<sup>35</sup> Some interesting support effects were already described in these former works, in particular the change of *trans/cis* selectivity toward the *cis* isomers, even with a slight *cis* preference (47:53) in some cases. In general, the results obtained with the supported catalysts were superior to those obtained in the homogeneous phase with the same complexes, which was undoubtedly due to the poor performance of the complexes based on copper(II) chloride.<sup>36,37</sup> In subsequent works,<sup>38–40</sup> <sup>t</sup>BuBox and Cu(OTf)<sub>2</sub> were also used for catalyst immobilization. In general, lower enantioselectivities with regard to the homogeneous catalytic systems were observed, as well as lower *trans/cis* ratios. Recoverability of these systems was tested from the very first work,<sup>34</sup> and some of these immobilized catalysts proved to be recoverable and reusable with similar results, constituting the first example described of a recyclable enantioselective catalyst for this reaction.

Different clays both natural (K10 montmorillonite, bentonite, which are aluminosilicates) and synthetic (laponite, which is a magnesiumsilicate) have been tested as supports,<sup>38</sup> the results obtained in the catalytic experiments being very



**Figure 9.** [(BINAP)Rh(cod)]clay, [(QUINAP)Rh(cod)]clay, and [(BDPP)Rh(cod)]clay.

#### Scheme 4



similar. This indicates the consistent behavior of the support toward the immobilization of these complexes. In most subsequent works, laponite has been the clay of choice because of its synthetic nature, which warrants the chemical purity and homogeneity of the support. Natural clays usually contain other elements, like iron, that can interfere in the catalytic processes.

Some efforts have been devoted to find the best immobilization conditions, by using different exchange solvents (always with high dielectric constant) and different exchange strategies (one step, by exchanging the whole complex, or stepwise, by first exchanging the copper and then adding the chiral ligand).<sup>41</sup> Although some improvements were found with the adequate combination of ion-exchange conditions, the enantioselectivity results of the catalysts bearing the bulkier <sup>t</sup>BuBox were far from those obtained in homogeneous phase, and furthermore, the recoverability of these systems was poor. The origin of this behavior lies in the loss of chiral ligand by decomplexation, probably due to unfavorable steric interactions with the support and a low stability of the complex (see section 2.2 for a more comprehensive description of this point).

Azabis(oxazoline) (azaBox) ligands (Figure 11) possess a higher coordinating ability with regard to their analogous Box ligands, as shown by theoretical calculations and competitive catalytic experiments.<sup>42</sup> This property was exploited to prepare more stable immobilized catalysts, in which the loss of chiral ligand by decomplexation was minimized. Thus, when the catalytic results of Cu(II) complexes of alkylBox and azaBox ligands (alkyl = isopropyl and *tert*-butyl), immobilized onto laponite are compared, much better results, close to those obtained in homogeneous phase catalysis, were obtained with the latter.<sup>42</sup> Furthermore, these catalysts were recoverable at least once without loss of catalytic activity or selectivity.

On the other hand, one of the most interesting effects found with this kind of supported catalysts is the already mentioned *cis*-preference observed in the cyclopropane products. This particular effect was ascribed from the beginning to the two-dimensional nature of the clay surface, which would make difficult the *trans* approach of the alkene to the copper-carbene intermediate (Figure 12).<sup>43</sup>

This surface effect can therefore be magnified if a solvent with a dielectric constant lower than dichloromethane (the solvent used in the first studies) is employed. Under these conditions, the cationic complex forms a tighter ion pair with the anionic surface, and the steric effect of the latter increases. Thus, when the cyclopropanation reactions were catalyzed by the laponite-exchanged PhBox-Cu complex, in hexane

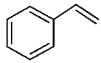
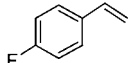
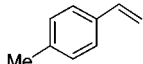
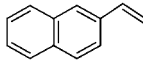
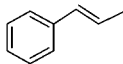
or styrene, a complete reversal of the *trans/cis* diastereoselectivity (31:69) was observed.<sup>43,44</sup> Even more interestingly, the major *cis*-cyclopropane obtained had the opposite absolute configuration, with regard to homogeneous phase results. Trying to improve the support surface effect, *C*<sub>1</sub>-symmetric chiral ligands, namely, (*S*)-4-substituted-2-(pyridin-2-yl)-4,5-dihydrooxazoles (Figure 13), were tested in the same systems.

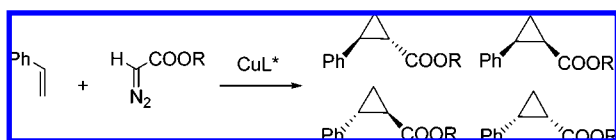
With these ligands, the same *cis* preference was obtained, but no reversal in the absolute configuration of the major *cis*-cyclopropane was observed.<sup>45</sup> A possible explanation to this fact would lie in the size of the chelate complex, which is five-membered for these ligands. It is well-known that five-membered chelate copper complexes lead to poor enantioselectivities in related systems. Therefore, the same group tested the structurally related (*S*)-4-substituted-2-(quinolin-8-yl)-4,5-dihydrooxazoles (Figure 13),<sup>46</sup> able to form six-membered chelate complexes with copper. However, the catalytic results were not so different from those obtained with 2-(pyridin-2-yl)-4,5-dihydrooxazoles. In particular, the clay-supported complexes displayed a high *cis/trans* selectivity (up to 85:15), but enantioselectivities were low, and no reversal in the absolute configuration of the major *cis*-cyclopropane was observed.

Previous theoretical studies on the mechanism of this reaction,<sup>33</sup> including the origin on the stereoselection in homogeneous phase,<sup>47</sup> allowed to propose a model to explain the behavior observed in the case of the *C*<sub>2</sub>-symmetric ligands, based on the steric effect of the support surface on the incoming alkene (Figure 14). The transition state lacking this steric interaction turns to be the most stable in the heterogeneously catalyzed reactions, leading to the major product observed.

In the case of the *C*<sub>1</sub>-symmetric ligands, the higher *cis* preference (up to 15:85) can be explained by the better accommodation of the copper-carbene intermediate to the support surface when both the ligand substituent and the ester group lie in the opposite side from the support, minimizing steric repulsions and maximizing electrostatic interactions. The *cis* transition state corresponding to this disposition is more favorable than any *trans* TS, where some complex-support steric repulsions must appear, as illustrated in Figure 15. On the other hand, it must be realized that the use of *C*<sub>1</sub>-symmetric ligands doubles the number of possible reaction channels, as immobilization does. Therefore, from four possible reaction channels using a *C*<sub>2</sub>-symmetric ligand in homogeneous phase (eight, if the possible conformations of the ester group are taken into account), we arrive to 16 reaction channels for a supported *C*<sub>1</sub>-symmetric complex (32 if ester conformations are considered again). Clearly, this fact complicates the comprehension of the factors influencing the stereoselectivity of the reaction, and molecular modeling studies become more necessary. The attractive possibility of directing the stereoselectivity of a reaction with a suitable

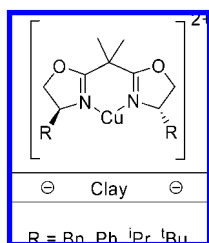
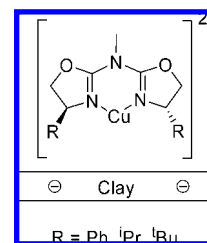
**Table 2. Results from the Enantioselective Hydroboration of Alkenes with [(QUINAP)Rh(cod)]<sup>+</sup> Supported on Clays<sup>a</sup>**

Substrate	K10				Bentonite			
	Run	Yield (%)	Branched (%)	ee (%)	Yield (%)	Branched (%)	ee (%)	
	Homog	99	95	88				
	1	51	68	50	33	26	5	
	2	98	97	89	93	77	73	
	3	92	97	86	93	89	85	
	4	98	98	88	90	87	82	
	Homog	97	95	78				
	1	38	59	40	54	72	61	
	2	83	89	75	77	85	74	
	3	92	90	73	86	88	83	
	4	82	87	67	82	87	83	
	Homog	96	99	91				
	1	31	74	70	57	85	87	
	2	98	97	89	86	90	87	
	3	92	97	86	70	90	85	
	4	98	98	88	75	89	86	
	Homog	95	99	98				
	1	26	98	54	-	-	-	
	2	71	95	70				
	3	95	98	97				
	Homog	92	99	93				
	1	5	99	13	15	99	7	
	2	66	99	87	33	99	61	
	3	66	99	86	61	99	83	
	4	64	99	85				

<sup>a</sup> Data from refs 31 and 32.**Scheme 5**

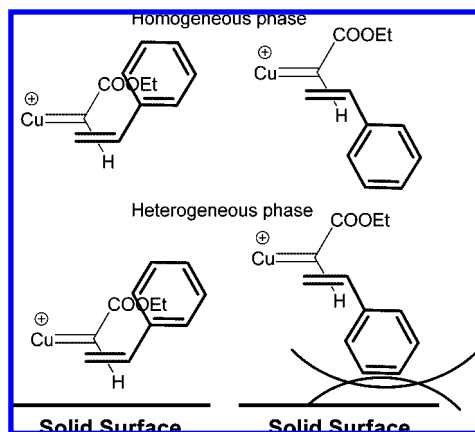
combination of ligand design and support choice is an interesting goal, which will deserve more fundamental studies.

A recent application of these catalytic systems has been reported by Fraile et al.<sup>48</sup> The enantioselective C–H carbene insertion of ethyl 2-phenyl-diazoacetate on THF (Scheme 6) was efficiently catalyzed for the first time with copper

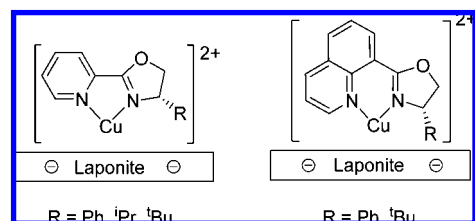
**Figure 10.** Box–Cu complexes immobilized on clays by cation exchange.**Figure 11.** Clay-immobilized azaBox–Cu complexes.

complexes. Only those ligands bearing phenyl substituents (PhBox and AzaPhBox) lead to moderate enantioselectivities (between 40% and 60% ee) in homogeneous phase. But interestingly, when the PhBox–Cu(OTf)<sub>2</sub> complex was immobilized on laponite, a more active and selective catalyst was obtained, up to 88% ee in the major *syn* product. Furthermore, the catalyst was recoverable and can be used up to four times with the same results of yield and selectivity.

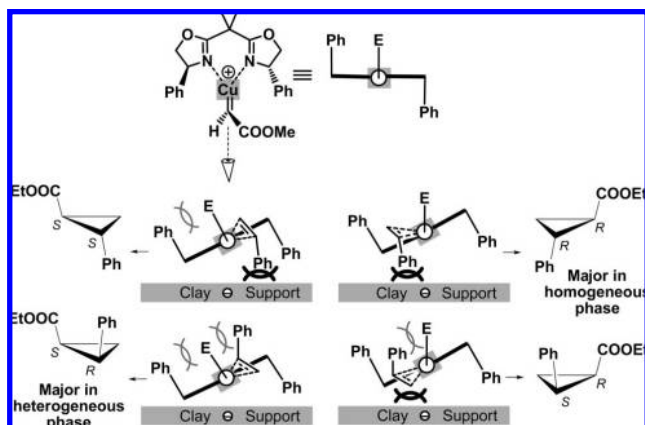
This constitutes another example of positive support effect by the clay support, and the search for new ligands and catalytic systems able to exploit these beneficial effects is an interesting work line to explore in depth in the near future, together with the mechanistic comprehension of the role of the support on the stereoselectivity of the catalytic systems.



**Figure 12.** Possible steric interaction between the incoming styrene and the clay surface disfavoring the *trans* reaction channel.



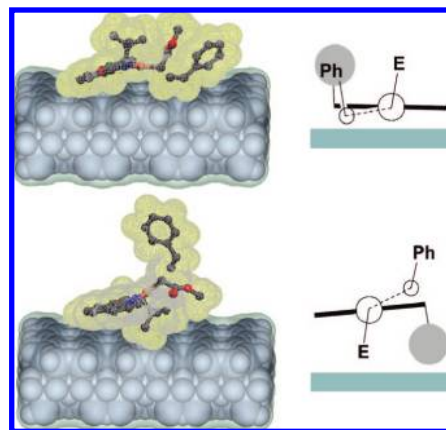
**Figure 13.** Laponite-immobilized 2-(pyridin-2-yl)-4,5-dihydrooxazole-Cu and 2-(quinolin-8-yl)-4,5-dihydrooxazole-Cu complexes.



**Figure 14.** Model of the steric interactions between the different transition states of the cyclopropanation reaction and the surface of the clay support responsible for the stereochemical changes observed in the heterogeneously catalyzed reactions.

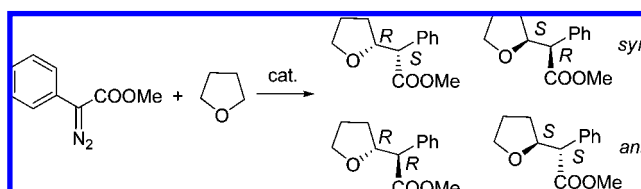
The use of clay-supported Box-copper catalysts in the closely related aziridination reaction of styrene with  $\text{PhN}=\text{IPh}$ <sup>49</sup> (Scheme 7) has also been investigated. PhBox- and <sup>t</sup>BuBox-Cu(II) complexes immobilized onto laponite were also tested in the aziridination reaction. Rather poor results were obtained, with 75% yield and 25% ee for the PhBox catalyst, which was otherwise recoverable once with similar results.

Apart from carbene and nitrene transfer reactions, clay-immobilized Box-copper complexes have also been tested in Lewis acid promoted reactions, such as Diels-Alder and Mukaiyama aldol reactions. The first attempt to use the cationic exchange method in Diels-Alder reactions was described by Fraile et al.<sup>50</sup> Cationic complexes of PhBox and Cu, Zn, and Mg salts were exchanged on laponite clay (Figure 16). This ligand was chosen because of the higher stability of its copper complex in comparison with <sup>t</sup>BuBox,

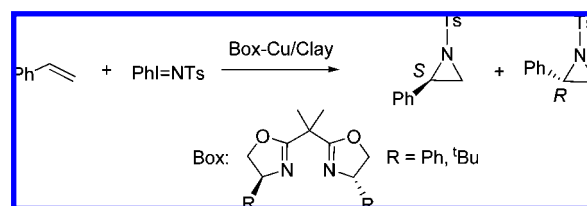


**Figure 15.** Idealized models to explain the *cis* preference observed in the cyclopropanation reaction of styrene with ethyl diazoacetate, catalyzed by quinolineoxazoline-copper complexes supported onto a clay.

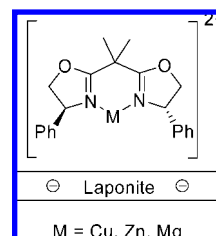
### Scheme 6



### Scheme 7

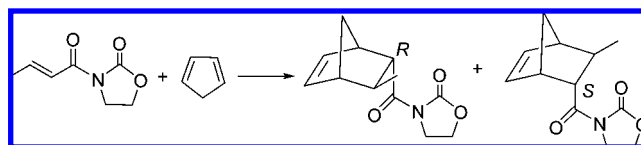


as previously commented. In general, the results in Diels-Alder reactions between cyclopentadiene and (*E*)-3-(but-2-enyl)-oxazolidin-2-one (Scheme 8) were poorer than those obtained in homogeneous phase, with enantioselectivities ca. 10% ee (for copper and zinc complexes). Analysis of the solids

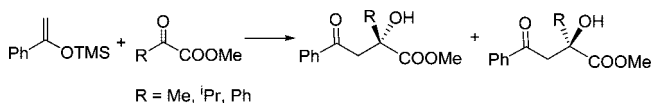


**Figure 16.** Laponite-supported PhBox-metal complexes.

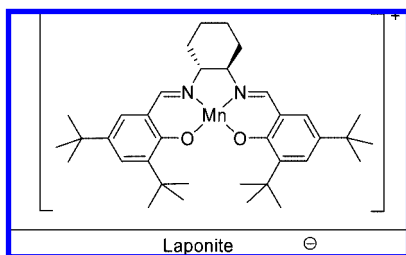
### Scheme 8



### Scheme 9

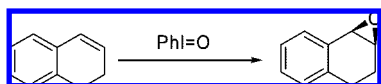






**Figure 17.** Laponite-supported Jacobsen's complex.

#### Scheme 10



demonstrated that Zn and Mg complexes were not efficiently exchanged, and most of the chiral ligand was also lost during the exchange process.

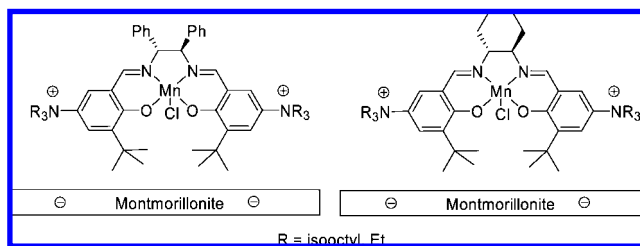
Mayoral and co-workers tried to apply Box- and azaBox-copper complexes immobilized in laponite by cationic exchange in Mukaiyama aldol reactions (Scheme 9).<sup>51,52</sup>

In the case of the reactions with methyl pyruvate (Scheme 9, R = Me),<sup>51</sup> supported PhBox-Cu complex was active in both THF and CH<sub>2</sub>Cl<sub>2</sub>. In the former solvent, the immobilization showed a positive effect on enantioselectivity, 86% ee vs 45% ee in solution, but this catalyst was almost completely deactivated. In CH<sub>2</sub>Cl<sub>2</sub>, the enantioselectivity (67% ee) was nearly the same as in solution, and the catalyst was partially recoverable. Interestingly, these deactivated catalysts could be successfully used in another reaction, namely, the cyclopropanation of styrene with ethyl diazoacetate (Scheme 5), showing the multitask nature of these solid catalysts. In contrast, supported azaBox complexes were nearly inactive toward the Mukaiyama aldol reaction, probably due to the higher coordinating character of the ligand that leads to a reduced Lewis acidity.

In a subsequent work,<sup>52</sup> the study was extended to other Mukaiyama aldol reactions with bulkier  $\alpha$ -ketoesters (Scheme 9). In all cases, enantioselectivities lower than those obtained with methyl pyruvate were observed. The recoverability of the catalysts in the case of the methyl pyruvate reactions was shown to be related to the reaction solvent used. Thus, with dichloromethane, the catalyst could be recovered once, with a slight loss of yield and enantioselectivity (67% ee vs. 58% ee upon recovery). With THF, although the enantioselectivity was higher with the freshly prepared catalyst (86% ee), the catalyst was almost totally deactivated upon recovery. But this deactivation was not permanent; once the catalyst became inactive in THF, it could be reused twice in dichloromethane, with moderate yields and the same enantioselectivity as that for the fresh catalyst (59% and 62% ee, respectively).

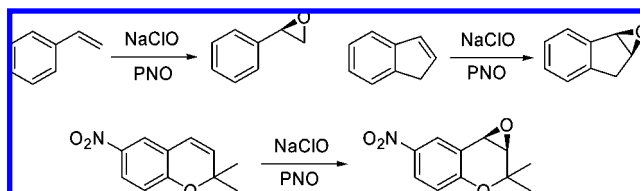
Again an incipient support effect on the stereoselectivity seems to indicate that immobilized catalyst may present interesting features *per se*, apart from the possibility of recovery, and that support can introduce a beneficial influence on the reaction stereoselectivity.

The cationic nature of Mn<sup>III</sup>(salen) complexes has been used to immobilize them onto the surface of anionic supports after a cationic exchange process. This method was first used with clays.<sup>53</sup> After several tests with a nonchiral (salen)Mn complex, synthetic laponite was chosen as the best support for this type of catalyst, and the direct exchange with the

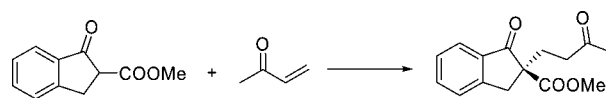


**Figure 18.** Montmorillonite-supported Mn complexes with salen ligands bearing charged moieties.

#### Scheme 11



#### Scheme 12

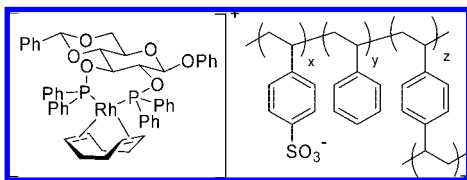


preformed complex in methanol was the chosen method, instead of the complex formation on Mn-exchanged clay. Jacobsen's complex (Figure 17) was immobilized in this way and the resulting catalyst led to moderate enantioselectivity (34% ee) in the epoxidation of 1,2-dihydronaphthalene (Scheme 10) with iodobenzene.

This result represented a slight reduction from the value obtained in solution (46% ee) but was consistent with the use of an additional axial ligand, such as pyridine, and showed the possible role of the clay sheets not only as anions but also as ligands for the catalytic complex. Probably the most relevant finding in this paper was the demonstration of complex degradation under the reaction conditions, a process that is responsible for the loss of catalytic activity and enantioselectivity in this and probably other immobilized catalysts. The IR spectrum of the recycled catalyst showed that most of the bands corresponding to the initial complex were lost, whereas the N/Mn ratio remained constant, thus demonstrating the absence of ligand leaching.

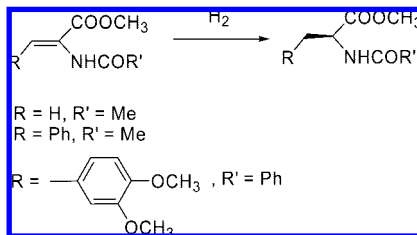
A different strategy for the immobilization of Mn(salen) complexes by electrostatic interactions is the modification of the chiral ligand with charged substituents in the aromatic rings (Figure 18). Positive charges were introduced in the form of quaternary ammonium salts and the complexes were exchanged on a montmorillonite clay from an ethanolic solution.<sup>54,55</sup> The catalyst loading was very low, which is consistent with the large size of the complexes, and exchange mainly took place on the outer surface of the clay.

All these catalysts showed very high activity in the epoxidation of alkenes with NaOCl using pyridine *N*-oxide as an additive (Scheme 11). In the case of styrene, 70% ee was obtained, representing an improvement on the result in homogeneous phase (up to 52% ee). Similar enantioselectivity was obtained in the epoxidation of indene, although in this case the immobilization was slightly detrimental. The best results, with up to 99% ee, were obtained in the epoxidation of 2,2-dimethyl-6-nitrochromene. The possibility of recycling the catalyst was tested in the epoxidation of styrene, with five consecutive reactions in which loss of



**Figure 19.**  $[(\text{Ph-}\beta\text{-glup})\text{Rh}(\text{cod})](\text{O}_3\text{S-PS-DVB})$ .

### Scheme 13



enantioselectivity was not observed and only slow deactivation of the catalyst occurred.

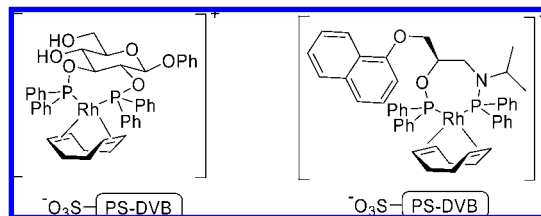
The only example described in the literature using a noncrystalline solid different from clays is La-exchanged hydroxylapatite (HAP) or fluoroapatite (FAP) modified with chiral diacids.<sup>56</sup> The catalysts were used in the Michael addition of methyl vinyl ketone on a  $\beta$ -ketoester (Scheme 12) in a heterogeneous way as shown by filtration experiments. The addition of tartaric, malic, or *O,O'*-dibenzoyl-tartaric acids led to enantioselective reactions with strange and unexplained results. Despite using a La/tartaric ratio of 6:1 in the final solid, moderate enantioselectivities were obtained (30–60% ee), whereas it was null with homogeneous  $\text{La}(\text{OTf})_3$ . The most surprising effect was the reversal of enantioselection described with tartaric acid when changing from FAP (60% ee of *S* enantiomer) to HAP (30% ee of *R* enantiomer) supports, whereas all the other acids on FAP gave rise to an *S* preference. Moreover recovery was not described.

## 2.2. Immobilization on Polymers and Related Hybrid Materials

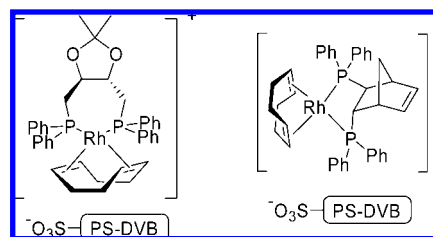
Cation-exchange resins have been well-known materials for more than 70 years, and they were the second choice to immobilize cationic chiral catalysts, in a parallel development to the clay-supported ones.

Probably the first example of immobilization on polymers was described by Selke in 1986.<sup>57</sup> The chosen support was a sulfonated poly(styrene–divinylbenzene) copolymer ( $\text{O}_3\text{S-PS-DVB}$ ) with 2% cross-linking degree to immobilize the Rh complex with a diphosphine derived from a  $\beta$ -D-glucopyranoside (Figure 19). Exchange was carried out in methanol on the acidic form of the resin in two ways: (i) with a prehydrogenation in homogeneous phase (cod is substituted by solvent or substrate) and (ii) in situ formation of the complex from  $[\text{Rh}(\text{cod})(\text{acac})]$  without prehydrogenation. Most tests were carried out with the catalyst prepared by the first method, because it showed higher stability against Rh leaching.

The catalysts were tested in the hydrogenation of dehydroamino acid derivatives (Scheme 13) with excellent enantioselectivities, 85–94% ee. Activity of the supported catalysts was much lower than that of the homogeneous analogues, corresponding to a diffusion-limited reaction rate. The catalyst showed a great stability in recycling experi-



**Figure 20.**  $[(\beta\text{-glup})\text{Rh}(\text{cod})]^+$  and  $[(\text{Propaphos})\text{Rh}(\text{cod})]^+$  immobilized on ( $\text{O}_3\text{S-PS-DVB}$ ).



**Figure 21.**  $[(\text{DIOP})\text{Rh}(\text{cod})]^+$  and  $[(\text{Norphos})\text{Rh}(\text{cod})]^+$  immobilized on ( $\text{O}_3\text{S-PS-DVB}$ ).

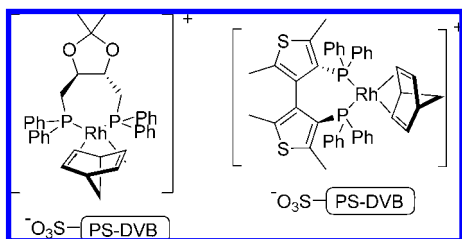
ments, keeping  $t/2$  between 10.9 and 17.1 min along 10 cycles with 94–95% ee. Activity decayed from the 11th cycle. Combined Rh leaching of several runs was analyzed, showing a progressive increase from 0.3% in the runs 1–4 to 5.2% in the runs 9–12. The stability greatly depended on the substrate and deactivation was faster with cinnamic derivatives.

In a subsequent work<sup>58</sup> other two complexes were immobilized (Figure 20), and their performance was compared with that of  $[(\text{Ph-}\beta\text{-glup})\text{Rh}(\text{cod})](\text{O}_3\text{S-PS-DVB})$ . The exchange was carried out on the acidic form of several sulfonated PS–DVB analogues with different cross-linking degrees. This immobilization method seems to produce the hydrolysis of the acetal group in Ph- $\beta$ -glup, leading to  $\beta$ -glup in the immobilized catalyst, explaining in this way the slight increase in enantioselectivity observed in the hydrogenation of methyl (*Z*)-2-acetamidocinnamate.

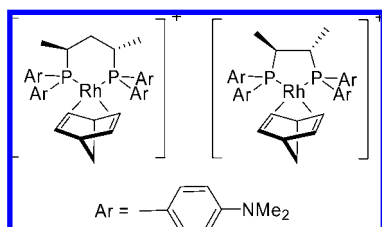
Lowering the cross-linking degree from 2% to 0.5% increased the catalytic activity, due to the improved swelling properties of the resin. Direct exchange of the complexes on the basic form of the resin was also possible, but the exchangeable cation showed an important influence, with  $\text{Li}^+$  being the most efficient regarding activity (higher swelling ability) but with reduced amount of exchanged complex (slower exchange kinetics). This method was more suitable for the hydrolysis-sensitive Propaphos ligand. The best results were obtained with  $\beta$ -glup ligand, with high enantioselectivity irrespective of the exchange method, high stability upon recycling ( $93.6\% \pm 0.3\%$  ee along 15 cycles) and low Rh leaching degree (0.5% average per cycle).

Brunner and co-workers carried out an extensive study of immobilization of  $[(\text{DIOP})\text{Rh}(\text{cod})]\text{PF}_6$  and  $[(\text{Norphos})\text{Rh}(\text{cod})]\text{PF}_6$  complexes (Figure 21) on the same type of sulfonated polymeric resins, as well as some carboxylic ones.<sup>59</sup> Exchange was also carried out on both the acidic and  $\text{Na}^+$  forms of the resins and the catalysts were tested in the hydrogenation of (*Z*)-2-acetamidocinnamic acid and its methyl ester.

The exchange on the acidic form of the sulfonic resins led to low enantioselectivity with DIOP complex, which was increased in the subsequent recycles, for example, from 28% to 60% ee in the fifth use. This effect was not as important with Norphos ligand, and the best results were obtained with



**Figure 22.**  $[(\text{DIOP})\text{Rh}(\text{nbd})]^+$  (nbd = norbornadiene) and  $[(\text{TMBTP})\text{Rh}(\text{nbd})]^+$  immobilized on  $(\text{O}_3\text{S-PS-DVB})$ .



**Figure 23.** Nafion-supported Rh complexes of amino-modified BDPP and Chiraphos ligands.

catalysts prepared by true exchange from the  $\text{Na}^+$  form, up to 75% ee with DIOP complex and 80% ee with Norphos complex. Results with the macroporous Dowex resin were slightly better than those obtained with the gel-type resin, probably due to the improved diffusion. Results with carboxylic resins were much poorer, showing the counterion effect.

The same type of immobilization was described more recently by Barbaro et al.,<sup>60</sup> using in this case the  $\text{Li}^+$  form of a gel-type Dowex resin as a support. DIOP and 4,4'-bis-(diphenylphosphino)-2,2',5,5'-tetramethyl-3,3'-bithiophene (TMBTP) complexes were tested (Figure 22) in the hydrogenation of methyl 2-acetamidoacrylate (Scheme 13). The catalysts showed a loss in activity in the second use, but afterward they kept the same activity. Excellent enantioselectivity (99.9% ee) was obtained with TMBTP ligand, both in homogeneous and in heterogeneous phase. Leaching was lower than 2%.

An alternative polymeric sulfonic support is Nafion. A superacidic character is conferred by its perfluorinated chains, and as a consequence the corresponding anion is less coordinating than a normal sulfonate anion. Nafion was used for the first time as support for a chiral catalyst by Hanson and co-workers.<sup>61</sup> In this first work, acidic and  $\text{K}^+$  forms of Nafion NR-50 were used as supports for amino derivatives of BDPP and Chiraphos ligands (Figure 23). The acidic form of Nafion was able to protonate the four amino groups of the chiral ligand in methanol, leading to species with five positive charges that were quickly and efficiently immobilized onto the resin.

The supported complexes were tested in the hydrogenation of methyl (*Z*)-2-acetamidocinnamate, methyl (*Z*)-2-benzamidocinnamate (Scheme 13), and (*Z*)-2-acetamidocinnamic acid (Scheme 1), with moderate enantioselectivity (72%, 56%, and 76% ee, respectively). Alternatively a BDPP complex with four trimethylammonium groups was exchanged on the  $\text{Na}^+$  form of Nafion. In that case exchange had to be carried out in water. Other sulfonic resins such as Amberlyst-15-H gave rise to lower enantioselectivities. The most interesting feature of these catalysts was the absence of detectable Rh leaching, probably because charges in the ligand are not dependent on the oxidation state of the metal, in contrast with charge in Rh atom, which may lead to a

Rh(0) species through reduction. The slow decay in enantioselectivity in the case of methyl (*Z*)-2-acetamidocinnamate (73%, 73%, 73%, 67%, 64%, and 63% ee in six consecutive runs) was ascribed to traces of oxygen.

An alternative method of immobilization was tried in a subsequent work.<sup>62</sup> When a 5% solution of Nafion in water was added to a methanol solution of Rh complexes with amino-modified BDPP or Chiraphos ligands, an orange gel-type solid precipitated. It was possible to filter these solids and use them as heterogeneous catalysts for the hydrogenation of (*Z*)-2-acetamidocinnamic acid and methyl (*Z*)-2-benzamidocinnamate. The protonation of the four amino groups of the ligand probably produces a cross-linking effect between the Nafion chains, making the final material insoluble. An advantage of this material is the higher catalytic activity compared with Nafion NR-50 beads, completing the reaction with the methyl ester in only 10–30 min, compared with 24–48 h with beads. The solid was quite stable, although some Rh leaching was detected, on the order of 1.5% in the first recycle and less than 1% in the subsequent reuses.

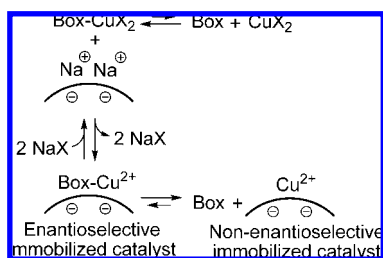
Cationic Box–Cu(II) complexes immobilized on different organic anionic supports were used as catalysts in the cyclopropanation reaction of styrene with ethyl diazoacetate (Scheme 5). In a former study from Mayoral and co-workers,<sup>39</sup> PhBox, BnBox, and <sup>t</sup>BuBox ligands were used to form the copper complexes, which were further immobilized onto Nafion and a Nafion–silica nanocomposite, prepared by gelation of a mixture of a sodium silicate solution with a Nafion-containing solution at pH 7, drying, and reacidification with 25%  $\text{HNO}_3$ .

With the PhBox ligand, results virtually identical to those obtained in homogeneous phase have been described (ca. 60% ee in *trans*-cyclopropanes). Furthermore, the catalyst was easily recoverable and reusable with the same results. Nafion itself has a very low surface area ( $<0.02 \text{ m}^2 \text{ g}^{-1}$ ), but the Nafion–silica nanocomposites have much better values ( $>80 \text{ m}^2 \text{ g}^{-1}$ ), allowing better accessibility and hence better catalytic performance. Unfortunately, the best ligand in the homogeneous phase, <sup>t</sup>BuBox, did not exhibit similar performance when its copper complexes were immobilized onto the same supports, and only modest enantioselectivities were obtained, probably due to the leaching of ligand and the concurrence of nonenantioselective reaction. The same effect was subsequently reported with other Nafion–silica supports, such as SAC-13 and SAC-40, obtained following a similar procedure.<sup>44</sup>

Nafion–silica nanocomposites have a low cation-exchange capacity (typically  $0.15 \text{ mequiv g}^{-1}$ ), so other similar supports were also tested, based on the grafting of fluoro-sulfonic acids on silica. Although the copper content increased up to  $0.55 \text{ mequiv g}^{-1}$ , enantioselectivity results with the <sup>t</sup>BuBox ligands remained lower than those obtained in homogeneous phase, and they were even lower upon reuse.<sup>41</sup>

Other cation-exchange polymeric supports, based on sulfonic acid groups, such as Dowex 50W×8 resin and Deloxan I/9 were also tested, but with these supports, even the immobilized PhBox–Cu(II) complexes led to low enantioselectivities, which were almost completely lost upon reuse.<sup>40</sup> The origin of these negative results was ascribed to the high coordinating ability of the sulfonate counteranion, since it is known that in the homogeneous phase these kinds of catalysts require the use of low coordinating anions, such

Scheme 14



as triflate, perchlorate, tetrafluoroborate, or hexafluorophosphate. This fact also helps to explain why fluorosulfonic materials, such as Nafion, lead to better results.

As already mentioned, a key point for the recoverability of these Box-based catalysts is the stability of the Box–copper complex, and this issue has also been thoroughly investigated.<sup>41,44</sup> Thus, when the *t*-BuBox–Cu(OTf)<sub>2</sub> complex was immobilized by cationic exchange on a Nafion–silica nanocomposite (SAC-13), only about 20% ee for *trans*- and *cis*-cyclopropanes was obtained (compared with over 90% ee in homogeneous phase) in the reaction of styrene with ethyl diazoacetate (Scheme 5), which indicated the probable leaching of the ligand from the immobilized catalysts because of steric interactions with the support. This hypothesis was validated by adding free *t*-BuBox ligand to the heterogeneously catalyzed reaction. Under these conditions, 91% ee in *trans*-cyclopropanes and 88% ee in *cis*-cyclopropanes was obtained,<sup>44</sup> showing the role of complexation equilibria on the enantioselectivity (Scheme 14).

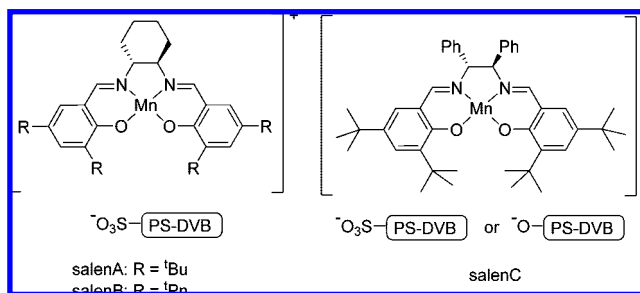
Azabis(oxazoline) (azaBox) ligands possess a higher coordinating ability with regard to their analogous Box ligands, as shown by theoretical calculations and competitive catalytic experiments.<sup>42</sup> This property was exploited to prepare more stable immobilized catalysts.

When the aza*t*-BuBox–Cu(OTf)<sub>2</sub> complex was exchanged on Nafion–silica SAC-40, spectroscopic and analytical results evidenced the integrity of the complex.<sup>42</sup> When this immobilized catalyst was used in the benchmark cyclopropanation reaction, 90% ee in *trans*-cyclopropanes and 84% ee in *cis*-cyclopropanes were obtained. Furthermore, in a second run 88% ee and 80% ee were obtained in these products, indicating that most of the chiral complex remains immobilized on the support. A more extensive study, using different ligands, supports, and Cu salts, corroborated these conclusions.<sup>42</sup>

Other reactions have also been tested with these kinds of supports. In the case of aziridination reaction (Scheme 7),<sup>49</sup> using Nafion–silica nanocomposites as the anionic supports led to results not as good as those described using CuHY exchanged zeolites (see section 2.3).

Cationic complexes of PhBox and Cu, Zn, and Mg salts exchanged on Nafion–silica nanocomposite were also tested as catalyst in the Diels–Alder reaction of cyclopentadiene with (*E*)-3-(but-2-enoyl)-oxazolidin-2-one (Scheme 8).<sup>50</sup> The catalysts showed slightly lower activity than their homogeneous counterparts, and almost no enantioselectivity.

Polymeric supports have seldom been used for the electrostatic immobilization of other types of chiral catalysts, and on some occasions, the ionic nature of the metal–support bond is not clear. (Salen)Mn complexes were immobilized in poly(styrene–divinylbenzene) (PS–DVB, 15% cross-linking) polymers modified with sulfonic and phenolic groups (Figure 24).<sup>63</sup> The immobilization was carried out by



**Figure 24.** (Salen)Mn complexes immobilized in sulfonic or phenolic PS–DVB resins.

treatment of the sodium salts of the polymers with an ethanolic solution of (salen)MnCl, as a truly cation exchange. The solids were tested in the epoxidation of five different alkenes with aqueous NaClO, and the most significant results are collected in Table 3.

In the case of 1-phenylcyclohexene, 6-cyano-2,2-dimethylchromene, and styrene, enantioselectivity was identical or slightly lower than that obtained with the homogeneous catalyst. The most interesting results were obtained with *cis*- $\beta$ -methylstyrene and  $\alpha$ -methylstyrene. In the first case, the immobilization hindered the rotation of the radical intermediate, reducing in this way the amount of *trans*-epoxide obtained and noticeably increasing the enantioselectivity of the *cis*-epoxide, 67% vs 25% ee in solution. This enhanced enantioselectivity was also observed in the case of  $\alpha$ -methylstyrene with a fully recoverable immobilized catalyst.

Because the nature of the phenoxy–Mn link may be considered as not fully ionic, the same happens in the case of the dirhodium complexes immobilized on carboxylate-functionalized PS–DVB (Figure 25).<sup>64</sup> The supported catalysts were prepared by carboxylate exchange from (M)-Rh<sub>2</sub>(L-protos)<sub>2</sub>[(*p*-X-C<sub>6</sub>H<sub>3</sub>)P(*p*-X-C<sub>6</sub>H<sub>4</sub>)<sub>2</sub>]<sub>2</sub> with carboxyethyl polystyrene (1% cross-linking) under reflux in dichloromethane. Optimum loading was 0.1 mmol/g.

Immobilized catalysts were tested in the cyclopropanation reaction between styrene and ethyl diazoacetate. The nature of the X substituent was crucial both for diastereo- and enantioselectivity. With X = H, F, Cl, Br, CF<sub>3</sub>, or Me, a slight *trans* preference (53–61%) was obtained together with moderate enantioselectivities for *trans* (51–70% ee) and *cis* (34–66% ee) diastereomers. In the case of X = *t*-Bu or SiMe<sub>3</sub>, *cis* isomers were the preferred diastereomer (68%) with moderate enantioselectivity (56% ee) but very low enantioselectivity for the *trans* isomers (12–15% ee). The same trend was observed with the analogous homogeneous catalysts (3-phenylpropionate bridges), which led in general to lower enantioselectivity. Recycling was tested in some cases, showing great stability for eight to nine cycles, with only moderate decrease in catalytic activity.

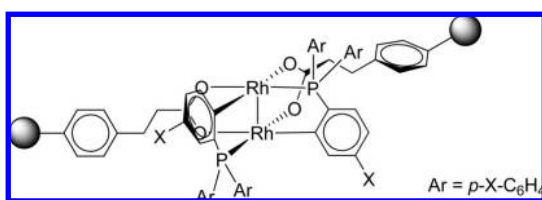
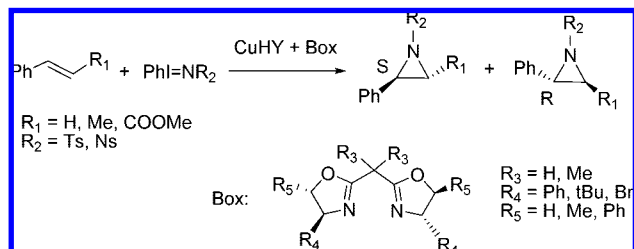
### 2.3. Immobilization on Zeolites and Mesoporous Crystalline Materials

Zeolites are crystalline three-dimensional aluminosilicates, where some aluminum atoms occupy framework positions by substituting silicon atoms. The Al/Si ratio determines the zeolite acidity and also its cation-exchange capacity. Although zeolites have been extensively used as strong solid acid catalysts by themselves, for instance, in the petrochemical industry, they can also act as supports for cationic catalytic complexes, although the immobilization nature, electrostatic or entrapment, is still under debate. In this

**Table 3. Results from the Epoxidation of Different Alkenes with NaClO Catalyzed by (Salen)Mn Complexes Immobilized in Sulfonic or Phenolic PS–DVB Resins<sup>d</sup>**

Alkene	Catalyst (% mol)	Time (h)	Yield (%)	Ee (%)
	(salenB)MnCl <sup>a</sup> (1.5)	6	94	84
	(salenB)Mn(O <sub>3</sub> S-PS) <sup>a</sup> (0.5)	24	93	71
	(salenA)MnCl <sup>a</sup> (1.5)	6	100	90
	(salenA)Mn(O <sub>3</sub> S-PS) <sup>a</sup> (1.0)	24	99	88
	(salenC)MnCl <sup>a</sup> (1.5)	6	100	58
	(salenC)Mn(O-PS) <sup>a</sup> (0.5)	24	76	61
	(salenC)MnCl (1.5)	6	25/55 <sup>b</sup>	25/93 <sup>b</sup>
	(salenC)Mn(O <sub>3</sub> S-PS) (1.5)	24	43/43 <sup>b</sup>	67/89 <sup>b</sup>
	(salenC)Mn(OPh) (1.5)	6	100	24
	(salenC)Mn(O-PS) (0.5)	24	36-41-36 <sup>c</sup>	77-75-76 <sup>c</sup>

<sup>a</sup> Results with 4-phenylpyridine N-oxide (PPNO) as additional axial ligand. <sup>b</sup> Results for *cis* and *trans* epoxide, respectively. <sup>c</sup> Results of three consecutive runs. <sup>d</sup> Data from ref 63.

**Figure 25.** Supported dirhodium complexes.**Scheme 15**

section, we will include the examples in which the authors consider that the immobilization method was clearly cationic exchange, whereas the cases of entrapment will be discussed in section 5.2. Similarly, other mesoporous silicas, doped with aluminum or other metals, can also be employed with the same purpose.

Most of the studies on the use of zeolites as supports are due to Hutchings and co-workers, who extensively studied aziridination reactions (Scheme 15) catalyzed by bis(oxazoline)–copper complexes.

Catalysts were obtained by adsorbing the ligand on a copper-exchanged HY zeolite. The final ligand/Cu ratio was 0.5, showing that not all the copper was accessible to the bis(oxazoline). In fact the use of an excess of ligand reduced the final yield, probably due to pore blocking.<sup>65–67</sup> Regarding the alkene, the best enantioselectivity was obtained with methyl (*E*)-cinnamate; however, higher aziridine yields were obtained with styrene and (*E*)- $\beta$ -methylstyrene. Another important factor was the solvent, and the best results were obtained in acetonitrile. The nature of the nitrene donor was crucial, the enantioselectivities were higher with [*N*-(*p*-nitrophenylsulfonyl)-imino]phenyliodinane ( $\text{R}_2 = \text{Ns}$ ) than with [*N*-(*p*-tolylsulfonyl)-imino]phenyliodinane ( $\text{R}_2 = \text{Ts}$ ).<sup>68</sup> In most of the aziridination reactions, an excess of alkene was used to avoid side reactions and, as a consequence,

increase the yield. However the best results with the immobilized catalysts were obtained using about 1.5 equiv of nitrene donor.<sup>68,69</sup> As expected the nature of the chiral ligand was very important;<sup>68</sup> in this regard, the best results, considering both yield and enantioselectivity (94% ee with 1.4 equiv of Ns nitrene donor), were obtained using PhBox ( $\text{R}_3 = \text{Me}$ ,  $\text{R}_4 = \text{Ph}$ ,  $\text{R}_5 = \text{H}$ ) and CuHY.<sup>70</sup> The influence of the ligand was not the same under homogeneous and immobilized conditions; for example, with PhBox ( $\text{R}_3 = \text{H}$ ) and CuHY enantioselectivities up to 79% ee were reached with both nitrene donors, whereas with the same ligand and Cu(OTf)<sub>2</sub>, the best result was 28% ee. Although the conditions (excess of Cu) favored the presence of nonchiral Cu catalytic centers under homogeneous conditions, these differences led the authors to propose that the confined space of the zeolite improves the behavior of some ligands.<sup>71</sup>

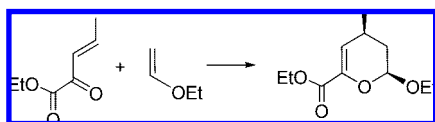
Copper leaching increased with both reaction time and nitrene donor concentration. Although filtration experiments showed that at long reaction times some active species were leached, they did not have an important influence on the reaction results.<sup>69</sup> A slight decrease in copper leaching, accompanied by a slight decrease in final yield, was observed when  $\text{H}^+$  in CuHY was substituted by group I metal cations.<sup>72</sup>

The influence and formation of byproducts was studied too. Thus, the amount of benzaldehyde, obtained by oxidation of styrene with the byproduct PhIO, depended on the substitution of the styrene phenyl ring, and in this regard, both homogeneous and immobilized catalysts showed a similar behavior.<sup>73</sup>

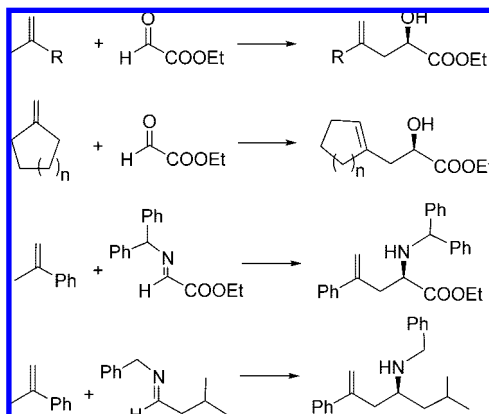
The same authors carried out some interesting mechanistic studies. EPR experiments showed the presence, in the zeolite, of square planar and square pyramidal complexes of Cu(II) with PhBox. Aziridination with PhI=NTs led to a paramagnetic intermediate that regenerated Cu(II) by reaction with styrene.<sup>74</sup>

Another interesting observation was the increase of enantioselectivity with time. Several experiments showed that, in the presence of the catalyst, aziridine reacts with the nitrene precursor and with the sulfonamide byproduct. These reactions are able to interconvert the aziridine enantiomers, playing an important role in the reaction outcome.<sup>75</sup> These opening reactions could take place via coordination of the aziridine to  $\text{Cu}^{2+}$  behaving as a Lewis acid, as suggested by

## Scheme 16



## Scheme 17



DFT calculations.<sup>76</sup> These results illustrate the importance of having a deep mechanistic knowledge of the catalytic reactions in order to correctly interpret the experimental results.

Only one example has been reported that uses a mesoporous crystalline material instead a zeolite as support for these reactions.<sup>66</sup> The mesoporous Al-MCM-41 support was first exchanged with Cu(II) acetate, and then the chiral ligands were added to form the immobilized complex. The results obtained with these solids were modest, reaching up to 87% yield and 37% ee in the best cases.

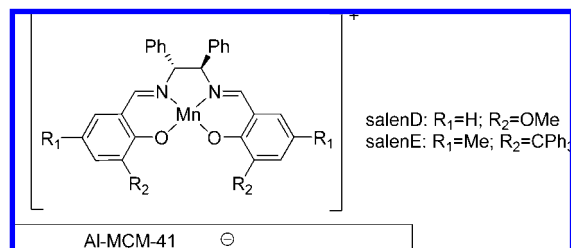
Only a few applications of zeolites and mesoporous crystalline materials as supports for electrostatic immobilization of enantioselective catalysts refer to Lewis-acid catalyzed processes.

Thus, the hetero-Diels–Alder reaction between ethyl (*E*)-2-oxo-3-pentenoate and vinyl ethyl ether (Scheme 16) was catalyzed by a PhBox–Cu complex immobilized on different crystalline mesoporous solids (Cu-MCM-41, Cu-AISBA-15, and Cu-MSU-2).<sup>77</sup> The immobilized catalysts were much less active than their homogeneous counterparts. Regarding enantioselectivity, all the mesoporous catalysts gave results lower than the 20% ee obtained in solution.

Carbonyl- and imino-ene reactions (Scheme 17) were also catalyzed by the PhBox–Cu(II) exchanged on Y zeolite.<sup>78</sup> The enantioselectivities obtained with the supported catalysts were similar to or better than those obtained in homogeneous phase with the same ligands. As relevant examples, enantioselectivity was improved with  $\alpha$ -methylstyrene, from 66% to 80% ee, and methylenecyclopentane, from 57% to 93% ee. Less than 1% copper leaching was detected under the reaction conditions, and it was demonstrated that the system is truly heterogeneous. Furthermore, the catalyst was efficiently recovered by filtration and washing. The catalyst was reused up to three times with the reagent alternatively changed from ethyl glyoxylate to methyl pyruvate without loss of activity or enantioselectivity.

The use of mesoporous materials, mainly Al-MCM-41, for electrostatic immobilization of (salen)Mn complexes has been also explored by Hutchings and co-workers.

The mesoporous character of MCM-41 overcomes the size limitations imposed by the use of zeolites (see section 5.2),



**Figure 26.** (Salen)Mn complexes immobilized on Al-MCM-41 by electrostatic interactions.

**Table 4.** Results of the Alkene Epoxidation Reactions with *m*-CPBA Catalyzed by (salen)Mn Complexes Immobilized on Al-MCM-41 by Cationic Exchange<sup>a</sup>

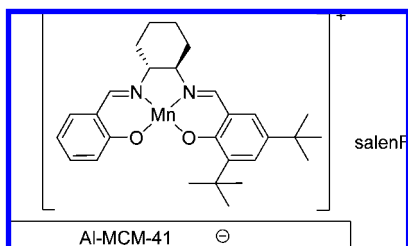
ligand	catalysis	substrate	<i>T</i> (°C)	yield (%) <sup>b</sup>	ee (%) <sup>b</sup>
salenE	homogeneous	styrene	0	95	56
	heterogeneous <sup>c</sup>	styrene	0	82	70
	heterogeneous <sup>c</sup>	styrene	−80	75	86
	heterogeneous <sup>d</sup>	styrene	0	76, 78, 75	66, 64, 64
	homogeneous	$\alpha$ -methylstyrene	0	71	23
	heterogeneous <sup>d</sup>	$\alpha$ -methylstyrene	−80	47	54
Jacobsen	heterogeneous <sup>c</sup>	$\alpha$ -methylstyrene	0	81	32
salenF	heterogeneous <sup>c</sup>	$\alpha$ -methylstyrene	0	83	55

<sup>a</sup> Data from refs 82 and 83. <sup>b</sup> Numbers separated by commas indicate results in successive reuses. <sup>c</sup> Prepared by direct exchange. <sup>d</sup> Prepared by refluxing Mn-MCM-41 with the chiral ligand.

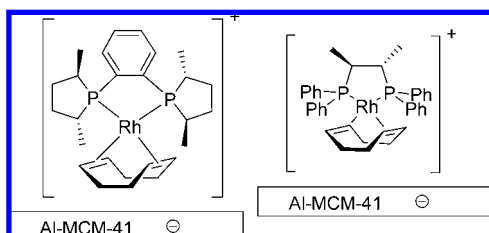
and it is possible to prepare the complex by refluxing the chiral Jacobsen's ligand in the presence of Mn<sup>2+</sup>-exchanged Al-MCM-41.<sup>79–81</sup> However, this method only allowed the complexation of 10% of Mn, as shown by elemental analysis, and good results were only possible due to the very low catalytic activity of the uncomplexed Mn sites. The immobilized catalyst was used in the epoxidation of (*Z*)-stilbene with iodosylbenzene, and this led to a mixture of *cis* (nonchiral) and *trans* (chiral) epoxides. Enantioselectivity in the *trans* epoxides was up to 70% ee, close to the value obtained in solution (78% ee). However, this value was much lower when (*E*)-stilbene was used as a substrate (25% ee). As occurred with other immobilized catalysts, reuse of the catalyst led to a significant loss in activity and, to a greater extent, in enantioselectivity.

Two new salen ligands (Figure 26) were synthesized and immobilized in Al-MCM-41 using two methods: direct exchange of the (salen)MnPF<sub>6</sub> complex or treatment of Mn<sup>II</sup>-exchanged Al-MCM-41 with the chiral ligand and subsequent oxidation to Mn(III).<sup>82</sup>

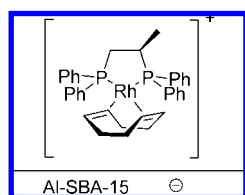
The behavior of the two types of immobilized catalysts was quite similar, although those prepared by direct exchange showed slightly higher activity and selectivity in the epoxidation of styrene and  $\alpha$ -methylstyrene with *meta*-chloroperoxybenzoic acid (*m*-CPBA) in the presence of *N*-methylmorpholine *N*-oxide (Table 4). Better results were obtained with ligand salenE probably due to the bulkiness of the triphenylmethyl substituent in position 3 of the salicylaldehyde. The immobilized catalyst led to better enantioselectivity than the homogeneous one, especially at 0 °C, and excellent enantioselectivity (86% ee) was obtained at −80 °C. Despite the fact that the results with  $\alpha$ -methylstyrene were not as good, the effect of immobilization on enantioselectivity was again observed. Recycling was attempted with one catalyst, and it was shown that three consecutive reactions with the same activity and enantioselectivity could be performed.



**Figure 27.** Nonsymmetrical (salen)Mn complex immobilized on Al-MCM-41 by electrostatic interactions.



**Figure 28.** [(MeDuPhos)Rh(cod)]<sup>+</sup> and [(Chiraphos)Rh(cod)]<sup>+</sup> complexes immobilized on Al-MCM-41.



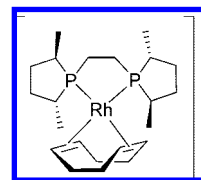
**Figure 29.** [(Prophos)Rh(cod)](Al-SBA-15).

The same authors described the synthesis of nonsymmetrical salen ligands.<sup>83</sup> As expected, the nonsymmetrical analogue of Jacobsen's ligand (salenF, Figure 27), was less efficient in the epoxidation of styrene but, surprisingly, was better for  $\alpha$ -methylstyrene (Table 4).

In contrast with clays, Rh–phosphine complexes were immobilized on mesoporous crystalline materials rather late, when the incorporation of Mn(salen) and Cu(box) complexes had been already described.

Hoelderich and co-workers described the electrostatic immobilization of four different Rh–diphosphine complexes, [(MeDuPhos)Rh(cod)]<sup>+</sup>, [(Chiraphos)Rh(cod)]<sup>+</sup> (Figure 28), [(DIOP)Rh(cod)]<sup>+</sup>, and [(Norphos)Rh(cod)]<sup>+</sup> (Figure 21), on Al-MCM-41.<sup>84</sup> The methodology was the adsorption of the complex from a dichloromethane solution and thorough washing of the solid with methanol to ensure the total extraction of the physisorbed complex. <sup>31</sup>P-MAS NMR confirmed the absence of free phosphine ligand, but the only signal of the spectrum was shifted from that of the starting complex, although no explanation for this behavior was given. [(MeDuPhos)Rh(cod)]<sup>+</sup> was the best catalyst for the hydrogenation of dimethyl itaconate (Scheme 2), both in activity (TON > 4000) and enantioselectivity (92% ee). This performance was retained for at least 8–10 runs.

Given the success of this approach, the same group described the immobilization of four complexes, [(MeDuPhos)Rh(cod)]<sup>+</sup>, [(Chiraphos)Rh(cod)]<sup>+</sup> (Figure 28), [(DIOP)Rh(cod)]<sup>+</sup> (Figure 21), and [(Prophos)Rh(cod)]<sup>+</sup> (Figure 29), on another type of mesoporous support, Al-SBA-15, following the same procedure.<sup>85</sup> The absence of adsorption on a purely siliceous SBA-15 support demonstrated the electrostatic nature of the catalyst–support interaction. The performance of the four catalysts was compared in the hydrogenation reactions of dimethyl itaconate (Scheme 2)



**Figure 30.** [(MeBPE)Rh(cod)]<sup>+</sup>.

**Table 5.** Comparison of Different Mesoporous Solids As Supports for Electrostatic Immobilization of Rh–Diphosphine Hydrogenation Complexes<sup>a</sup>

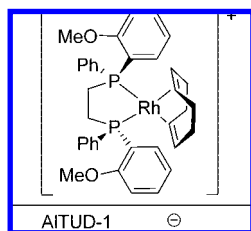
Substrate	Support	MeDuPhos		MeBPE
		TOF (h <sup>-1</sup> )	ee %	ee %
	none	n.d.	94	92
	MCM-41	166	92	84
	MCM-48	234	98	92
	SBA-15	44	89	84
	none	n.d.	94	90
	MCM-41	83	97	94
	MCM-48	120	97	95
	SBA-15	43	93	82
	none		96	89
	MCM-41		99	84
	MCM-48		98	82
	SBA-15		90	76

<sup>a</sup> Data from refs 85 and 86.

and methyl 2-acetamidoacrylate (Scheme 13). In both cases, [(MeDuPhos)Rh(cod)]<sup>+</sup> was the best catalyst (89% and 93% ee, respectively), whereas the other three showed only moderate enantioselectivity (62–78% ee). The best catalyst was recovered four cycles with itaconate and 10 cycles with 2-acetamidoacrylate.

In this paper and in a more recent one,<sup>86</sup> the same authors compare the performance of [(MeDuPhos)Rh(cod)]<sup>+</sup> (Figure 28) and [(MeBPE)Rh(cod)]<sup>+</sup> (BPE = 1,2-bis[(2*R*,5*R*)-2,5-dimethylphospholano]ethane; Figure 30) immobilized on three different supports (Al-MCM-41, Al-MCM-48, and Al-SBA-15) as catalysts for the two above commented hydrogenations and that of methyl (*Z*)-2-acetamidocinnamate (Scheme 13).

One first remark was that the amount of complex exchanged was much lower than the theoretical one, in the range of 25–50%. One possible explanation might be the difficulty for the exchange of the sites in the most inner part of the pore systems when the most external sites are already (kinetically favored) exchanged. Despite having less diffusion problems due to the larger pore size (9.2 vs 3–3.5 nm diameter) SBA-15 showed consistently worse results (Table 5) than MCM solids, both in catalytic activity and in enantioselectivity. This worse performance of SBA-15 might be due to the different preparation method of Al insertion in the support during synthesis for MCM solids and postsynthesis for SBA-15. The catalysts based on MCM supports and with MeDuPhos ligand were able to efficiently carry



**Figure 31.** [(DiPAMP)Rh(cod)](AITUD-1).

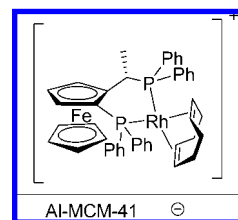
out the hydrogenation reactions with very high substrate/catalyst ratio (2000–6000), which together with the efficient reuse made it possible to reach total TON > 20 000.

Sheldon and co-workers described the electrostatic immobilization of [(MeDuPhos)Rh(cod)]<sup>+</sup> and [(DiPAMP)Rh(cod)]<sup>+</sup> (DiPAMP = (1*S*,2*S*)-1,2-bis[(2-methoxyphenyl)phenylphosphino]ethane; Figure 31) in a large pore support (AITUD-1, 15 nm pore diameter with broad distribution) by cationic exchange from alcoholic solutions.<sup>87</sup>

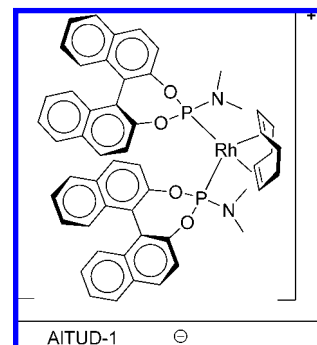
The results obtained with [(MeDuPhos)Rh(cod)]<sup>+</sup> in the hydrogenation of dimethyl itaconate (Scheme 2) were highly dependent on the reaction vessel (due to mass-transfer limitations conditioned by the stirring method) and solvent. As first conclusions, all the reactions were highly enantioselective (96–98% ee), with better activity in isopropanol and lower leaching level (below 1%) in less polar aprotic solvents (dichloromethane, ethyl acetate, or methyl *tert*-butyl ether (MTBE)). In the hydrogenation of methyl 2-acetamidoacrylate (Scheme 13) with [(MeDuPhos)Rh(cod)]<sup>+</sup>, enantioselectivity was more dependent on the solvent, from 75% ee in isopropanol to 98% ee in methanol, and again leaching was lower in less polar solvents. With [(DiPAMP)Rh(cod)]<sup>+</sup>, enantioselectivities were even more variable (MeOH, 92% ee; EtOH, 79% ee; H<sub>2</sub>O, 64% ee; EtOAc, 30% ee), with leaching also varying from less than 1% (EtOAc) up to 20% (MeOH). However this leaching was not of active species, as demonstrated by filtration experiments. Recycling was better in the case of [(DiPAMP)Rh(cod)]<sup>+</sup>, with the same or improved performance for four cycles.

Hutchings and co-workers<sup>88</sup> also described the cationic exchange of [(MeDuPhos)Rh(cod)]<sup>+</sup> in Al-MCM-41 from methanol solution. The catalyst was extremely active in the hydrogenation of methyl 2-acetamidoacrylate (Scheme 13) and dimethyl itaconate (Scheme 2). In the first case, five consecutive runs were carried out to complete conversion in 10–20 min with 95%, 99%, 97%, 97%, and 92% ee. In the second case, eight consecutive runs (1 h each) were carried out with conversions from 95% to <99% and also 95–99% ee. Recovery was not so efficient when high substrate/catalyst ratio (5000) was used. SBA-15 support was much less efficient and extensive leaching was observed. The immobilization was alternatively performed by adding the chiral ligand to the support exchanged with [Rh(cod)<sub>2</sub>]<sup>+</sup>, a method used more commonly with entrapped catalysts (see section 5). Supported [(Josiphos)Rh(cod)]<sup>+</sup> complex (Figure 32) prepared with this method was used in 10 consecutive runs of dimethyl itaconate hydrogenation reaction, with 98–99% conversion and 90–94% ee in all of them.

Not only diphosphines can be used as ligands for supported Rh catalysts. Sheldon and co-workers described the immobilization of [(MonoPhos)<sub>2</sub>Rh(cod)]<sup>+</sup> complex (Figure 33) in AITUD-1 using the conventional method of cationic exchange.<sup>89</sup> Again the use of a protic solvent (isopropanol) led to good results in the hydrogenation of methyl 2-aceta-



**Figure 32.** [(Josiphos)Rh(cod)](Al-MCM-41).



**Figure 33.** [(MonoPhos)<sub>2</sub>Rh(cod)](AITUD-1).

midoacrylate (97% ee) but with considerable leaching (8.4%) and the corresponding deactivation upon recovery. The catalytic performance was maintained when the catalyst was used in aprotic solvents, such as CH<sub>2</sub>Cl<sub>2</sub>, EtOAc, or MTBE, or in water and the enantioselectivity even slightly increased (up to 94% ee) from the second cycle. One advantage of this method is the possibility of using water, a solvent in which the complex is not soluble, as the reaction medium.

In a subsequent paper,<sup>90</sup> the same authors compared the performance of several supports in the immobilization of the same [(MonoPhos)<sub>2</sub>Rh(cod)]<sup>+</sup> complex. Cationic exchange was carried out on mesoporous AITUD-1, Nafion, and Nafion–silica nanocomposite SAC-13. Rh loading was much higher on the mesoporous material, 0.117 mmol/g, than on SAC-13, 0.0136 mmol/g, or Nafion, although in this case the loading was highly dependent on the solvent used, 0.005 mmol/g from isopropanol and 0.076 from methanol, probably due to the swelling ability of Nafion in the different solvents. Hydrogenation of methyl 2-acetamidoacrylate (Scheme 13) was used as catalytic test, and results were highly dependent on the reaction solvent, mainly regarding catalytic activity. Higher TOF values were obtained in dichloromethane, except with Nafion, which presented the highest activity in water. Variability of enantioselectivity was 83–97% ee with AITUD-1, 87–98% ee with SAC-13, and 92–98% ee with Nafion (exchanged in isopropanol). Rh leaching was also highly dependent on solvent, due in part to the different solubility of the complex, explaining the very low leaching level in water. In contrast, alcohols (isopropanol or methanol) provoked the highest Rh leaching with all the supports.

## 2.4. Immobilization on Organically Modified Inorganic Supports

Polymers present several advantages for electrostatic interactions, such as the variability of anionic centers, but some disadvantages from a practical point of view, such as the fragility or the swelling properties. In this regard, organically modified inorganic supports may join the advantages of the polymeric materials together with the mechanical strength and the defined pore structure of the inorganic supports.



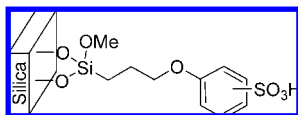


Figure 34. Sulfonic acid grafted on silica.

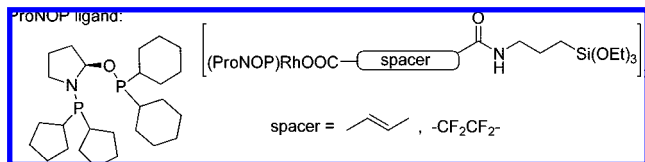
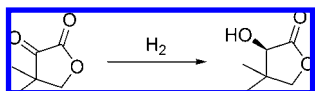


Figure 35. ProNOP–Rh complex with linkers to be immobilized on silica.

#### Scheme 18



This strategy was already tested by Selke and Čapka in 1991 by grafting a phenyl moiety on silica and subsequent sulfonation to obtain the benzenesulfonic acid (Figure 34).<sup>91</sup> This anionic support was used to immobilize  $[(\text{Ph-}\beta\text{-glup})\text{Rh}(\text{cod})]^+$  (Figure 19) and  $[(\beta\text{-glup})\text{Rh}(\text{cod})]^+$  (Figure 20) complexes, either from the acidic form or from the  $\text{Li}^+$  form. As in the case of polymeric supports,<sup>58</sup> the acidic form produces the partial hydrolysis of the ketal, leading to slightly higher enantioselectivities in the hydrogenation of methyl 2-acetamidocrylate. Catalysts were very active and stable,  $t/2$  between 2.0 and 3.5 min with enantioselectivity  $94.1\% \pm 0.2\%$  ee in 20 cycles. This high activity was very important to speed up the recycling process and prevent deactivation, mostly due to phosphine oxidation.

In contrast with polymeric materials, the type of alkaline cation of the support had no influence, given that the hybrid material was not swellable. The detrimental effect of larger tetraalkylammonium cations was probably due to pore occlusion, more important with bulkier substrates, such as cinnamic derivatives (Scheme 13). Rh leaching was in the range of 1% per cycle, unacceptable for practical use from the authors. The performance decreased when substrate/catalyst ratio increased. In the hydrogenation of methyl (Z)-2-acetamidocinnamate with substrate/catalyst = 500, supported  $[(\beta\text{-glup})\text{Rh}(\text{cod})]^+$  deactivated after two runs with 95% ee. Recyclability and stability against Rh leaching were improved by using toluene as a solvent with a support preloaded with aniline. Seven runs were possible with slight reduction in activity;  $t/2$  increased from 8 to 20 min, and enantioselectivity decreased from 92% to 87% ee.

Five years later Rh complexes with a ProNOP ligand were functionalized with carboxylates bearing spacers with trialkoxysilane ends (Figure 35) to be immobilized onto silica.<sup>92</sup> In this case again, the nature of the Rh–O bond may not be considered as fully ionic, but it is included in this section due to the resemblance with the other examples.

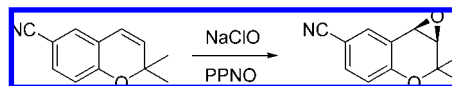
The dimeric complex was grafted on silica, although there was no evidence about the number of links (one or two) to the surface. Catalysts were evaluated in the enantioselective hydrogenation of ketopantolactone (Scheme 18). Results of conversion (52–100%) and enantioselectivity (75–91% ee) were satisfactory in the first run, but leaching was important in all cases, and recovered solids showed an important drop in performance.

Table 6. Results from the Epoxidation of *cis*- $\beta$ -Methylstyrene with Jacobsen's Catalyst in Homogeneous and Heterogeneous Phase<sup>a</sup>

support	<i>cis</i> epoxide		<i>trans</i> epoxide	
	yield (%)	ee (%)	yield (%)	ee (%)
none	27.5	55	72.5	100
MCM-41 (1.6)	66.0	95	3.8	76
SBA-15 (7.6)	36.2	95	2.8	77
silica (9.7)	21.2	94	1.3	100

<sup>a</sup> Data from ref 94.

#### Scheme 19



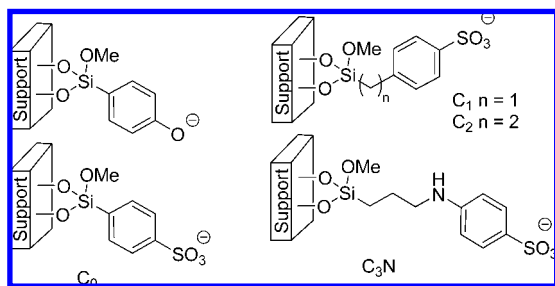
After these pioneering works, two research lines have been followed in this subject: the use of Nafion–silica hybrid materials as supports for Box–Cu complexes, already discussed in section 2.2,<sup>39,41,42,44</sup> and the grafting of different organic moieties on mesoporous materials to immobilize (salen)Mn complexes.<sup>93–97</sup>

In a first report,<sup>93</sup> Li and co-workers demonstrated how a phenoxide group grafted on MCM-41 was able to immobilize Jacobsen's (salen)Mn complex through cation exchange in refluxing ethanol, although the ionic nature of the Mn–O bond is not clear. The immobilization proved to be positive for the epoxidation of  $\alpha$ -methylstyrene with aqueous NaClO, because the enantioselectivity increased from 56% ee in solution to 72% ee with the heterogeneous catalyst in the same solvent. The catalyst was stable during three cycles. Interestingly the solid was unable to epoxidize 1-phenylcyclohexene, due to the bulkiness of the substrate, demonstrating the placement of the catalytic sites in the mesopores of the support.

In a subsequent work by the same group, a benzenesulfonic moiety was grafted on supports with different porosity: two different MCM-41s (1.6 and 2.7 nm pore diameter), SBA-15 (7.6 nm), and activated silica (9.7 nm).<sup>94</sup> Three (salen)Mn complexes (Figure 24) were immobilized and used as catalysts in the epoxidation of  $\alpha$ -methylstyrene with aqueous NaClO in the presence of PPNO. In all cases, the immobilization was positive for enantioselectivity, from 26–57% ee in solution to 74–78% ee with the supported catalysts. The effect was even more clear in the case of *cis*- $\beta$ -methylstyrene epoxidation (Table 6).

As can be seen, the yield of *trans*-epoxide is greatly reduced by the use of supported catalysts, irrespective of the support, and the enantioselectivity in the *cis*-epoxide is noticeably improved, from 55% to 95% ee. The hypothesis proposed for this effect is the restricted rotation of the radical intermediate, also reported in the case of the purely organic support PS–DVB.<sup>63</sup>

The use of the grafted phenoxide anion was studied more in depth by using also different supports, complexes, and substrates.<sup>95</sup> Results were quite puzzling, given that immobilization proved to have almost no influence on the epoxidation enantioselectivity of some alkenes (styrene), a clear detrimental effect on other substrates (1-phenylcyclohexene), and positive effect only in the case of  $\alpha$ -methylstyrene. Also yields were affected differently depending on the substrate, with no clear relationship between activity and porosity. The restricted formation of *trans*-epoxide in the reaction of *cis*- $\beta$ -methylstyrene was also detected. Several



**Figure 36.** Supports used for Jacobsen's (salen)Mn epoxidation catalyst.

**Table 7. Results from the Epoxidation of 6-Cyano-2,2-dimethylchromene with NaClO Catalyzed by Jacobsen's (Salen)Mn Complex Immobilized on Hybrid Materials<sup>a</sup>**

anion	support	spacer	time (h)	yield (%)	ee (%)
Cl			6	97	80
PhO			6	100	85
PhO	MCM-41 (1.6)	C <sub>0</sub>	24	77	49
PhO	MCM-41 (2.7)	C <sub>0</sub>	24	32	26
PhO	SBA-15 (6.2)	C <sub>0</sub>	24	100	85
PhO	SBA-15 (7.6)	C <sub>0</sub>	24	73	77
PhO	silica (9.7)	C <sub>0</sub>	24	84	69
PhSO <sub>3</sub>	silica (9.7)	C <sub>0</sub>	24	26	45
PhSO <sub>3</sub>	silica (9.7)	C <sub>1</sub>	24	54	60
PhSO <sub>3</sub>	silica (9.7)	C <sub>2</sub>	24	89	79
PhSO <sub>3</sub>	silica (9.7)	C <sub>3</sub> N	24	87	83
PhSO <sub>3</sub>	SBA-15 (7.6)	C <sub>2</sub>	24	89	85
PhSO <sub>3</sub>	SBA-15 (7.6)	C <sub>3</sub> N	24	91	89
PhSO <sub>3</sub>	MCM-41 (1.6)	C <sub>3</sub> N	24	77	71
PhSO <sub>3</sub>	Me-silica (9.7) <sup>b</sup>	C <sub>2</sub>	6	98	87
PhSO <sub>3</sub>	Me-silica (9.7) <sup>b</sup>	C <sub>3</sub> N	4.5	100	91
	reuse 1		4.5	95	87
	reuse 2		6	77	83

<sup>a</sup> Data from ref 96. <sup>b</sup> Methylated support.

hypotheses were proposed: restriction or enhancement of alkene approach pathways, changes in the stereochemical communication, modification of transition states, and reaction through different processes. However, the lack of evidence for any of those hypotheses made it impossible to explain the observed modifications in activity and enantioselectivity.

An exhaustive study by the same group described the effect of pore size and spacer length on the enantioselectivity of 6-cyano-2,2-dimethylchromene epoxidation (Scheme 19).<sup>96</sup>

Five supports, namely, MCM-41 with 1.6 and 2.7 nm pore diameters, SBA-15 with 6.2 and 7.6 nm pore diameters, and activated silica with 9.7 nm pore diameter, in combination with a phenoxide and four benzenesulfonic groups with different spacers (Figure 36) were tested as supports for Jacobsen's (salen)Mn complex. The most relevant results are gathered in Table 7.

The effect of anion in solution was negligible when changing from chloride to phenoxide. In the case of supported phenoxide, the use of MCM-41 (1.6) was considered as representative of grafting on the external surface of the support, which produced a detrimental effect on both activity and enantioselectivity. The confinement effect inside the mesopores was considered as superimposed on this detrimental effect. The optimal pore size was found to be 6.2 nm diameter, both for activity and for selectivity, reproducing in this way the enantiomeric excess obtained in solution (85% ee). The effect of the spacer was tested in the case of sulfonic anions. Increasing the spacer length in the support with largest pore size had a positive effect on

enantioselectivity, from 45% ee with C<sub>0</sub> spacer up to 83% ee with the longer C<sub>3</sub>N spacer, and even higher (89% ee) if a support with slightly smaller pore size was used. These results were explained from the free space in the nanopores between the catalytic complex and the walls of the pores. When this space fits well with the size of the substrate, optimal enantioselectivity is obtained.

Activity and enantioselectivity were further increased by methylation of the support surface, attributed to the higher hydrophobicity of surface, favoring in this way the adsorption of the more hydrophobic substrate.

In the last paper of this series,<sup>97</sup> several effects of PPNO additive, pore size of support, substrate structure, and methylation of support were described, resulting in rather puzzling results. Unfortunately in no case was the enantioselectivity obtained with the immobilized catalysts better than that obtained with the homogeneous catalyst.

An analogous strategy was used by Sabater and co-workers<sup>98</sup> to immobilize Jacobsen's (salen)Mn complex on three supports, MCM-41, ITQ-2, and ITQ-6 (two delaminated zeolites), with two types of spacers. The chloride present in the original complex was first substituted by a carboxylate or alkoxide bearing a terminal olefin that was made react with 3-mercaptopropyl-modified support (Scheme 20). Afterward the solids were silanized to eliminate residual silanol groups.

Results from the epoxidation of 1-phenylcyclohexene with NaOCl were excellent: 89–98% conversion, 78–90% selectivity to epoxide, 76–86% ee. Delaminated zeolites were better supports regarding selectivity to epoxide but slightly worse for enantioselectivity. Catalysts suffered a significant drop in performance upon recycling, although data about possible metal or complex leaching were not provided.

Hultman et al. described the immobilization of dirhodium–carboxamide complexes by substitution of one carboxamide group with a grafted carboxylate (Scheme 21).<sup>99</sup>

Only modest to low enantioselectivities were obtained<sup>100</sup> in the cyclopropanation reaction of styrene and ethyl diazoacetate (35–45% ee) and in the carbene insertion to the Si–H bond (20–33% ee) (Scheme 22). Small improvements of enantioselectivity compared with the results in solution were described, but the reversal was true with a related carboxamide ligand.

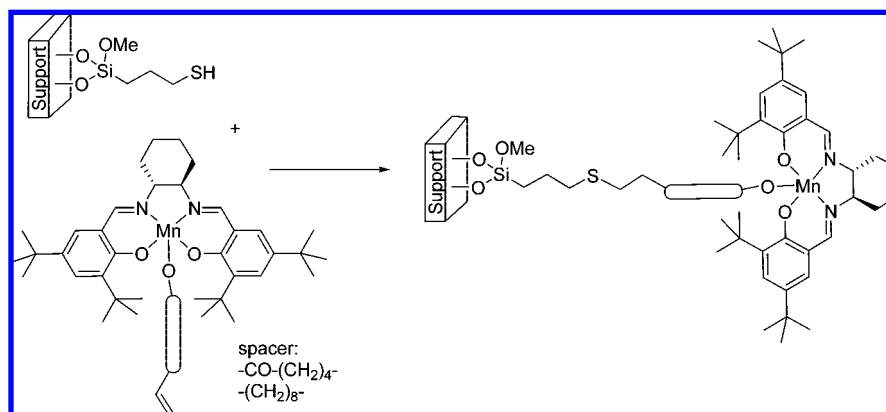
## 2.5. Immobilization on Cationic Supports

Chiral catalysts bearing anionic groups can be immobilized by electrostatic interaction with cationic supports, although this strategy has been less often used than the cationic exchange.

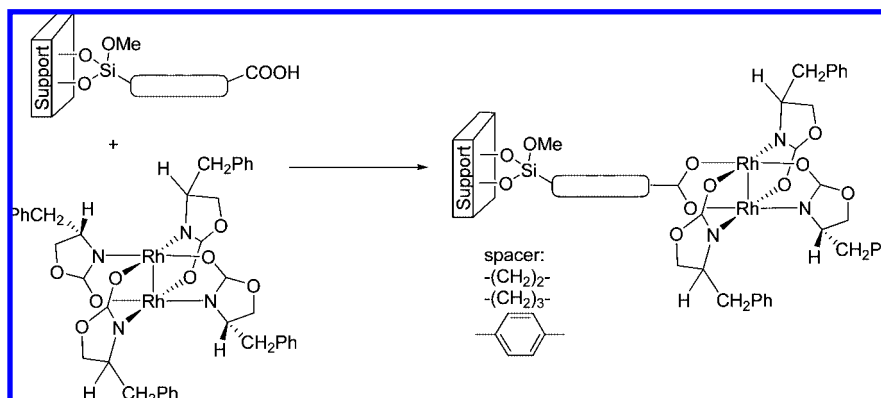
In the first report using this strategy Tas et al.<sup>101</sup> immobilized a sulfonated Ru–BINAP complex (Figure 37) on layered double hydroxides (LDHs), more precisely on the external surface as shown by XRD. These catalysts were tested in the hydrogenation of dimethyl itaconate and geraniol, and the results are shown in Table 8.

In the case of dimethyl itaconate, the activity and enantioselectivity of the complex remained practically unchanged after immobilization on Mg–Al/Cl LDH, whereas on Zn–Al/NO<sub>3</sub> LDH activity remained unchanged but enantioselectivity decreased. It is not easy to explain this behavior, but the authors suggested that the differences between the solid supports might be the origin for these differences. Mg–Al/Cl LDH shows a basic behavior in aqueous solution in contrast with the acidic character of Zn–Al/NO<sub>3</sub> LDH. In

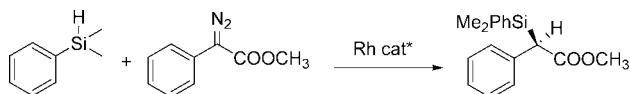
Scheme 20



Scheme 21



Scheme 22



the case of geraniol, reduced activity with unchanged enantioselectivity was observed after immobilization. In this case, the support did not have any influence on the results. Although catalyst recovery was not studied, leaching was not observed. Interestingly, when the sulfonated complex was immobilized onto organic anion exchangers, no activity was observed.

A related strategy is the creation of a three-dimensional polymeric network, around the catalyst, held together by electrostatic interactions. This strategy was used with Rh- and Ru-BINAP complexes, using ligands modified with phosphate groups<sup>102,103</sup> (Figure 38). The homogeneous catalyst was mixed with an aqueous solution of a suitable polyelectrolyte. The Rh-catalyst was tested in the hydroformylation of different alkenes.

With a suitable polyelectrolyte, poly(diallyl-dimethylammoniumchloride) was the best one, and toluene as the solvent, 39% ee was reached in the hydroformylation of vinyl acetate, an enantioselectivity slightly lower than the 45–60% ee obtained with homogeneous Rh-BINAP catalysts. The results

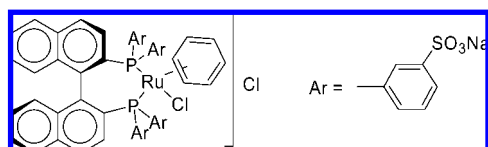


Figure 37. Anionic (BINAP)Ru complex.

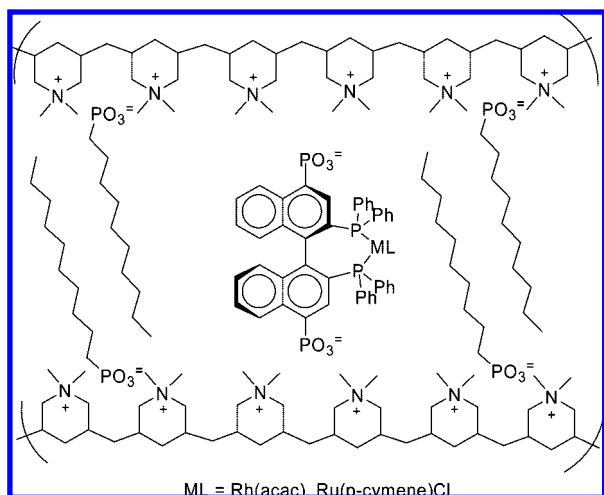
Table 8. Results Obtained in the Hydrogenation Reactions Promoted by Chiral Catalysts Immobilized on LDHs<sup>a</sup>

Substrate	Support	TOF (h <sup>-1</sup> )	ee %
	-	29	51
	Mg-Al/Cl LDH	27	48
	Zn-Al/NO <sub>3</sub> LDH	25	11
	-	4	100
	Mg-Al/Cl LDH	2	100
	Zn-Al/NO <sub>3</sub> LDH	2	100

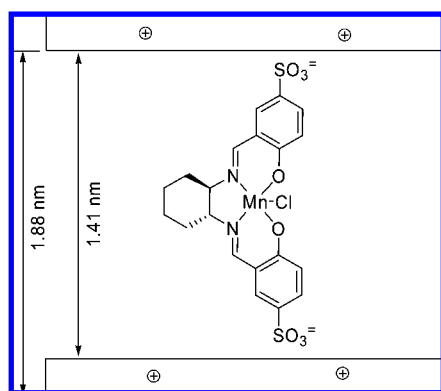
<sup>a</sup> Data from ref 101.

depended on the olefin, and very low enantioselectivities were reached with the nonpolar styrene. The Ru complex led to 90% ee, comparable to the 91% ee obtained in solution, in the asymmetric hydrogenation of dimethyl itaconate in EtOH. Catalysts were reused several cycles with negligible decrease in chemo- or enantioselectivity and without experimentally observable metal leaching.

In the same field, Anderson and co-workers<sup>104–107</sup> have studied the immobilization of Mn(salen) catalysts in which the salen ligand was modified by the introduction of anionic sulfonate groups. In the first papers, the complex was intercalated into Zn-Al LDH by aqueous exchange of the benzoate anion from Zn<sub>2</sub>Al/PhCOO LDH, and the solid was characterized by XRD, IR, and UV-visible spectroscopies and TGA analysis. Thermogravimetric analysis was consistent with the presence of the complex within the LDH host, whereas spectroscopic studies indicated that no change of the

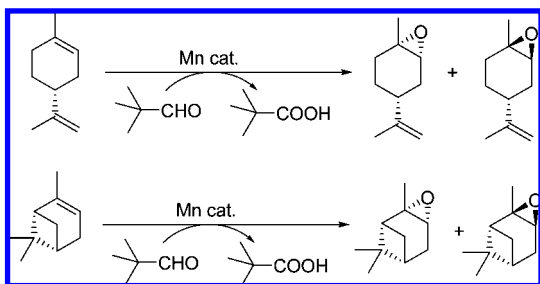


**Figure 38.** Anionic Rh and Ru complexes entrapped in a polyelectrolyte support.



**Figure 39.** Disulfonated (salen)Mn complex intercalated between LDH layers.

### Scheme 23



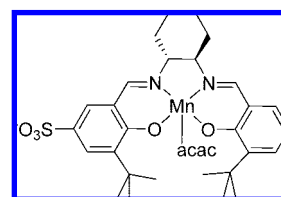
complex occurred during intercalation. XRD pattern of exchanged material showed that the basal spacing increased from 15.22 to 18.78 Å, which suggested the successful intercalation of the complex with the possible configuration shown in Figure 39.<sup>104–106</sup> However theoretical calculations showed that the catalysts presented smaller *d* spacings than required to locate a perpendicularly orientated Mn complex.<sup>106</sup> Although it would be possible for the complex to adopt such an orientation by penetration of the sulfonate groups into the layers, a different orientation with an angle lower than 90° was also suggested.<sup>106</sup>

The catalyst were tested in the oxidations of (*R*)-(+)-limonene<sup>104–106</sup> and (*-*)- $\alpha$ -pinene<sup>105,106</sup> with oxygen or air in the presence of a sacrificial aldehyde (Scheme 23). In the first work,<sup>104</sup> it was shown that (*R*)-(+)-limonene was efficiently converted into the (+)-*cis*-limonene-1,2-epoxide with 100% conversion, 85.6% epoxide selectivity, and 34%

**Table 9. Results from the Epoxidation of Different Alkenes with Anionic Mn(salen) Supported on LDH<sup>a</sup>**

Substrate	TOF (h <sup>-1</sup> )	Epoxide selectivity %	ee %
	234.2	90	68
	165.0	86	27
	360.2	70	28
	327.1	70	62
	121.8	88	18

<sup>a</sup> Data from ref 107.



**Figure 40.** Monosulfonated (salen)Mn complex.

de, using 75 psi of O<sub>2</sub>. Whereas an increase of the pressure did not modify the results, both epoxide selectivity and diastereomeric excess increased, to 89% and 55%, respectively, upon addition of *N*-methylimidazole.

Both terpenes<sup>105,106</sup> were oxidized using oxygen at atmospheric pressure and toluene as the solvent. Although high conversions (95–100%) and epoxide selectivities (87–93%) were reached in both cases, de was higher in the epoxidation of (*-*)- $\alpha$ -pinene (98% de vs up to 43% de with limonene). Furthermore the catalyst was recovered with the same behavior.<sup>105</sup> Even the change of solvent to acetone and the use of air instead of oxygen did not have an important influence on the results, although the epoxidation of (*R*)-limonene was somewhat slower using air.<sup>106</sup>

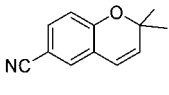
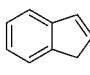
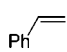
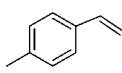
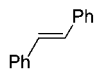
The same catalyst was used in the epoxidation of several styrene derivatives and cyclic alkenes,<sup>107</sup> using molecular oxygen at atmospheric pressure and room temperature, in the presence of pivalaldehyde (Table 9).

Results were dependent on the structure of the alkene. TOF decreased in the order:  $\alpha$ -methylstyrene > 4-methylstyrene > styrene and 1-methylcyclohexene > 1-phenylcyclohexene > cyclohexene. Epoxide selectivity was higher for cycloalkenes, and the enantioselectivity was low to moderate; the highest values were obtained with  $\alpha$ -methylstyrene and 1-methylcyclohexene. No evidence for leaching or catalyst decomposition were observed; in fact catalyst was reused in all the reactions, up to three times, with almost identical performance.

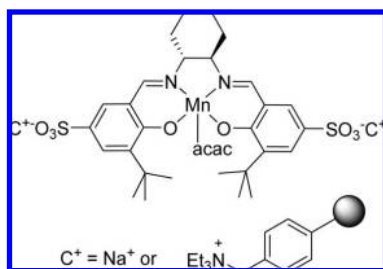
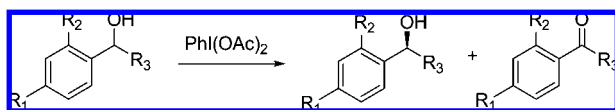
More recently Choudary et al.<sup>108</sup> compared a closely related Mn(salen) catalyst (A) (Figure 40) immobilized by hydrogen bond (as shown by IR) to silica (B), by electrostatic interaction onto a Mg–Al LDH (C), or on a Merrifield resin modified with triethylammonium groups (D). The catalysts were compared in the *m*-CPBA oxidation of various alkenes (Table 10).

Except the catalyst immobilized on silica (B), solid catalysts were more active and more enantioselective than

**Table 10. Results Obtained from the Epoxidation of Different Alkenes with *m*-CPBA Catalyzed by Monosulfonated (Salen)Mn Complex<sup>b</sup>**

Substrate	Catalyst	Time (min)	Yield %	ee %
	A	<5	100 (75) <sup>a</sup>	89 (56) <sup>a</sup>
	B	<5	100 (79) <sup>a</sup>	95 (45) <sup>a</sup>
	C	<5	100 (92) <sup>a</sup>	94 (93) <sup>a</sup>
	D	<5	100 (90) <sup>a</sup>	96 (96) <sup>a</sup>
	A	<10	100	92
	B	<10	100	94
	C	<5	100	93
	D	<5	100	97
	A	<10	100	25
	B	10	100	40
	C	<5	100	44
	D	<5	100	48
	A	<10	100	26
	B	10	100	30
	C	<5	100	31
	D	<5	100	33
	A	60	100	18
	B	120	100	42
	C	<5	100	29
	D	<5	100	35

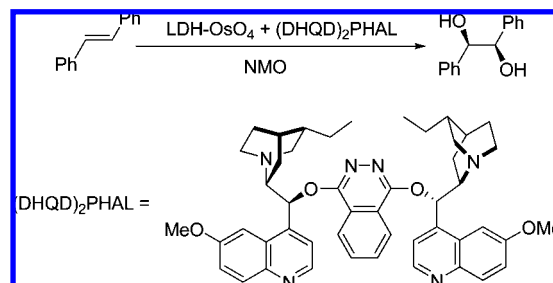
<sup>a</sup> Values corresponding to the fourth reaction. <sup>b</sup> Data from ref 108.

**Figure 41.** Homogeneous and supported disulfonated (salen)Mn catalyst.**Scheme 24**

catalyst A, which was explained by the spatial constraints imposed by immobilization. Whereas the silica catalyst showed an important leaching of metal, this was negligible for the catalysts immobilized by strong electrostatic interactions; therefore the later catalysts were recovered with the same enantioselectivity and only slight decreases in activity.

The same group used a  $[(^-O_3S)_2\text{salen}]\text{Mn}$  catalyst, immobilized by electrostatic interactions on an ammonium-modified Merrifield resin (Figure 41) as catalyst for the oxidative kinetic resolution of secondary alcohols in water (Scheme 24).<sup>109</sup>

Solvent had a noticeable influence on the results, as shown in the kinetic resolution of 1-phenylethanol. In this reaction, 38% ee was obtained in homogeneous phase, whereas low

**Scheme 25**

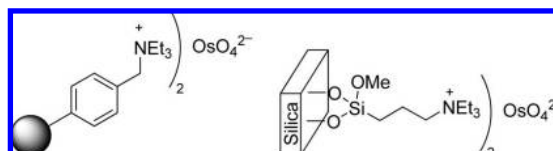
values or even no enantioselectivity at all were obtained with most of organic solvents tested, either alone or in aqueous mixtures. Enantioselectivity increased with various additives, reaching 55% ee with KBr. The scope of the reaction was studied with both soluble and immobilized catalysts. Whereas substitution in the 4-position of the aromatic ring only showed a slight influence on the results, substitution in position 2 or longer R<sub>3</sub> chains were highly detrimental. The best results were obtained with cyclic alcohols, up to 96% ee with 1,2,3,4-tetrahydro-1-naphthol. In all cases, the immobilized catalyst led to enantioselectivities 1–4% lower than the homogeneous counterpart. Filtration experiments, as well as analysis of the filtrate, showed the heterogeneous character of the reaction, allowing three reuses with the same results.

Following a closely related strategy osmate anions have been immobilized onto cationic supports. In a first report,  $\text{OsO}_4^{2-}$  was immobilized on Mg–Al LDH, and onto tetraalkylammonium groups bound to silica and resin supports.<sup>110</sup> IR and UV-DRS indicated that osmate was unaffected, whereas the  $d_{001}$  basal spacing of the LDH, determined by XRD, remained unchanged after anion exchange, so that  $\text{OsO}_4^{2-}$  was mainly located in edge positions.

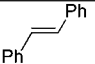
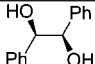
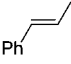
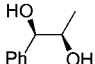
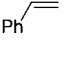
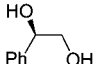
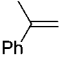
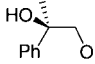
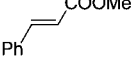
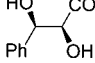
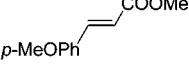
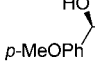
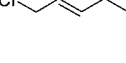
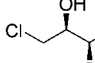
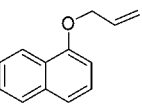
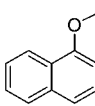
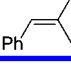
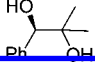
In a catalytic experiment, *trans*-stilbene was added to a mixture of  $\text{LDH}-\text{OsO}_4^{2-}$ , 1,4-bis-(9-dihydroquinidyl)phthalazine (DHQD)<sub>2</sub>-PHAL, and *N*-methylmorpholine *N*-oxide (NMO); the diol was obtained with 96% yield and 99% ee (Scheme 25). Similar excellent results were obtained with the osmate immobilized onto tetraalkylammonium-functionalized silica and resin (Figure 42). Excellent results were obtained with other olefins and the LDH catalyst, provided slow addition was warranted (Table 11).

The LDH–OsO<sub>4</sub> catalyst was quantitatively recovered by simple filtration and the chiral ligand by acid/base extraction. The recovered catalyst was used, with addition of chiral ligand, and consistent activity was observed after the fifth cycle. Os leaching was not detected. The influence of the composition of the M(II)–Al LDH (M = Mg, Ni), the interlayer anion, and  $\text{OsO}_4^{2-}$  loading were studied<sup>111</sup> in the non-asymmetric reaction. Regarding enantioselectivity, the solvent had a slight influence on it, the best ee in the oxidation of *trans*-stilbene was obtained with <sup>t</sup>BuOH/H<sub>2</sub>O.

The role of the oxidant was examined in the oxidation of  $\alpha$ -methylstyrene. LDH–OsO<sub>4</sub> showed an excellent activity for several cycles using NMO as the co-oxidant, but rapid

**Figure 42.** Immobilized osmate species on cationic supports.

**Table 11. Results from Enantioselective Dihydroxylation of Alkenes with  $\text{OsO}_4^{2-}$  Supported on LDH in the Presence of  $(\text{DHQD})_2\text{-PHAL}^a$** 

Substrate	Diol	Yield %	ee %
		96	99
		97	97
		94	95
		89	90
		96	99
		93	99
		90	82
		94	77
		92	91

<sup>a</sup> Data from ref 110.

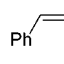
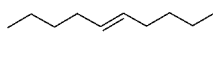
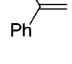
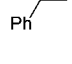
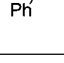
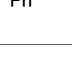
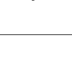
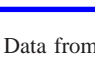
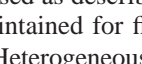
deactivation was observed using  $\text{K}_3\text{Fe}(\text{CN})_6$  or oxygen as the co-oxidants. This result was attributed to the displacement of  $\text{OsO}_4^{2-}$  by ferricyanide and ferrocyanide in the case of  $\text{K}_3\text{Fe}(\text{CN})_6$  or by phosphate anion from the phosphate buffer used in the case of oxygen.

In an attempt to overcome this serious limitation, an ammonium resin and an ammonium silica were used as osmate supports, in the belief that these anion exchangers would prefer divalent over trivalent anions (Figure 42).

In fact both solids showed consistent performance for various cycles in the oxidation of  $\alpha$ -methylstyrene irrespective of the co-oxidant used. Due to swelling properties, the resin displayed higher activity, and it was explored in the asymmetric reaction with 1 mol % resin- $\text{OsO}_4$  and 1 mol %  $(\text{DHQD})_2\text{PHAL}$  (Table 12). Conditions had to be adjusted for each co-oxidant, so with NMO, slow addition of the olefin was necessary to reach higher enantioselectivities. This slow addition was not necessary with the system  $\text{K}_3\text{Fe}(\text{CN})_6/\text{K}_2\text{CO}_3/\text{OsO}_4$ . With oxygen, maximum yield was obtained at pH = 10.4 and 40–50 °C. With NMO and  $\text{K}_3\text{Fe}(\text{CN})_6$  excellent yields and enantioselectivities were obtained with all the olefins, but in the case of trisubstituted olefins, an additive (tetraethylammonium acetate (TEAA) or  $\text{CH}_3\text{SO}_2\text{NH}_2$ ) was added to accelerate the hydrolysis of osmate ester. In the case of oxygen results were good for aliphatic olefins and aromatic olefins without  $\alpha$ -hydrogen, due to the over oxidation of the obtained benzyl alcohols.

It is important to note that an increase in the L\*/Os ratio did not lead to any improvement of the % ee of the diol. No leaching of Os was observed during or at the end of the reactions. Catalyst and chiral ligand were recovered and

**Table 12. Results from Enantioselective Dihydroxylation of Alkenes with  $\text{OsO}_4^{2-}$  Supported on Tetraalkylammonium Resin in the Presence of  $(\text{DHQD})_2\text{-PHAL}^a$** 

Substrate	Oxidant	Yield %	ee %
	NMO	92	95
	$\text{K}_3\text{Fe}(\text{CN})_6$	89	97
	$\text{O}_2$	50	89
	NMO	94	67
	$\text{K}_3\text{Fe}(\text{CN})_6$	92	95
	$\text{O}_2$	91	88
	NMO	93	91
	$\text{K}_3\text{Fe}(\text{CN})_6$	92	93
	$\text{O}_2$	99	84
	NMO	92	99
	$\text{K}_3\text{Fe}(\text{CN})_6$	91	99
	$\text{O}_2$	17	91
	NMO	95	96
	$\text{K}_3\text{Fe}(\text{CN})_6$	92	98
	$\text{O}_2$	47	86
	NMO	95	92
	$\text{K}_3\text{Fe}(\text{CN})_6$	90	92
	$\text{O}_2$	53	87
	NMO	90	91
	$\text{K}_3\text{Fe}(\text{CN})_6$	88	99
	$\text{O}_2$	80	90
	NMO	94	98
	$\text{K}_3\text{Fe}(\text{CN})_6$	92	99
	$\text{O}_2$	-	-
	NMO	-	-

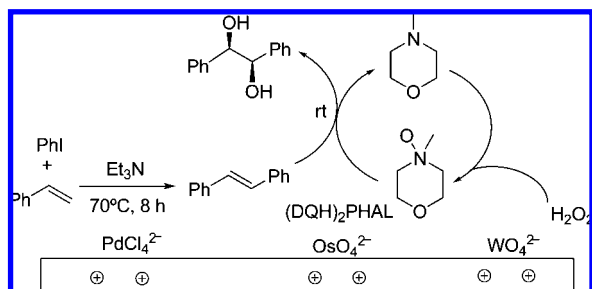
<sup>a</sup> Data from ref 111.

reused as described above, and activity and selectivity were maintained for five cycles.

Heterogeneous bifunctional  $\text{OsO}_4^{2-}-\text{WO}_4^{2-}$  and trifunctional  $\text{OsO}_4^{2-}-\text{WO}_4^{2-}-\text{PdCl}_4^{2-}$  catalysts were prepared by ion exchange using MgAl LDH, leading to LDH- $\text{OsW}$  and LDH- $\text{OsWPd}$ , respectively.<sup>112</sup> FTIR and UV spectra indicated that the divalent anions were unaffected and were anchored to the LDH support in their monomeric forms. XRD showed that basal spacing remained unchanged after anion exchange, which indicated the location of the divalent anions on the external positions of the LDH. The bifunctional catalysts (LDH- $\text{OsW}$ ) were tested in the one-pot dihydroxylation of *trans*-stilbene using NMO generated by the in situ oxidation of *N*-methylmorpholine (NMM) with  $\text{H}_2\text{O}_2$ , affording higher yields than the homogeneous system or the biphasic catalyst immobilization by interaction with quaternary ammonium salts covalently bound to a resin or to silica.

Both LDH- $\text{OsW}$  and the homogeneous  $\text{K}_2\text{OsO}_4-\text{Na}_2\text{WO}_4$  system were efficient in the simultaneous *N*-oxidation of NMM and asymmetric dihydroxylation using the Sharpless  $(\text{DHQD})_2\text{PHAL}$  ligand (Scheme 26). Mono- and disubstituted olefins (Table 13) were dihydroxylated with high yields and enantioselectivity. The presence of tetraethylammonium acetate was necessary in the case of trisubstituted olefins, due to the slower hydrolysis of the corresponding osmate esters. Similar yields and enantioselectivities

Scheme 26

Table 13. Selected Results from the Asymmetric Dihydroxylation with the LDH–OsW/NMM/H<sub>2</sub>O<sub>2</sub> System<sup>b</sup>

Alkene	Run	Yield (%)	Ee (%)
	1	92	96
	1	93	99
	1	89 <sup>a</sup>	91 <sup>a</sup>
	1	92	99
	5	90	99

<sup>a</sup> Two equivalents of tetraethylammonium acetate added. <sup>b</sup> Data from ref 112.

were obtained with both homogeneous and heterogeneous catalysts, although the former needed longer reaction times. Being water soluble, the homogeneous composite catalyst could be easily separated from the organic phase and reused, whereas recovery of the heterogeneous catalyst was carried out by simple filtration. Both catalysts were reused for five cycles with almost the same results. The main advantage of the heterogeneous system was the excellent enantioselectivities obtained with an equimolar ligand to Os ratio, whereas a large excess of ligand (3 equiv) was used to obtain the optimum enantioselectivity in the homogeneous phase.

The trifunctional LDH–OsWPd catalyst was tested in a tandem Heck/N-oxidation/asymmetric dihydroxylation reaction system (Scheme 26). This strategy proved to be useful with several alkyl halides and olefins (Table 14). The LDH–OsWPd catalyst was quantitatively recovered by filtration and the chiral ligand (>95%) by acid–base extraction. Consistent activity was observed even after the fifth cycle. This methodology was used as a first step in the synthesis of diltiazem and taxol side chains.

More recently, osmate-exchanged chloroapatite (CAP–OsO<sub>4</sub>) was used in the asymmetric dihydroxylation of alkenes.<sup>113</sup> In general, results and recyclability were similar to those obtained with LDH–OsO<sub>4</sub>,<sup>110</sup> together with the dihydroxylation of some *N*-arylacrylamides (Scheme 27).

The same LDH–OsO<sub>4</sub> catalyst<sup>110</sup> was tested in the asymmetric aminohydroxylation of olefins<sup>114</sup> (Scheme 28) and the oxidation of sulfides<sup>115</sup> (Scheme 29). In the first reaction, moderate isolated yields and enantioselectivities were obtained, with diols being formed in significant amounts. LDH–OsO<sub>4</sub> was recycled three times in the aminohydroxylation of stilbene. Although enantioselectivity was constant, the catalyst was deactivated after each cycle due to osmium leaching, with a reduction of the osmium content to 40% of the initial amount after four reactions.

Oxidation of alkyl aryl sulfides was carried out with NMO, with good yields but moderate to low enantioselectivities, lower than 51% ee in all cases (Scheme 29).

Although osmium leaching was not observed, activity decreased in the third reuse, and enantioselectivity was reduced from the first reuse, as observed in the oxidation of methyl phenyl sulfide (28%, 15%, 9%, and 4% ee).

From the examples described in this section, we can conclude that immobilization through electrostatic interactions is a simple and efficient method, very useful when complexes have a formation constant high enough to be stable under the immobilization conditions, in order to prevent the need for extra ligand addition in the reaction medium. The methodology is less attractive, from a practical point of view, when the ligands must be modified with charged groups, because the number of steps in the preparation of the immobilization complex increases. Changes in oxidation state of the metal, generation of ionic species in the catalytic process, or effects of anion on catalytic performance are some of the points to be considered when designing an immobilized catalyst using this methodology.

### 3. Coordinative Methods

In this section, we will review those methods in which the metal responsible for the catalytic activity is linked to the support by a coordinative interaction, that is, the presence of a group from the support in the coordination sphere of the metal, either saturating a positive charge or not. This can be achieved either by a direct metal–support interaction or by means of an interposed molecule, previously attached to the support, via covalent bonding. In this section, the methods that use coordination to form a solid network supporting the catalyst are also considered.

#### 3.1. Unmodified Supports as Ligands

As previously stated, in this subsection, we will consider those immobilization strategies where the catalytic metal is directly bonded to one or several atoms of the unmodified support. Of course, there are always borderline or dubious cases, where it can be discussed whether this metal–support interaction is better described as a genuine coordination interaction or as covalent bonding. Anyway, all immobilized catalytic systems comprising direct metal–support interactions are considered here.

Probably the first example of preparation of an enantioselective catalyst by direct metal–support interaction is due to Mayoral and co-workers,<sup>116</sup> who in 1996 described the grafting of a chiral aluminum catalyst to inorganic supports (silica and alumina) by means of Al–O interactions. To this end, (1*R*,2*S*,5*R*)-menthol and AlEt<sub>2</sub>Cl were made to react in several proportions and then heated in toluene under reflux in the presence of alumina or silica gel. The resulting solids were tested as catalysts in the Diels–Alder reaction of methacrolein with cyclopentadiene (Scheme 30). The best result was obtained with the silica-supported catalyst and 1:1 Al/menthol ratio at –50 °C. Under these conditions, 81% conversion, 90:10 *exo/endo* selectivity, and 31% ee in the major *exo* cycloadduct was obtained, which is comparable with the results in homogeneous phase with the same Al/menthol ratio.

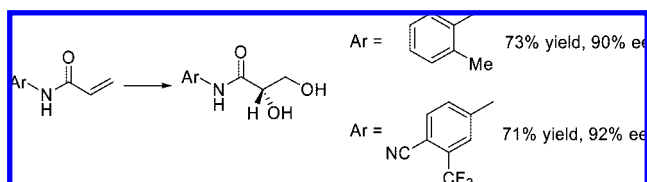
A related strategy to immobilize Lewis acid catalysts onto MCM-41 silica was described by Anwander and co-workers, first in the case of nonchiral catalysts<sup>117</sup> and subsequently

Table 14. Results of Tandem Heck/N-Oxidation/Asymmetric Dihydroxylation Reactions with LDH–OsWpd Catalyst<sup>a</sup>

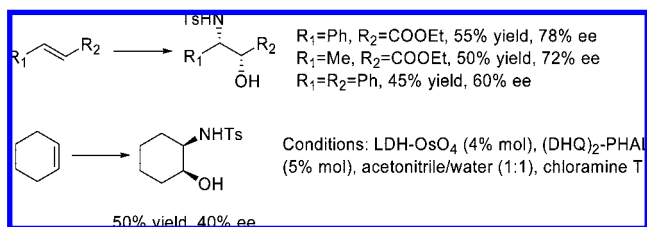
Aryl halide	Alkene	Product	Run	Yield (%)	Ee (%)
PhI			1	85	99
PhI			5	82	99
PhI			1	93	99
			1	93	99
PhI			1	92	98
PhI			1	90	47

<sup>a</sup> Data from ref 112.

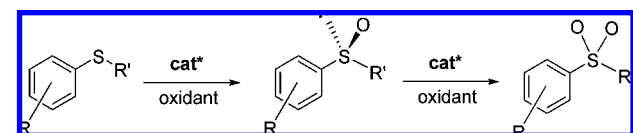
## Scheme 27



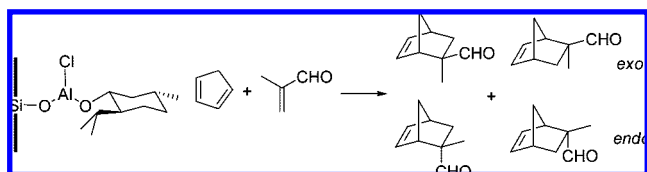
## Scheme 28



## Scheme 29



## Scheme 30



in their chiral versions.<sup>118</sup> The strategy consists of a two-step synthesis, in which silylamides are used as reactive precursors to graft  $[M\{N(\text{SiHMe}_2)_2\}_3(\text{THF})_x]$  ( $M = \text{Sc}, \text{Y}, \text{La}, \text{Al}$ ) onto the MCM-41 silica surface. Subsequent surface-confined ligand exchange  $[MCM-41]M(L)_x(\text{THF})_y$  leads to the immobilized catalysts (Scheme 31). It is worth noting that the support gets partially silanized during this process.

In the case of the nonchiral catalysts, the ligand used was fod (1,1,1,2,2,3,3-heptafluoro-7,7-dimethyl-4,6-octanedionate), whereas in the chiral versions of the catalyst, a variety of ligands were tested. In this case, only yttrium complexes were considered for catalytic tests.

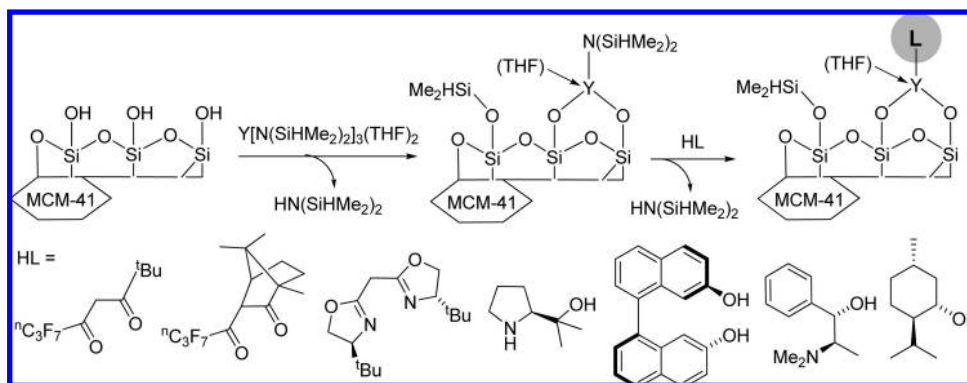
The benchmark reaction was the hetero-Diels–Alder reaction between Danishefsky diene and benzaldehyde (Scheme 32). Whereas the nonchiral catalysts showed very promising features (good activities, even better than their homogeneous counterparts, and recoverability up to six times keeping the same activity), the chiral catalysts displayed a disappointing behavior. In general, the immobilized catalysts led to diastereoselectivities similar to or lower than their homogeneous counterparts. The L-(–)-3-(perfluorobutyl)-camphor derivative  $[MCM-41]Y((-)\text{-hfc})_x(\text{THF})_y$  produced the highest diastereomeric and enantiomeric excesses (67% de, 37% ee at  $-35\text{ }^\circ\text{C}$ ). In most cases, enantioselectivities observed for the immobilized catalysts were almost zero. Another noticeable drawback of the systems tested is that all the experimental procedures are carried out in a glovebox, making difficult a wide applicability of these catalysts. Silanization of the silica support, as a result of the preparation process of the catalysts, was demonstrated to be important for the catalytic results.

Immobilization of chiral titanium complexes onto silicas by reaction of the metal with surface silanol groups has been also used to prepare oxidation catalysts. Thus, Mayoral and co-workers described for the first time the enantioselective sulfide to sulfoxide oxidation of *p*-tolyl methyl sulfide (Scheme 29), catalyzed by tartrate–Ti complexes immobilized onto silica gel (Figure 43).<sup>119</sup> Although catalyst were highly active and selective to sulfoxide production (up to 99:1 sulfoxide/sulfone product with almost quantitative conversions), only modest enantioselectivities (up to 13% ee) were obtained although some Ti leaching was observed. Both *tert*-butyl hydroperoxide (TBHP) and hydrogen peroxide ( $\text{H}_2\text{O}_2$ ) were used as oxidants.

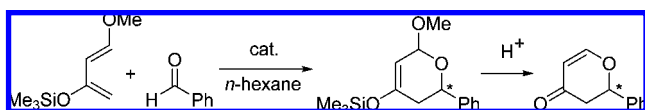
A similar strategy was described by Iwamoto and co-workers, using mesoporous MCM-41 silica as the support.<sup>120,121</sup> The chiral immobilized catalyst was prepared in a four-step



Scheme 31



Scheme 32



procedure. First, the MCM-41 was obtained by hydrothermal synthesis. Next, the metal was introduced by the template-ion-exchange method, which consists of vigorously stirring the support in the presence of an aqueous solution of a salt of the target metal. The resulting solid was calcined in air to remove the template ions. Finally, the chiral modifier was added to the solid. Preliminary studies with nonchiral catalysts showed that only Ti (TiM-41) leads to solids with enough catalytic activity toward the oxidation of phenyl methyl sulfide to the corresponding sulfoxide. The chiral catalysts were prepared by addition of (*R,R*)-tartaric acid to the TiM-41 solid (Figure 43). In most cases, these catalysts displayed low or no enantioselectivity at all. The role of factors such as oxidant and solvent were investigated. Thus,  $\text{H}_2\text{O}_2$  was preferred over TBHP, and nonoxygenated solvents, such as dichloromethane and *n*-hexane, were better than alcohols and acetonitrile, probably because of the loss of Ti ions in the presence of the later solvents. Under the best conditions, only a modest 30% ee could be obtained at high sulfide conversion, but with low sulfoxide/sulfone selectivity (60:40). A kinetic study demonstrated that this enantioselectivity was mainly due to a kinetic resolution process, in which one of the sulfoxide enantiomers reacts faster to give the sulfone, in the presence of the chiral catalyst.

A closely related family of catalyst was described by Basset and co-workers for the enantioselective epoxidation of allylic alcohols.<sup>122,123</sup> In this case, the catalytic metal was tantalum, which was supported onto silica through reaction with surface silanol groups in a two-step procedure. The chiral modifier (either diethyl tartrate, DET, or diisopropyl tartrate, DIPT) was subsequently added by impregnation of the solid (Scheme 33). Tantalum presents two advantages over titanium for the preparation of these immobilized chiral catalysts. First, its larger coordination sphere allows the simultaneous presence of the chiral modifier, the reagents, and the link to the support, which is more difficult in the

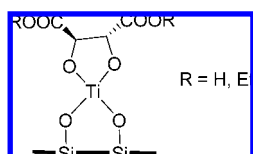


Figure 43. Proposed structure of grafted Ti-tartrate species.

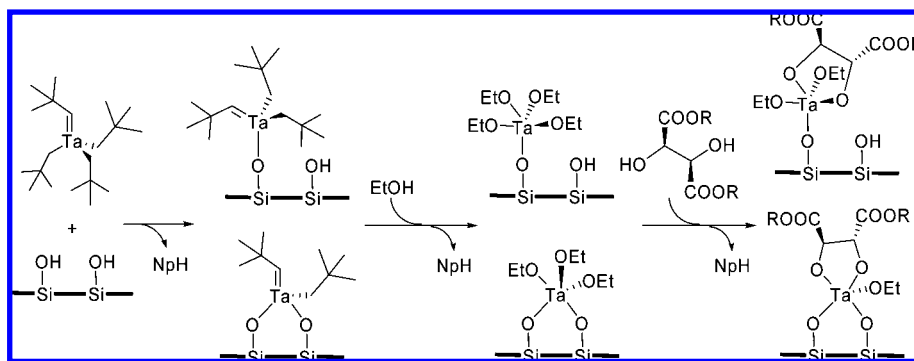
case of Ti. Second, Ta exhibits a low activity in the homogeneous phase, thus minimizing the possible effect of concurrent homogeneous catalysis by metal leaching. Site isolation of the catalytic sites in the solid was invoked to explain the greater activity of the immobilized catalyst with regard to the homogeneous counterpart.

The immobilized chiral Ta catalysts were active toward the epoxidation of allyl alcohol (up to 94% ee, but with low conversion, 20%) and (*E*)-2-hexen-1-ol (up to 93% ee with 35% conversion). The catalysts were truly heterogeneous, and no leaching (<2% of metal) and therefore no catalytic activity in filtration experiments was observed. Several factors were important to determine the activity and selectivity of these catalysts. Impregnation duration of the chiral modifier was an important factor, and long times (over 12 h) were necessary to reach the best enantioselectivities. Regarding the oxidant, the use of organic hydroperoxides (TBHP, cumyl hydroperoxide) was mandatory, since  $\text{H}_2\text{O}_2$  led to high conversions, but with no enantioselectivity under the same conditions. Poisoning effects were observed with oxygenated molecules, as water, *tert*-butanol, or some of the reaction products, for example, glycerol. All these molecules can block the catalytic sites by competitive coordination. Substrate initial concentration and metal/substrate ratio were also important factors. With an initial concentration of 1 M in allyl alcohol, enantioselectivity rises to 98% ee with a 45% conversion but with a decrease in selectivity to glycidol. This result was interpreted as a kinetic resolution effect, one of the glycidol enantiomers being hydrolyzed faster in the reaction medium. Finally, the reaction was also very sensitive to temperature. Best results are obtained at 0 and 10 °C, although in the later case, kinetic resolution effects are probably also involved (91% ee, but with only 76% selectivity to the epoxide). Unfortunately, no systematic studies of recoverability were described, and only one single experiment of reuse was reported.

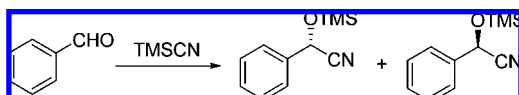
Titanium complexes supported on MCM-41 silica have also been described as efficient enantioselective catalysts for the trimethylsilylcyanation of benzaldehyde (Scheme 34) by Kim and co-workers.<sup>124</sup>

The chiral ligands employed for this reaction were salen-type ligands, both symmetrical ( $C_2$ -symmetric) and unsymmetrically substituted. The chiral salen-Ti(IV) catalysts were prepared in situ by reacting  $\text{Ti}(\text{O}^i\text{Pr})_4$  with the corresponding salen ligand, and the resulting Ti complexes being anchored over mesoporous MCM-41 silica by reflux in MeOH solution (Figure 44). The integrity of the supported complexes was demonstrated by comparing the IR and UV spectra of the homogeneous complex in solution and that anchored to the

Scheme 33



Scheme 34



MCM-41. The catalytic tests showed that the supported complexes led to almost the same conversions and enantioselectivities as the homogeneous catalysts. The best results were obtained with one of the unsymmetrical salen ligands, bearing *tert*-butyl groups in only one of the salicylaldehyde moieties, the other one remaining unsubstituted. With this ligand, 94% ee was obtained in heterogeneous conditions (90% ee in homogeneous phase). The analogous  $C_2$ -symmetric chiral ligand, bearing four *tert*-butyl groups, led to lower enantioselectivities (83% ee in heterogeneous phase and 77% ee in homogeneous phase). In a second work,<sup>125</sup> comparative studies were carried out by considering not only different salen ligands but also different supports and immobilization methods. With the same  $C_2$ -symmetric ligand, amorphous silica led to lower enantioselectivity (48% ee vs 64% ee with MCM-41), as did the immobilization by cationic exchange, using an Al-MCM-41 silica as support (43% ee). Better results were obtained by covalent bonding of the salen ligand to the support (up to 93% ee), but this strategy is out of the scope of this review. As in other studies, no recovering and reusing experiments were carried out, so the main possible advantage over homogeneous catalysis, given the similar activity and selectivity exhibited by both systems, remains unrevealed.

The same strategy of catalytic complex anchoring through metal–silanol interactions has been successfully used by Iwasawa and co-workers<sup>126</sup> to immobilize vanadium–Schiff-base complexes onto silica. The catalytic tests indicate that

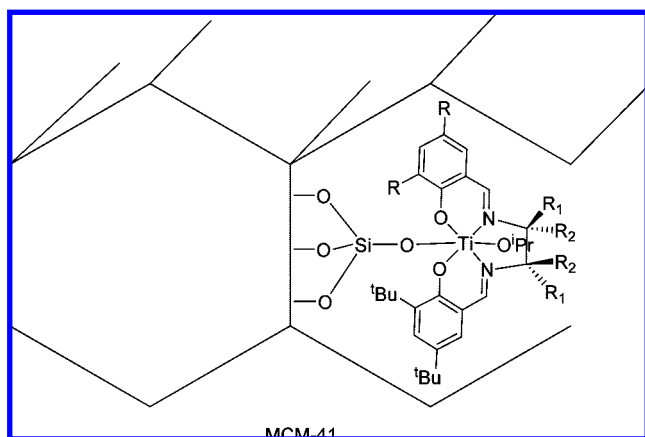
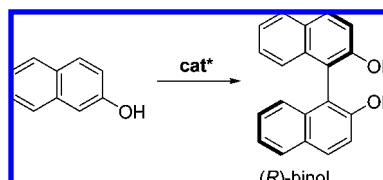


Figure 44. Grafted (salen)Ti complex.

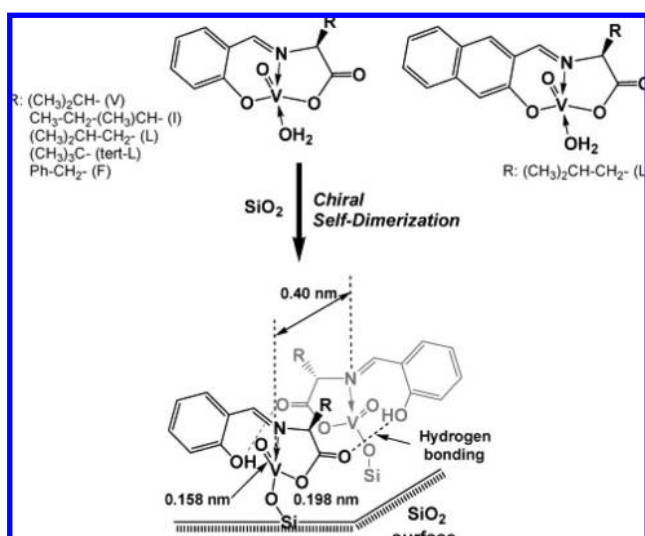
Scheme 35



the supported catalysts are active toward the asymmetric oxidative coupling reaction of 2-naphthol to give 2,2'-binaphthol (BINOL) (Scheme 35). Up to 90% enantioselectivity at 96% conversion was obtained with total chemoselectivity to BINOL when the amount of supported catalyst reached full surface coverage (3.4 wt % vanadium), as estimated by the concentration of surface silanols. Under homogeneous conditions, the same complexes do not catalyze the reaction. The best heterogeneous catalyst was reused once, keeping the same activity and enantioselectivity.

In depth spectroscopic and theoretical studies were carried out by the same group, in order to determine the exact nature of the supported catalytic centers.<sup>127</sup> The authors found new chirality creation by the self-dimerization of the vanadyl complexes on the surface. The chiral self-dimerization and the role of surface silanols in the self-assembly were investigated by means of XANES, EXAFS, DR-UV/vis, XPS, FT-IR, and ESR. The surface vanadyl complexes had a distorted square-pyramidal conformation with a V=O bond. FT-IR spectra revealed that the aryl-O moiety of Schiff-base ligands was transformed into a phenolic OH by a surface-concerted reaction between the vanadium precursors and surface silanol groups. The phenolic OH in an attached vanadyl complex interacted with a COO moiety of another vanadyl complex by hydrogen bonding to form a self-dimerized structure at the surface (Scheme 36). The self-dimerized V structure on silica was modeled by DFT calculations, which demonstrated that two vanadium monomers with phenol moieties linked together by two hydrogen bonds and their V=O groups were directed opposite to each other. The surface self-dimerization of the vanadium precursors fixes the direction of the V=O bond and the plane of the Schiff-base ligand. Thus, a new chiral reaction field was created by two types of chirality: the chiral Schiff-base ligand and the chiral V center. The latter is directly responsible for the enantioselectivity of the coupling reaction, and therefore, this constitutes one of the few examples where there is a direct influence of support effects on the stereoselectivity performance of the catalytic system.

Not only silica supports can be used for this kind of immobilization. Basic carbons present oxygen donors on their surface, able to act in the same way as silanols. These

Scheme 36<sup>a</sup>

<sup>a</sup> Reprinted with permission from ref 127. Copyright 2005 American Chemical Society.

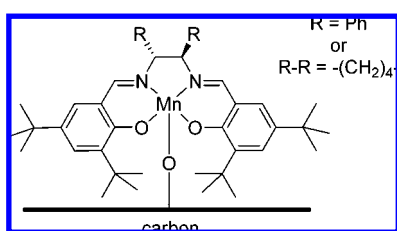


Figure 45. (Salen)Mn complexes grafted on basic carbon.

oxygenated groups were used by Silva et al. to immobilize two different (salen)Mn complexes (Figure 45) by refluxing the (salen)MnCl complex with the basic carbon in ethanol.<sup>128,129</sup> This bond may be considered as covalent, although it would resemble the phenoxide–Mn and alkoxide–Mn bonds reported by other authors.<sup>63,92,94,98</sup> However these catalysts have been included in this section to show the similarity also with the silica-bonded systems.

Epoxidation results were rather poor. In the case of styrene epoxidation with *m*-CPBA/NMO, enantioselectivity was significantly reduced from the values obtained in solution, 31% vs 45% ee with Jacobsen's catalyst, 5% vs 60% ee with ligand bearing  $R = Ph$  (Figure 45). The epoxidation of  $\alpha$ -methylstyrene with NaOCl was more efficient with regard to enantioselectivity, but catalysts were much less active, although stable upon recovery.

Barnard and co-workers described the immobilization of several [(diphosphine)Rh(nbd)] complexes via formation of a Rh–O bond (Figure 46).<sup>130</sup> [(Bophoz)Rh(nbd)]carbon and [(BDPP)Rh(nbd)]carbon were used in the enantioselective hydrogenation of dimethyl itaconate (Scheme 2), with slight but significant improvement from the enantioselectivity values obtained in solution, 91% vs 82% ee with Bophoz and 78% vs 70% ee with BDPP. The catalysts were stable along three reuses and leaching was below the detection limit of ICP, even in scaled-up experiments. [(Phanephos)-Rh(nbd)]carbon and [(xyl-phanephos)Rh(nbd)]carbon were used as catalysts in the hydrogenation of methyl 2-acetamidocrylate (Scheme 13) with excellent enantioselectivities (97–98% ee) and total conversion.

The last example of this section uses polyaniline as an organic support for the catalytic metal complex and has been

recently reported by Choudary and co-workers.<sup>131</sup> Polyaniline (PANI) has quinoid and benzenoid units along with amine and imine functional moieties, which makes it a suitable support to hold metal complexes (Scheme 37). Although several PANI-supported metal catalysts were described in this work, the only enantioselective catalysts involved osmium and rhenium. Thus,  $OsO_4$  was immobilized onto PANI, and the resulting material (PANI–Os) was characterized by FT-IR, UV–vis, and XPS. Methyl-trioxorhenium ( $MeReO_3$ ) was similarly immobilized to give PANI–Re. PANI–Os was tested as catalyst in the Sharpless asymmetric dihydroxylation of (*E*)-stilbene, using *N*-methylmorpholine *N*-oxide (NMO) as the oxidant and 1,4-bis(9-*O*-dihydroxyquinidyl)phthalazine [(DHQD)<sub>2</sub>PHAL] as the chiral modifier. The corresponding diol was obtained in 91% yield and 99% ee. Other olefins were also dihydroxylated with the same catalytic system, with good conversions (over 90%) and moderate to excellent enantioselectivities (Table 15).

$H_2O_2$  was also tested as co-oxidant, first using the PANI–Os–Re catalyst. The results obtained in the dihydroxylation of (*E*)-stilbene were also excellent (83% yield and 98% ee) and comparable to those previously described in homogeneous phase. When PANI–Os and PANI–Re were tested separately in the same reaction, the same results were obtained, disregarding any synergistic effect between Os and Re. Finally, possible metal leaching and recoverability of the catalysts were also investigated. The ICP-AES analysis of the reaction mixture did not detect the presence of Os or Re in solution. Furthermore, PANI–Os and PANI–Os–Re were recovered and used in five consecutive reactions, leading to the same yields and enantioselectivities. It must be mentioned that the chiral modifier can be recovered from the aqueous phase in the treatment of the reaction mixture, so that in each reuse, fresh chiral modifier must be added, which makes the reuse procedure less attractive.

### 3.2. Metal–Organic Frameworks

A totally different immobilization strategy is that described by Lin and co-workers,<sup>132</sup> that consists in the creation of a catalytically active chiral porous metal–organic framework (MOF), by using chiral bridging ligands containing orthogonal functional groups. The primary functional groups can be linked by metal-connecting units to form extended networks, whereas the orthogonal secondary functional groups can be used to generate the catalytic sites. Compared with other immobilization strategies, this methodology allows the preparation of asymmetric catalysts with high catalyst loading and more accessible catalytic centers. The bridging axially chiral ligand used in this work was 6,6'-dichloro-2,2'-dihydroxy-4,4'-di(4-pyridyl)-1,1'-binaphthyl (Figure 47).

By reaction of this ligand with  $CdCl_2$ , the MOF structure is obtained, in the form of colorless crystals. Cd(II) centers are octahedrally coordinated, and doubly bridged by chlorides to form zigzag chains that serve as secondary building units (Figure 48). The resulting structure has large chiral channels of 1.6–1.8 nm cross-section. Two of the three chiral ligands in the unit cell pair up are shielded by the naphthyl rings, so that only a third of the diol groups are available to form the catalytic sites, and point toward the chiral channels. The solid possesses a permanent porosity with a high specific surface area ( $> 600 \text{ m}^2 \text{ g}^{-1}$ ). The catalytically active solid was prepared by reaction with  $Ti(O^iPr)_4$ , and the resulting chiral catalyst was used in the  $ZnEt_2$  addition reaction to aromatic

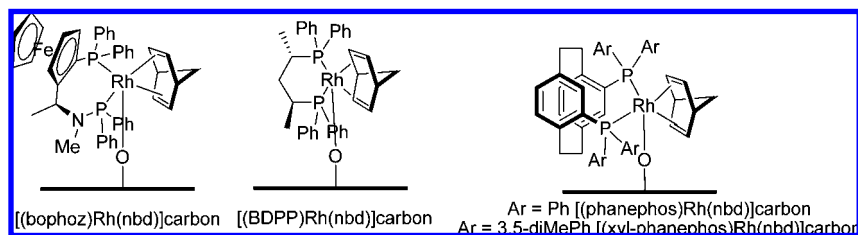


Figure 46. [(Diphosphine)Rh(nbd)] complexes grafted on basic carbon.

Scheme 37

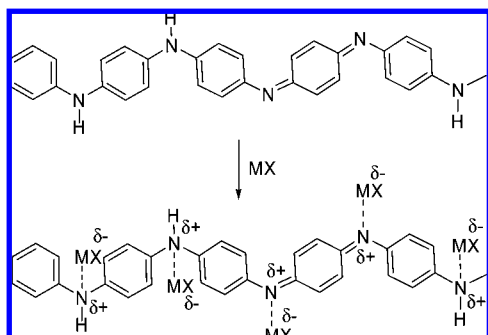


Table 15. Asymmetric Dihydroxylation of Olefins Using PANI-Os<sup>a</sup> and PANI-Os-Re<sup>b</sup> Catalysts<sup>c</sup>

Olefin	Isolated yield (%)	ee (%)
Ph-CH=CH-Ph	91 <sup>a</sup>	99 <sup>a</sup>
	83 <sup>b</sup>	98 <sup>b</sup>
p-MeOC <sub>6</sub> H <sub>4</sub> -CH=CH-COOEt	93 <sup>a</sup>	97 <sup>a</sup>
	91 <sup>a</sup>	86 <sup>a</sup>
Ph-CH=CH-COOMe	94 <sup>b</sup>	98 <sup>b</sup>
	94 <sup>a</sup>	86 <sup>a</sup>
Ph-CH=CH-Me	84 <sup>b</sup>	85 <sup>b</sup>
	93 <sup>a</sup>	73 <sup>a</sup>
Ph-C(=CH <sub>2</sub> )-Me	83	73 <sup>b</sup>
	93 <sup>a</sup>	71 <sup>a</sup>
Ph-CH=CH-Me	88 <sup>b</sup>	73 <sup>b</sup>
	90 <sup>a</sup>	62 <sup>a</sup>

<sup>a</sup> NMO as oxidant and (DHDQ)<sub>2</sub>PHAL as chiral modifier. <sup>b</sup> H<sub>2</sub>O<sub>2</sub> as oxidant and (DHDQ)<sub>2</sub>PHAL as chiral modifier. <sup>c</sup> Data from ref 131.

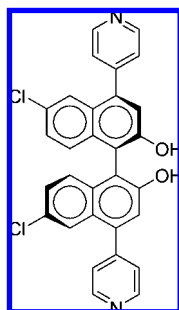


Figure 47. Bridging ligand to form chiral MOF.

aldehydes. With 1-naphthaldehyde and several benzaldehydes, total conversion and good enantioselectivities (80–93% ee) were obtained. These results were similar to those obtained in homogeneous conditions with the

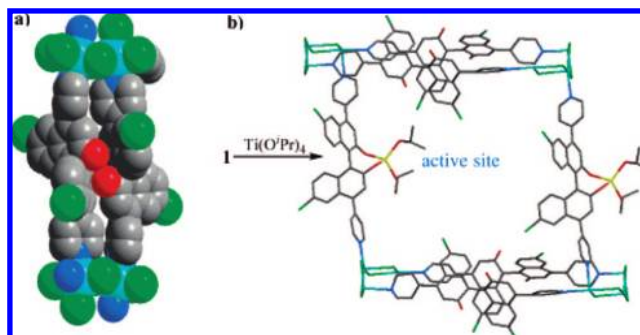


Figure 48. Schematic representation of the active (BINOLate)Ti(O<sup>i</sup>Pr)<sub>2</sub> catalytic sites in the open channels of the MOF. Cyan, green, red, blue, gray, and yellow represent Cd, Cl, O, N, C, and Ti atoms, respectively. Reprinted with permission from ref 132. Copyright 2005 American Chemical Society.

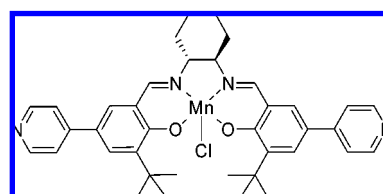
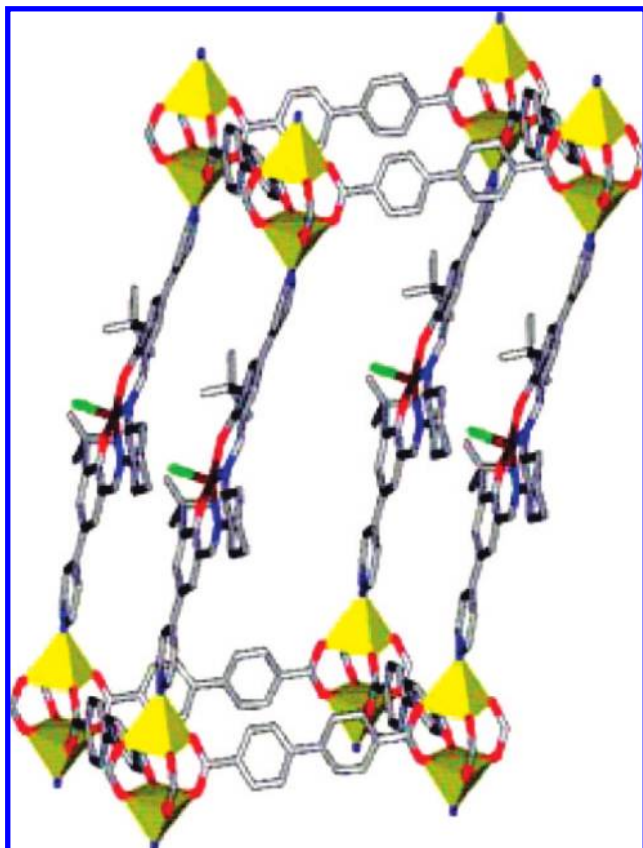


Figure 49. Salen ligand used to form a metal–organic framework (MOF).

BINOL–Ti(O<sup>i</sup>Pr)<sub>2</sub> complex. The catalyst was truly heterogeneous, since a supernatant solution of the reaction medium containing the immobilized catalyst did not show any activity. The use of bulkier substrates (dendritic aromatic aldehydes) allowed determination of the influence of the pore size on the catalytic activity. Thus, as the dendron size increased, the yield of the addition product steadily decreased, and no product was observed with the largest aldehyde, whose estimated size (~2.0 nm) exceeds the pore size of the catalyst. As in other studies of immobilized enantioselective catalyst, no recovery experiments were described by the authors. No metal leaching measurements were carried out either, a question particularly important being given the environmental and toxicological hazards of cadmium.

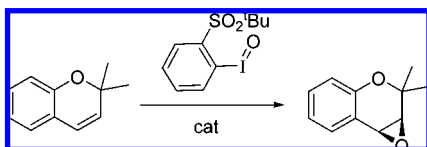
A similar approach has been also recently described by Hupp, Nguyen, and co-workers.<sup>133</sup> In this case, the chiral unit was a salen complex, *N,N'*-bis(3-*tert*-butyl-5-(4-pyridyl)salicylidene)[(*R,R*)-1,2-cyclohexanediamine]Mn<sup>III</sup>Cl (Figure 49), where the primary functional groups responsible for the MOF structure were the pyridine rings. Given that the MOF structure obtained by treatment with Zn(NO<sub>3</sub>)<sub>2</sub>·6H<sub>2</sub>O collapsed upon evacuation, a more robust pillared paddlewheel structure was obtained by addition of a second ligand, biphenyldicarboxylate (Figure 50).

In this case, all the Mn centers were available for catalysis. The resulting solid was tested in the asymmetric epoxidation



**Figure 50.** A POV-Ray view of the paddlewheel structure. Yellow polyhedra represent the zinc ions. Carbon, gray; oxygen, red; nitrogen, blue; chloride, green; manganese, brown. Reprinted by permission of the Royal Society of Chemistry, ref 133.

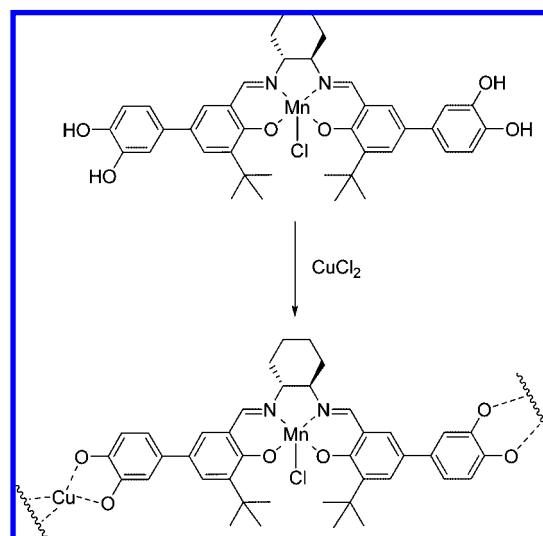
**Scheme 38**



reaction of 2,2-dimethyl-2H-chromene with 2-(*tert*-butylsulfonyl)iodosylbenzene (Scheme 38).

When compared with the homogeneous salen–Mn catalyst, the heterogeneous catalyst led to similar enantioselectivity (82% ee vs 88% ee), but more importantly, it displayed close to constant activity, in contrast with the homogeneous catalyst, which deactivates after 1 h. This resulted in higher total TON for the immobilized system. This behavior is probably due to the rigid structure of the catalytic complex, which avoids oxidation of the salen ligand by cross-reaction between two catalyst molecules. In this case, catalyst recovery and reuse was tested, and it was shown that at least three catalytic cycles can be achieved without loss of catalytic activity or enantioselectivity. Recycling was accompanied by MOF particle fragmentation. Analysis of the product solution by ICP showed that between 4% and 7% of the manganese was lost per cycle. Anyway, measurements of reaction progress after removal of MOF particles by filtration established that the remaining small quantity of dissolved manganese did not catalyze the reaction. Competitive size selectivity studies were performed, using a large porphyrin substrate and a smaller one, ethyl 4-vinylbenzoate, in 1:1 ratio, to check whether catalysis occurs predominantly within the channels of the MOF or on the external surface. The

**Scheme 39**

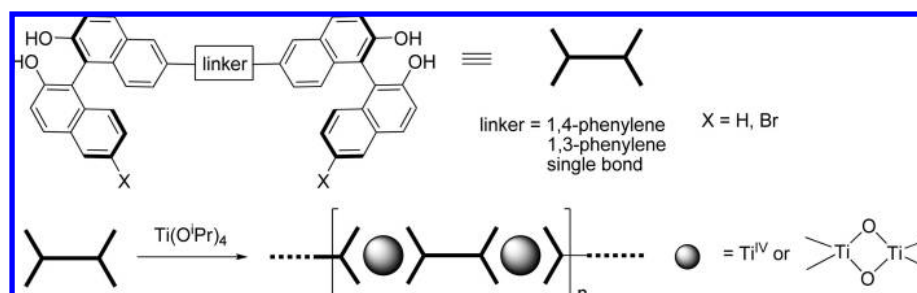


ratio of small to large substrate reactivity increased from 2 in the initial stage of the reaction to  $\sim 18$  at 45% conversion, indicating that at the beginning a significant fraction of the catalysis occurs on the MOF surface, but at later stages catalysis occurs chiefly within the MOF channels.

To improve the recoverability of these kinds of catalysts, by avoiding the MOF crystal fragmentation, the same authors tested amorphous coordination polymers formed by coordination polymerization of [bis(catechol)-salen]Mn with  $\text{CuCl}_2$  (Scheme 39).<sup>134</sup>

The coordination polymer thus formed was insoluble in a wide range of organic solvents (such as toluene, methanol, DMF, and DMSO) and water. Inductively coupled plasma (ICP) mass spectrometric measurements yielded a Mn/Cu ratio of ca. 1:1.1, suggesting a quasi-one-dimensional structure for the coordination polymer, in which salen moieties are connected by bis(catecholate)copper linkages. This polymer was tested as catalyst in the epoxidation of 2,2-dimethyl-2H-chromene with 2-(*tert*-butylsulfonyl)iodosylbenzene (Scheme 38). Although a slightly lower enantioselectivity was observed, relative to the homogeneous [bis(dimethoxyphenyl)salen]Mn complex (76% vs 86% ee), their epoxidation activities were comparable. This enantioselectivity decrease seemed to be related to structural constraints resulting from the immobilization. Indeed, when the polymer was dissolved in the presence of pyrocatechol and used as catalyst in the resulting homogeneous phase, the enantioselectivity increased up to 82% ee, closer to the value obtained with the homogeneous analogue. In the heterogeneous catalytic reactions, the coordination polymer was easily recovered by centrifugation and washing and reused in consecutive catalytic runs. The catalyst can be recycled up to ten times with little loss in activity (from 79% to 70% yield) and no loss in enantioselectivity (75–76% ee). Analyses of the metal leaching by ICP mass spectrometry revealed that most of the Mn and Cu leaching takes place in the first two cycles (4.7% of Cu and 3.1% of Mn). Comparative studies of the heterogeneous vs homogeneous catalysts were also carried out under high-oxidant conditions (ca. 13 times the concentration used in the normal experiments). The homogeneous catalyst was initially highly effective; however, it lost much of its activity after the first few minutes and completely deactivated in less than 0.5 h. In contrast, the heterogeneous catalyst exhibited a longer

Scheme 40



lifetime ( $>3$  h), with an enantioselectivity consistent throughout the reaction and a total turnover number (TON) greater than 2000 within 3 h (only 600 in the case of the homogeneous catalyst). On the other hand, the recoverability of this solid was not as good as that observed in the previous experiments, indicating that the high-oxidant conditions can facilitate catalyst degradation. Finally, other metals different from Cu(II) can also be used to obtain the coordination polymers. Using Cr(III), Cd(II), and Mg(II) led to polymers with similar catalytic performances (both in activity and in enantioselectivity), whereas other metals were clearly inferior (for instance, Fe(III) and Ni(II)).

In the preceding examples, the support is formed at the same time as the insoluble catalytic species, with the help of some auxiliaries, such as a second metal or ligand, necessary to build the MOF or the coordination polymer. In this sense, this strategy would be similar to a copolymerization using monomers different from those bearing the chiral ligand or to a sol-gel synthesis of a hybrid organic-inorganic catalytic material. Following this analogy, the homopolymerization of monomers bearing the chiral ligand would also find a counterpart in the self-support of a catalyst through the formation of a coordination homopolymer. This is a relatively new strategy, which has been exploited in the last years primarily by Ding and co-workers.<sup>135</sup> Since this strategy lacks of a true support and goes beyond the scope of this review, we will only summarize some of the most relevant results obtained with this approach.

Thus, different ditopic BINOL chiral ligands have been used to form coordination polymers with different metals, being applied to a variety of enantioselective organic reactions. For instance, the heterogenization of chiral titanium complexes by in situ assembly of bridged multitopic BINOL ligands with  $\text{Ti}(\text{O}^i\text{Pr})_4$  was carried out by these and other groups (Scheme 40), and the resulting solids were tested in

the carbonyl-ene reaction of  $\alpha$ -methyl styrene with methyl glyoxylate (Scheme 17).<sup>136–138</sup> Both the BINOL unit/Ti ratio and the spacer between two BINOL units were found to have significant impact on the catalytic results of this reaction. In general, good yields (up to 99%) and enantioselectivities (95–98% ee) were obtained with these catalysts. Upon completion, simple filtration of the reaction mixture allows the separation of the solid catalyst, which can be reused in further reactions. Recycling experiments showed that the catalyst can be used for five cycles with gradually decreased activity (from 87% to 70% yield) and enantioselectivity (from 97% to 79% ee).

Similar catalysts were also tested in the asymmetric sulfoxidation of sulfides with cumyl hydroperoxide (CMHP) (Scheme 29).<sup>138</sup> In general, chiral sulfoxides were obtained with very high enantioselectivities (from 96.4% to  $>99.9\%$  ee) in moderated yields (ca. 40%). Furthermore, no leaching of Ti was detected ( $<0.1$  ppm) by ICP spectroscopic analysis of the supernatant organic solution, and recycling experiments could be carried out for eight cycles without loss of enantioselectivity or activity.

The stereochemical characteristics of the multitopic ligands should, in principle, influence the microstructures of the metal-organic polymers, and hence they may have a substantial impact on the catalytic results obtained with such polymers. This influence was studied by varying the nature of the bridging spacers in the case of the heterogenization of Shibasaki's lanthanum catalysts (Figure 51).<sup>139</sup> Up to four types of multitopic ligands containing different bridging linkers (including linear, angular, trigonal planar, and tetrahedral spacers) were prepared, and the corresponding lanthanum complexes were tested as catalysts in the enantioselective epoxidation of  $\alpha,\beta$ -unsaturated ketones with CMHP (Scheme 41).

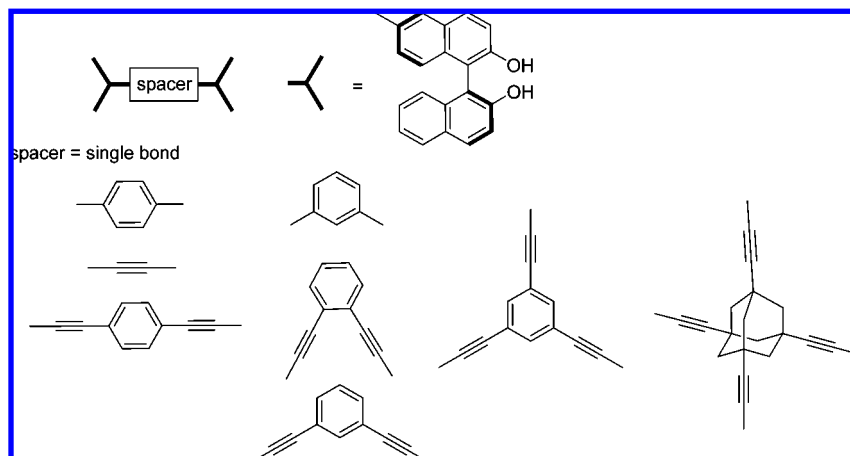
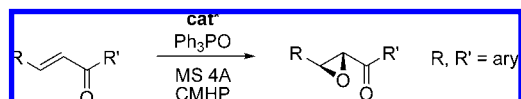
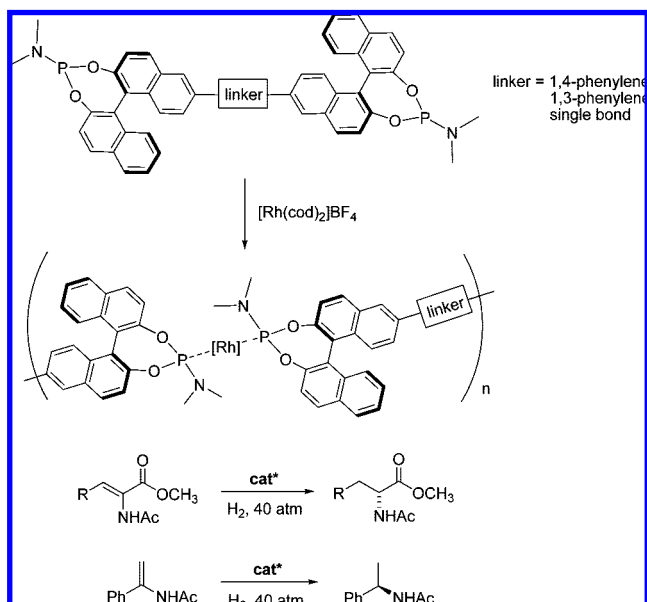


Figure 51. Structural variations of self-supported BINOL-La complexes.

## Scheme 41



## Scheme 42



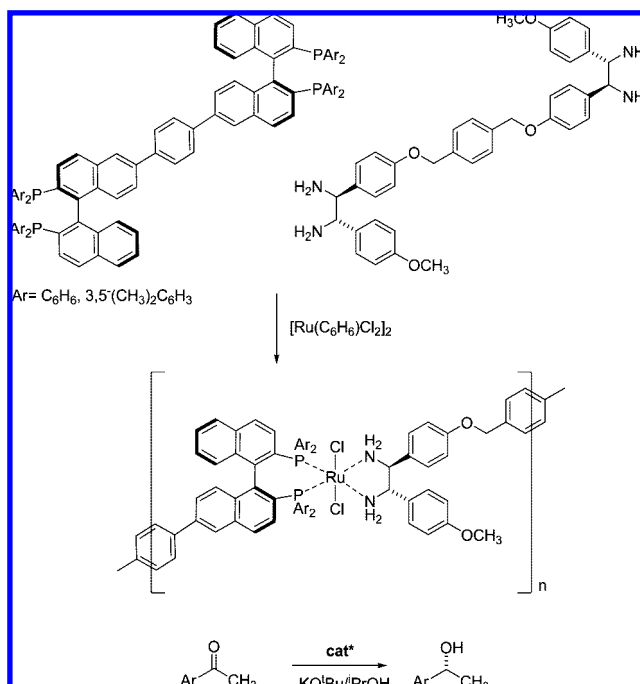
Under optimized reaction conditions, excellent yields in epoxide (91–99%) were obtained in all cases, as well as high enantioselectivities (85–98% ee). Lower enantioselectivities (ca. 84% ee) corresponded to the shortest linear spacer (a single bond between the two BINOL moieties) and to the angular spacer with the most acute angle (the *ortho*-di(eth-1-ynyl)benzene). Otherwise, it seems that if the BINOL groups are sufficiently far apart from each other, the resulting catalyst is excellent for these reactions, irrespective of the topology of the multitopic ligand. Recycling experiments were carried out with one of the catalysts bearing a linear spacer (the *para*-di(eth-1-ynyl)benzene). The corresponding lanthanum catalyst could be recycled at least six times without significant loss of activity or enantioselectivity. The lanthanum leaching in each run was determined to be less than 0.4 ppm by ICP analysis. Finally, the heterogeneous character of these catalysts was tested by the absence of activity of the supernatant solution under the same experimental conditions.

Self-supported MonoPhos–Rh(I) catalysts were prepared in a similar way and tested in enantioselective hydrogenations reactions of dehydro- $\alpha$ -amino acid and enamide derivatives (Scheme 42).<sup>138</sup>

In all cases, high yields (>99%) and enantioselectivities, comparable to those obtained with homogeneous catalysis at the same level of catalyst loading (1% mol), were observed. In particular, the self-supported catalysts demonstrated remarkably improved enantioselectivity (95–97% ee) in the hydrogenation of the enamide derivative in comparison with homogeneous catalysis using a MonoPhos–Rh(I) complex (88% ee). The catalysts could be readily recycled and efficiently reused for at least seven runs.

Variants on this self-supporting strategy have also been described. For instance, the assembly of two different multitopic chiral ligands with a single metal ion have been used to generate self-supported Noyori-type catalysts for the

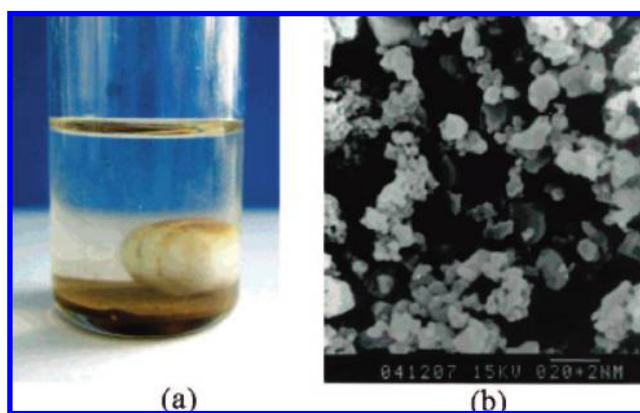
## Scheme 43



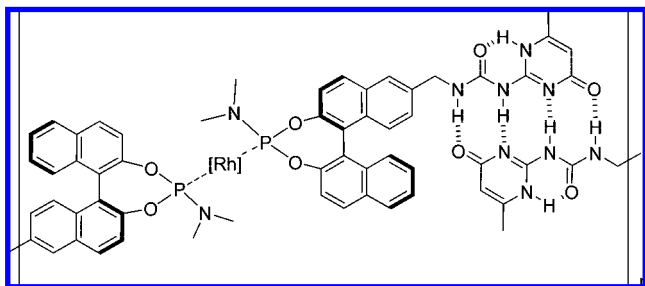
enantioselective hydrogenation of ketones.<sup>140</sup> In this case, bridged BINAP and chiral diamine ligands were assembled via coordination to a ruthenium center to generate the self-supported heterogeneous catalyst (Scheme 43). An image of the appearance of these coordination polymers, as well as a SEM image of the solid, is shown in Figure 52.

The subsequent application of these catalysts in the enantioselective hydrogenation of aromatic ketones (Scheme 43) was highly efficient, affording the corresponding 1-arylethanol in quantitative yield with a very low catalyst loading (0.1–0.01% mol). As in the preceding cases, the truly heterogeneous nature was tested by the lack of catalytic activity of the supernatant solution. Recovery and recycling experiments illustrated that the best catalyst can be reused for seven cycles without evident deterioration of catalytic activity or enantioselectivity.

Recently, self-assembly of a metal–ligand complex has been achieved through hydrogen bond interactions, leading to a supramolecular metal–organic polymer.<sup>141</sup> In this case,



**Figure 52.** (a) Self-supported chiral Ru(II) catalyst of Scheme 42 (pale brown solids at the bottom of the reactor) in 2-propanol and (b) SEM image of the self-supported Ru catalyst. The scale bar indicates 2  $\mu\text{m}$ . Reprinted with permission from ref 140. Copyright 2005 American Chemical Society.



**Figure 53.** Self-supported MonoPhos–Rh complex through hydrogen bonding.

the chiral ligand consists of a MonoPhos unit, modified by introducing a 6-methyl-2-ureido-4[1H]pyrimidone (Figure 53). Because the self-association constant of this group is very high ( $K_a = 6 \times 10^7 \text{ M}^{-1}$ ), it is very suitable for the construction of supramolecular structures. The resulting supramolecular metal–organic polymer is insoluble in less polar organic solvents, such as toluene, so it can be used in heterogeneously catalyzed hydrogenation reactions of dehydro- $\alpha$ -amino acids and enamides, like those shown in Scheme 42.

In all reactions tested, high conversions and enantioselectivities (91–96% ee) were obtained. ICP spectroscopic analyses did not provide any evidence of metal leaching within the detection limit of the instrument (1 ppm). However, although an efficient recovery and reuse of the catalyst was described (up to ten cycles, with enantioselectivities from 96% ee to 92% ee), a progressive loss of catalytic activity was detected (TOF from 180 to  $8 \text{ h}^{-1}$  in the tenth use), which was ascribed to partial decomposition of the catalyst during the recovery procedure, carried out in the absence of hydrogen atmosphere. Therefore, metal leaching under these conditions cannot be discarded (the authors do not offer data in this sense) and remains a question to be addressed in future developments.

Support strategies based on the formation of either MOF or metal–organic polymers are clearly in their beginning and have already offered encouraging results. Undoubtedly, they will be developed more extensively in the near future. An important question still unresolved lies in the determination of metal–organic polymer structures, which would help to efficiently design new catalytic systems.

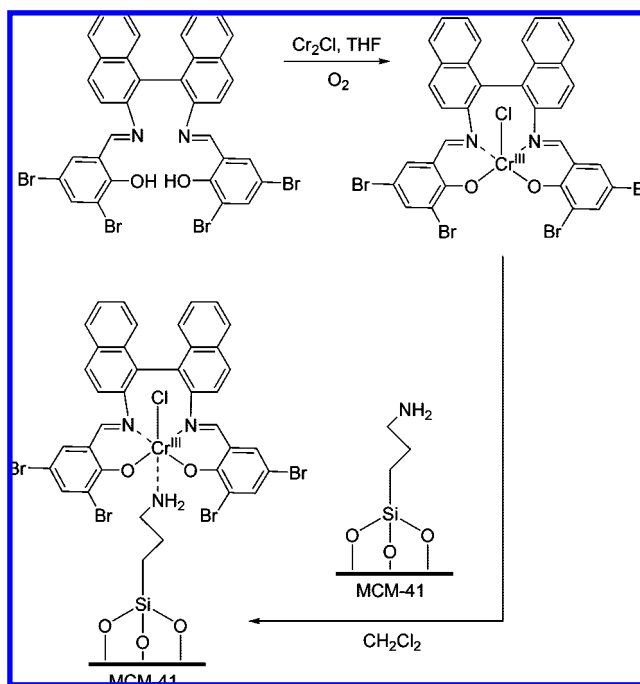
### 3.3. Modified Supports as Ligands

In this section, we will revise those strategies in which the coordinative interaction between the catalytic metal and the support requires the previous modification of the latter to introduce the coordinative element. In most cases, this modification is carried out by covalent grafting of a small molecule on the support surface.

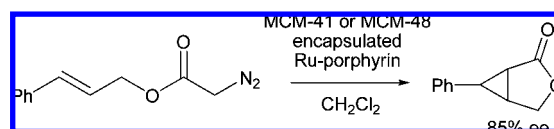
This immobilization strategy is particularly straightforward in those cases where the catalytic complex can bear axial ligands, as is the case of salen–metal complexes, given that the modified support can easily act as one of these ligands. Che and co-workers were one of the first in describing this kind of immobilization,<sup>142</sup> by using an aminopropyl-MCM-41 silica to immobilize a chromium binaphthyl Schiff base complex through coordination of the amino group to the chromium atom (Scheme 44).

The spectroscopic characterization of the supported catalyst showed that neither the support nor the complex changed noticeably upon immobilization. The supported enantio-

**Scheme 44**



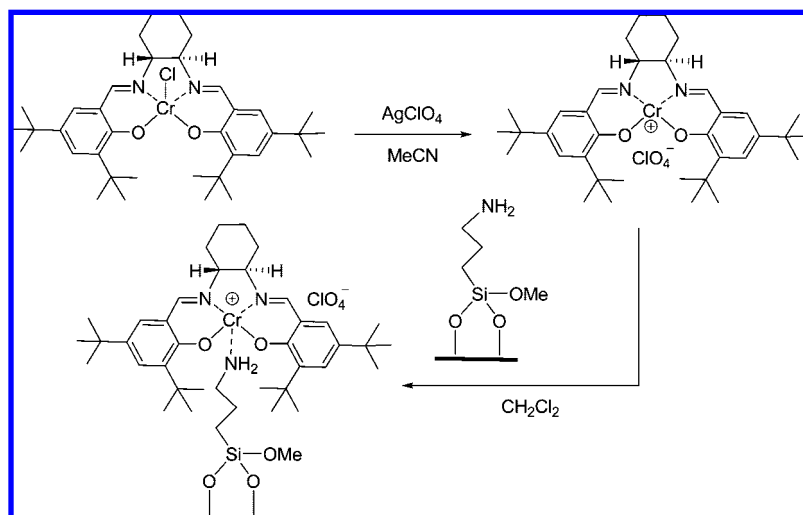
**Scheme 45**



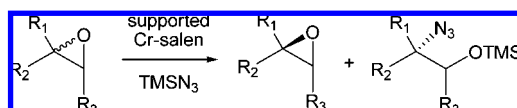
selective catalyst was tested in the asymmetric epoxidation of alkenes with PhIO. The authors reported that the supported catalyst exhibited better enantioselectivities than its homogeneous counterpart (up to 20% ee increase in the best case). They attributed this result to either an enhanced stability of the immobilized Cr complex or to the unique spatial environment created by the support surface. However, they did not consider the possible role of the axial ligand, absent in the homogeneous experiments, and that is known to improve enantioselectivity results also in solution. The solid catalysts were tested in reuse experiments. During the three first uses, yields and enantioselectivities were similar, but they significantly decreased from fourth use. In a subsequent work,<sup>143</sup> the same group used the same strategy to immobilize chiral ruthenium porphyrin complexes, tested as catalysts in asymmetric epoxidation of alkenes by 2,6-dichloropyridine *N*-oxide and intramolecular cyclopropanation. In this case, both MCM-41 and MCM-48 (containing a three-dimensional channel network) were used as supports. Amorphous silica was also used, for comparison. In the asymmetric epoxidation of styrene, both MCM-41 and MCM-48 displayed similar activities and enantioselectivities, up to 75% ee with the optimal loading of complex. On the other hand, the amorphous silica supported catalyst led to lower conversion and enantioselectivities. Other alkenes were also tested with moderate to good enantioselectivities. When a large size substrate, such as cholesterol acetate, was used, no epoxidation product could be detected, indicating that large molecules cannot diffuse into the channels of the mesoporous support and also that there is not significant leaching of the catalytic complex from the solid support during the reaction. An intramolecular cyclopropanation (Scheme 45) was also tested, leading to 85% ee in the first



Scheme 46



Scheme 47



use. The catalyst can be recovered and reused four times, but enantioselectivity dropped to 76% ee after two cycles.

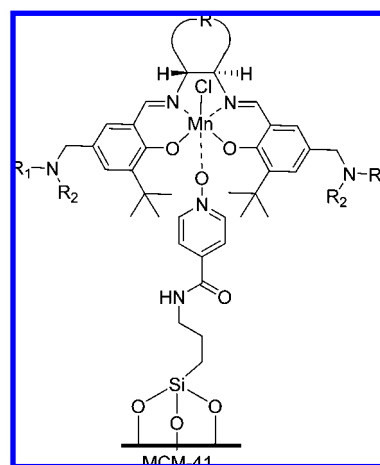
Chiral Cr–salen complexes were immobilized by Jacobs and co-workers<sup>144</sup> onto aminopropyl-functionalized silica, following the same strategy (Scheme 46),

In this case, the catalyst was used in the asymmetric ring opening reaction of epoxides with trimethylsilylazide (Scheme 47). Solvent choice was shown to be critical to avoid complex leaching from the support, apolar noncoordinating solvents, such as hexane, octane, or cyclohexane, being the best choices. Heterogeneity tests were carried out by taking aliquots from the supernatant solution at different reaction times and realizing that conversion levels do not further increase. The results obtained in the test reaction of desymmetrization of cyclohexene oxide with trimethylsilylazide were quite good. Catalyst could be recycled up to ten times keeping almost the same activity (quantitative conversions from 12 to 24 h reaction time) and enantioselectivity (>70% ee in most cases, up to 77%, which compares well with 85% ee in homogeneous phase). Total leaching after ten consecutive experiments was ca. 8%. The same catalytic system was also tested for other epoxides. In general, enantioselectivities were better for epoxides derived from long-chain terminal alkenes (1,2-epoxyhexane, 1,2-epoxyoctane), over 94% ee. However, catalyst leaching was also more important in this case, probably due of the amphiphilic nature of the reaction products, which increased the solubility of the complex in the reaction solvent (hexane).

Chiral salen–Mn complexes were also supported on modified MCM-41 silica, using pyridine *N*-oxide as the coordinating group, by Kureshy and co-workers (Figure 54).<sup>145</sup> As in the previous cases, the spectroscopic and XRD studies showed the integrity of the supports, as well as that of the catalytic complex, after immobilization. A large decrease in BET surface areas (from 1017 to 757 m<sup>2</sup> g<sup>-1</sup>) upon functionalization, accompanied with a reduction in the mesoporous diameter and pore volume, indicated that the chiral complex was present inside the channels of the modified MCM-41. The test reaction used was the epoxi-

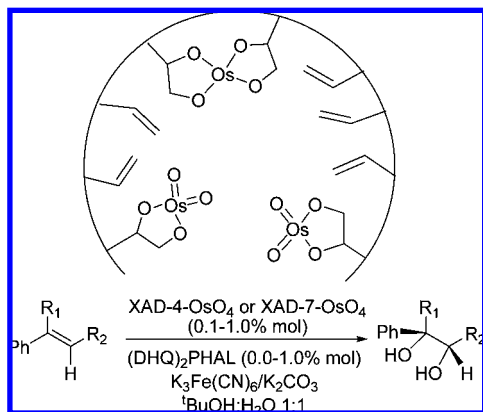
dation of styrene and other related aromatic alkenes (4-chlorostyrene, indene, 2,2-dimethyl chromene) with NaOCl in CH<sub>2</sub>Cl<sub>2</sub> at 0 °C. Good conversions to epoxide were obtained in all cases (75–99%). Significantly, enantioselectivities obtained for styrene (64–69% ee) and 4-chlorostyrene (62–67% ee) were higher than those with homogeneous catalysis (36–51% ee). However, the possible role of pyridine *N*-oxide as an axial ligand in the homogeneous phase does not seem to have been considered. Recycling experiments were also carried out in the epoxidation of styrene. Catalyst was recycled three times without loss of enantioselectivity, although longer reaction times were required to reach similar conversions. The characterization of the recycled catalyst suggested the partial degradation of the complex and the partial entrapment of reactant within the silica channels.

Polymer supports can also be modified for the immobilization of chiral catalysts. Song and co-workers exploited the immobilization of osmium tetroxide on different polymer matrixes to carry out asymmetric dihydroxylation and aminohydroxylation of olefins.<sup>146–148</sup> The underlying idea is that residual vinyl groups present in polystyrene-based resins can be osmylated with OsO<sub>4</sub>, leading to osmium glycolate reduced species, and freed from the support in situ by an oxidant. After the desired reaction with alkene is complete, the OsO<sub>4</sub> is taken up by other free vinyl groups



**Figure 54.** Supported (salen)Mn complex through coordination to a pyridine *N*-oxide.

Scheme 48



of the solid support, and thereby immobilized for reuse. Although the authors did not mention, it is obvious that this immobilizing strategy has an intrinsically limited capacity, since the number of free vinyl groups in the polymer decrease in each catalytic cycle. The first application of this strategy used Amberlite polystyrene (XAD-4) and polyacrylate (XAD-7) based cross-linked resins as supports for the asymmetric dihydroxylation (AD) of styrene and other related alkenes (Scheme 48). With both systems, excellent conversions and enantioselectivities were obtained (Table 16). Recycling experiments were also carried out for the reaction with styrene. Amberlite XAD-4 resin charged with 1 mol % Os showed good recyclability, allowing up to five catalytic cycles with high conversions and without decrease in enantioselectivity (95% ee).

However, from the third cycle, longer reaction times were required, due to the leaching of tiny amounts of  $\text{OsO}_4$  into solution. Therefore, although this catalyst represents a real improvement over the homogeneous system, it does not avoid the problem of the presence of highly toxic Os residues in the product mixture. Another drawback of these catalysts, already commented in section 3.1 is the separated recovery of the expensive chiral modifier,  $(\text{DHQD})_2\text{PHAL}$ , by acid aqueous extraction, which complicates the application of the catalytic method.

The same kind of immobilized catalyst was also applied to the asymmetric aminohydroxylation of olefins with  $\text{AcNHBr-LiOH}$  (Scheme 49),<sup>147</sup> also with excellent results in many cases (for instance, 93% yield and >99% ee for isopropyl (*E*)-cinnamate). Recovery of the catalyst showed the same pattern observed for AD, and three cycles could be accomplished with high yield and total enantioselectivity, although longer reaction times were necessary in each new cycle.

The recoverability of these catalytic systems has been further improved by using a different kind of resin support.<sup>148</sup> Thus, the use of macroporous resins bearing both residual vinyl groups and quaternary ammonium moieties achieves a better recyclability by allowing immobilization of  $\text{OsO}_4$  and osmate ions dissolved after the reaction, by simultaneous ion exchange and osmylation mechanisms (Scheme 50). As expected, the application of these modified immobilized catalysts led to results similar to those previously reported<sup>146</sup> for AD of styrene and related olefins. However, they displayed much better recyclability compared with both XAD-4  $\text{OsO}_4$  and  $\text{OsO}_4$  immobilized onto a Merrifield exchange resin, demonstrating the cooperative effect of both mechanisms of Os capture. With this catalyst, a total TON

as high as 1915 could be reached, although leaching of Os remains a problem to solve.

Another kind of modified polymeric support used to immobilize chiral catalyst bears pyridine groups in the modifier, able to coordinate to the metal of the catalytic complex. Davies and co-workers have thoroughly explored this strategy in the case of chiral dirhodium complexes.

Thus, in the first study, two different dirhodium tetraproline complexes were immobilized on a highly cross-linked polystyrene resin (Argopore) with a benzyloxymethylpyridine linker (Scheme 51),<sup>149</sup> by simple stirring of the solution containing the complex in the presence of the solid resin. The catalytic activity of these solids was evaluated in the cyclopropanation reaction of styrene with different methyl aryldiazoacetates.

From recovery experiments, it was concluded that the supported bridged proline catalyst  $\text{Rh}_2[(S)\text{-biTISP}]_2$  ( $\text{biTISP} = 5,5'-(1,3\text{-phenylene})\text{bis}[N-(2,4,6\text{-triisopropylbenzenesulfonyl})\text{proline}]$ ) is much more effective at maintaining high enantioselectivity (Figure 55). To further evaluate the catalytic activity of this system, reactions with different diazo compounds were carried out, as well as recycling experiments using different diazo compounds. In all cases, good activity and enantioselectivity results were described (Table 17).

Some attention was paid to the rather surprising fact that a pyridine-based support was so successful, because donor groups such as pyridine tend to deactivate rhodium tetracarboxylates. Control experiments were carried out using the same complexes in the homogeneous phase in the presence of 1.5 equiv of a 4-benzyloxyalkyl-pyridine (Figure 56). An important decrease in catalytic activity was observed, especially in the case of the  $\text{Rh}_2[(S)\text{-biTISP}]_2$  catalyst (only 18% yield in 12 h). In both cases, however, enantioselectivity remained high.

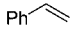
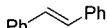
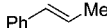



A second series of control experiments was carried out using an analogous polymeric support free of pyridine (Figure 56). With the phenyl-substituted resin catalysts, up to five cycles of cyclopropanation of styrene with phenyldiazoacetate could be carried out without decrease of final yield and enantioselectivity using both rhodium catalysts. These results suggest that the actual catalyst in the pyridine resin support is not the coordinated dirhodium complex, but probably the immobilization takes place through a microencapsulation effect, in analogy with examples gathered in section 5.1.

In a subsequent study, the C-H activation of 1,4-cyclohexadiene with methyl phenyldiazoacetate was catalyzed with the same kind of immobilized dirhodium complexes (Table 18).<sup>150</sup>

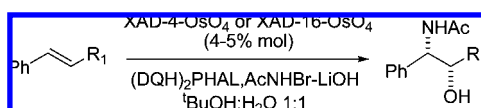
Good product yields and enantioselectivities were observed over ten cycles. Recycling experiments were also carried out using different aryldiazoacetates in each cycle. No cross-contamination between different cycles was detected. Several other C-H activation reactions with donor/acceptor carbenoids were tested, which can be considered as surrogates of classic organic synthesis reactions, such as Michael, aldol, Claisen, or Mannich reactions. In all cases, good yields and selectivities were described with catalytic systems recyclable at least three times. Finally, applications of these immobilized catalysts to the synthesis of key intermediates in the preparation of some pharmaceutical agents were also described.

The same group investigated the role of the polymer support on the performance of these catalytic systems.<sup>151</sup> Different aspects, such as polymer backbone, the

**Table 16. Results from Dihydroxylation of Olefins Catalyzed by OsO<sub>4</sub> Immobilized on Polymeric Matrixes<sup>a</sup>**

Olefin	XAD-4-OsO <sub>4</sub>				XAD-7-OsO <sub>4</sub>			
	cycle	time (h)	yield (%)	% ee	cycle	time (h)	yield (%)	% ee
	1	2	93	95	1	4	98	93
	3	2.5	90	95	3	15	73	91
	5	24	88	95	–	–	–	–
	1	8	94	>99	1	9	94	>99
	1	1.5	97	95	1	3.5	98	94
	1	0.5	96	89	1	2	97	88
	1	3.5	92	99	1	4.5	92	>99
	1	4.5	93	97	1	6	88	93

<sup>a</sup> With (DHQ)<sub>2</sub>PHAL 1%. Data from ref 146.

**Scheme 49**

linker, the terminal pyridine group, and the catalyst structure were proven to contribute to the efficiency of the immobilized catalyst. Studies using different polymer backbones demonstrated that the chemical environment around the pyridine group is crucial for effective immobilization, the best results being obtained with a pyridine group linked to the backbone through a Wang spacer in *para* position (Table 19). However, some resins lacking pyridine groups were also able to immobilize a significant amount of dirhodium complex and to catalyze the benchmark reaction of cyclopropanation of styrene with methyl phenyldiazoacetate. Some of them were also recyclable, although with noticeable decrease in enantioselectivity. These results point to combination of complex coordination and encapsulation in the immobilization process, as previously noted. It is known that pyridine deactivates dirhodium catalysts in homogeneous phase, so that the possibility of a release-and-capture mechanism (i.e., the active catalytic species is released to the solution during the reaction and captured through coordination to the support at the end) cannot be discarded *a priori*. Three phase tests, where the catalyst, the diazocompound, or both are immobilized on a support, demonstrated that the release-and-capture is not operating to a great extent in these catalytic systems.

The Argopore resin modified with benzyloxymethylpyridine groups was used as the support chosen by Davies' group to describe a so-called universal strategy for the immobilization of chiral dirhodium catalysts.<sup>152</sup> Up to five different dirhodium complexes with different electronic and steric features (Figure 57) were immobilized following the same strategy described in the preceding works. These immobilized catalysts were tested in several inter- and intramolecular cyclopropanation reactions, as well as in an asymmetric intramolecular C–H activation. In all cases, good enantioselectivities and recyclability of these catalysts were obtained, showing the high potential of this noncovalent immobilization strategy for the chiral dirhodium complexes.

Very recently, polyvinylpyridine has been used as support for immobilizing a chiral ruthenium(II)–salen complex.<sup>153</sup>

However, this immobilized complex has not been used for any enantioselective transformation, so it will not be discussed here.

As seen in this section, coordinative methods include a large variety of support–catalyst interactions. The knowledge of the nature of this interaction, its stability under reaction conditions, and the effect of the new coordination around the metal center seem to be crucial for a rational design of catalysts immobilized using this methodology.

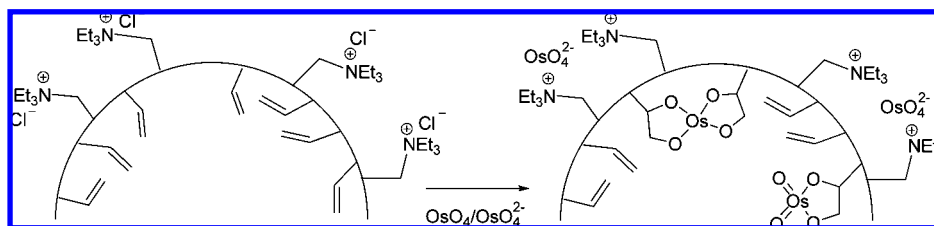
## 4. Adsorption Methods

In this section, immobilization methods that do not include specific metal–support coordination will be considered. Among them, we can cite physisorption through van der Waals interactions, formation of hydrogen bonds with ligands or anions, deposition of liquid phases, and formation of sulfur–gold bonds. In some cases, the existence of electrostatic or coordinative interactions cannot be discarded, but methods have been included in this section given that the formation of such specific interactions was not intended by the authors and their formation was not demonstrated by any method.

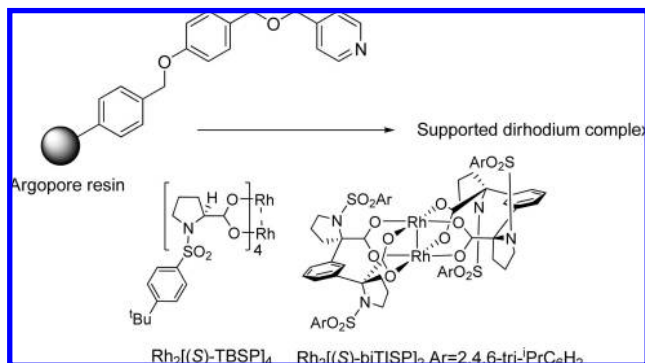
### 4.1. Immobilization by Physisorption

The possibility of immobilizing chiral catalysts by means of weak van der Waals type interactions with suitable supports was explored as early as in 1983.<sup>154</sup> Inoue et al. described the adsorption of [(DIOP)Rh(cod)Cl] and [(BPPM)Rh(cod)Cl] neutral complexes on charcoal. The importance of the support pretreatment was recognized, and the optimal results were obtained when charcoal was first treated with a metal acetate (Cr(OAc)<sub>3</sub> in the best case) and subsequently with triethylamine. Finally the complexes were adsorbed from ethanolic solutions. Although not intended by the authors, formation of O–Rh bonds in the case of treated carbons, in analogy with more recent works,<sup>130</sup> cannot be discarded. Enantioselectivities in the hydrogenation of (*Z*)-2-acetamidocinnamic acid (Scheme 1) were noticeably improved (Table 20), even over the results obtained in solution, 87% ee in the best case vs 79% ee in solution. Solvent was crucial for recovery, probably due to the solubility of the complex. Ethanol/water (1:1) was the best

Scheme 50

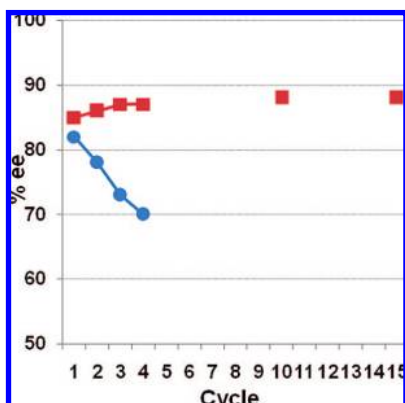


Scheme 51



choice, and catalysts were recoverable three times under O<sub>2</sub> exclusion. Leaching of Rh was detected, although 85% of the initial amount was still present on the catalyst after four runs.

The same group described the immobilization of the same type of complexes on methylated silica using hydrophobic interactions.<sup>155</sup> Neutral [(BPPM)Rh(cod)Cl] complex led to good results (88% ee) in the hydrogenation of a DOPA precursor (Scheme 52), but activity and enantioselectivity decreased significantly upon recycling (52% and 30% ee in consecutive runs). Reduction to metallic Rh was considered as the main factor for this deactivation. Cationic [(BPPM)-Rh(cod)]ClO<sub>4</sub> was more efficiently recovered under the same conditions (100% conversion, 85%, 77%, and 69% ee in three runs). Adsorption was carried out from methanol/water mixtures, showing that the maximum was reached at high water content. Hydrophobic character of the immobilization was invoked due to the lower adsorption observed for nonmethylated silica. In order to increase this hydrophobic interaction, the *tert*-butoxycarbonyl group of BPPM was substituted by a steraryl group, allowing in this way the use of methanol-rich mixtures for hydrogenation reactions,



**Figure 55.** Evolution of enantioselectivity with recycling for supported bridged (red squares) and nonbridged (blue circles) supported Rh–proline complexes (Scheme 55).

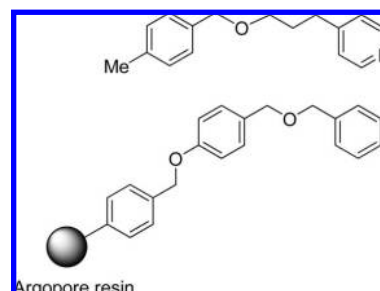
**Table 17. Results from Cyclopropanation Reactions with Supported Rh–Proline Catalyst<sup>a</sup>**

R	Catalyst (mol%)	time (min)	yield (%)	% ee
	0.04	180	88	88
	0.10	120	89	74
	0.10	60	90	80
	0.10	60	89	83
	0.10	60	87	90
	0.10	420	82	68

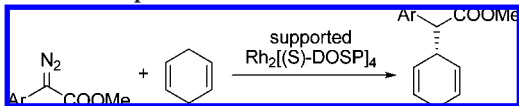
<sup>a</sup> Data from ref 149.

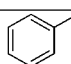
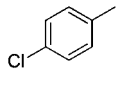
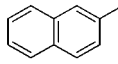
increasing the solubility of the substrate and hence reducing the reaction temperature. However recovery of this new catalyst was not described.

In 1990, Brunner and co-workers compared the immobilization of [(DIOP)Rh(cod)]PF<sub>6</sub> and [(Norphos)Rh(cod)]PF<sub>6</sub> by adsorption on different supports (BaSO<sub>4</sub>, cellulose, silica, alumina, carbon) and by cationic exchange<sup>59</sup> in the enantioselective hydrogenation of (*Z*)-2-acetamidocinnamic acid. Supported [(DIOP)Rh(cod)]PF<sub>6</sub> complex led to a continuous loss of enantioselectivity upon recovery, from around 60% ee in the first use to 35% ee in three to five runs depending on the support. [(Norphos)Rh(cod)]PF<sub>6</sub> was much more stable, allowing up to six runs with enantioselectivity over 60% ee. Silica was the best support, but results were slightly worse than those obtained with catalysts prepared by cationic exchange.



**Figure 56.** Additives for Rh–proline complexes.

**Table 18. Results from C–H Insertion Catalyzed by Supported Rh–Prolinate Complexes<sup>a</sup>**


Ar	cycle	time (min)	yield (%)	% ee
	1	20	79	88
	5	23	80	87
	10	30	84	84
	1	20	82	87
	1	20	85	85
	1	23	78	82
	1	24	60	87

<sup>a</sup> Data from ref 150.

The same group described the use of the same type of catalysts in the hydrogenation of the C=N bonds in the pyrazine ring of the folic acid (Scheme 53).<sup>156</sup> The catalysts were prepared by reaction of [Rh(cod)Cl]<sub>2</sub> (0.028 mmol) with the diphosphine ligand (0.033 mmol) in dichloromethane and adsorption on the support, shown by the disappearance of the orange color of the solution. The solvent was evaporated under vacuum, and the catalyst was used immediately because storage for some days resulted in decreased stereoselectivities.

In general better results were obtained with [(BPPM)-Rh(cod)Cl] compared with [(DIOP)Rh(cod)Cl]. Silica was shown to be again the best support, and independently of the particle size, yields were in the range of 80–92%. Catalysts immobilized on BaSO<sub>4</sub>, TiO<sub>2</sub>, MgO, molecular sieves, sephadex, and cellulose were inactive. Stereoselectivity depended on both the nature of the support and the particle size (80–84% de with DIOP and 88–92% de with BPPM). The best results were obtained using a silica gel with medium particle size (40 μm) and were worse with other silicas, alumina, celite, or charcoal.

Both yield and above all stereoselectivity decreased upon reuse. An attempt to recover the catalyst by addition of some fresh complex also led to reduced stereoselectivity. This result showed that some surface sites on silica were occupied in the first immobilization and were no longer available for the next catalyst loads. The nature of the catalyst–support interaction was not clear but the retention on the surface was probably related to the low solubility of the complex in the reaction medium.

In the case of adsorption through hydrophobic interactions, adsorption can be increased by using surfactant-modified supports. Flach et al.<sup>157</sup> studied the use of surfactants, both ionic and nonionic, covalently bonded to silica compared with dodecyl sulfate adsorbed on alumina (Figure 58) as supports for the hydrogenation of methyl (Z)-2-acetamidocinnamate with [(BPPM)Rh(cod)]BF<sub>4</sub> in aqueous medium. Table 21 compares the results obtained with the different supports.

In the homogeneous phase, the use of surfactants induced a large improvement in rate and selectivity. The same effect was observed using immobilized surfactants, although with lower increases in rate. The slower hydrogenation with silica Si2 was ascribed to an increased diffusion limitation related to pore filling. Probably the higher activity of alumina Al4 was related to a favorable bilayer structure. Some of the catalysts were recovered by sedimentation and reused. With both silicas, Si1 and Si2, traces of Rh were leached to the homogeneous phase; despite this, Si1 was reused several times. With Si2, activity was noticeably reduced after the first reaction, which was explained by the enrichment of the solid phase with insoluble product. Silica Si3 did not show Rh leaching after 10 reactions, probably due to an ion exchange of the tetraalkylammonium cations with the cationic Rh complex that would be then electrostatically fixed onto the support (as examples described in section 2.4). After 10 cycles, the solid system did not sediment sufficiently.

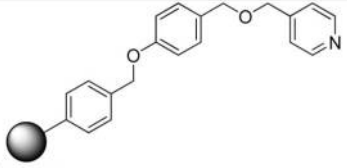
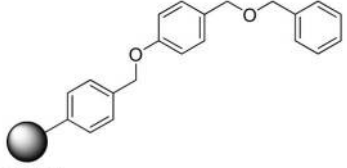
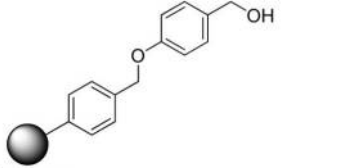
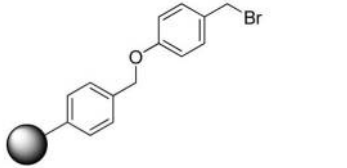
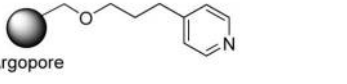
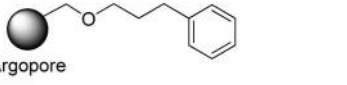
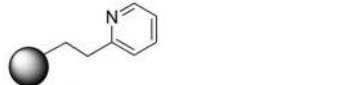
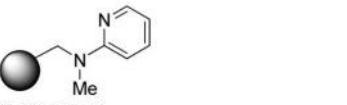

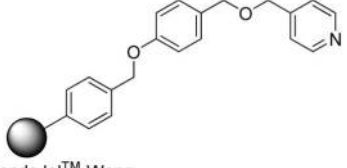
The pores of a mesoporous silica (HMS, average pore size 26 Å) were used to include catalysts with a good match between its dimension and the pore size.<sup>158</sup> So [(BINA-P)Ru(*p*-cymene)Cl]Cl and [(BPPM)Rh(cod)Cl] were incorporated from benzene solutions. Catalysts were used to carry out the hydrogenation of sodium (Z)-2-acetamidocinnamate in water. The results showed that the Rh catalyst was more active than the Ru one and the enantioselectivity was near 50% ee, lower than the values described in the homogeneous phase for the hydrogenation of the acid in organic solvents and the sodium salt in water. Pretreatment with NEt<sub>3</sub>, to eliminate acid sites from the support, did not have any noticeable influence. Whereas the recovered Rh catalyst (4% leaching) showed important decreases in activity and enantioselectivity, Ru catalyst was recovered with no changes in activity or enantioselectivity and less than 2% leaching. The same catalysts were tested in the hydrogenation of itaconic acid in aqueous medium, leading to enantioselectivities lower than 20% ee with both catalysts.

Attempts to hydrogenate the free (Z)-2-acetamidocinnamic acid in water required 50–60 °C to reach completion, due to the low solubility of the acid, and enantioselectivity reached 50–62% ee. The recovery of the product by washing the solid with methanol precluded any reuse of the catalyst due to the 90% leaching of Rh observed. The reaction in MeOH/H<sub>2</sub>O = 1:1 was probably homogeneous.

To try to improve these results, both catalysts were incorporated into silicas during sol–gel synthesis and tested in the water hydrogenation of sodium (Z)-2-acetamidocinnamate.<sup>159</sup> [(BINAP)Ru(*p*-cymene)Cl]Cl showed lower activity but led to similar enantioselectivity (69% conv and 44% ee), but both noticeably decreased after recovery. With [(BPPM)Rh(cod)Cl] only 37% conv and 21% ee were obtained in the first reaction; however total conversion without enantioselection was obtained with the recovered catalyst, consistent with the formation of very active but nonenantioselective sites, probably Rh particles. The use of MeOH/H<sub>2</sub>O = 1:1 improved the results (100% conv and 59% ee), but 41% Rh was leached under these conditions.

[(BINAP)Ru(*p*-cymene)Cl]Cl was also incorporated<sup>159</sup> onto preformed mesoporous silicas with a narrow range of pore size (26 and 37 Å) and one amorphous silica (average pore size 68 Å), modified by passivation of the external surface with Ph<sub>2</sub>SiCl<sub>2</sub> and derivatization of the internal surface with amino groups for potential tethering of the catalyst. Results with the modified large pore silicas were

Table 19. Effect of Different Resins as Supports for Immobilized Rh-Proline Catalysts for C–H Insertion Reactions<sup>a</sup>

Support	Immobilization (%)	Cycle	time (h)	%ee
 Argopore	86	1	10	86
		5	15	81
 Argopore	75	1	10	84
		5	10	71
 Argopore	71	1	10	80
		5	14	68
 Argopore	70	1	10	82
		5	14	68
 Argopore	92	1	10	86
		5	20	77
 Argopore	29	1	10	82
		5	30	67
 Functionalized Silica gel	8	1	10	78
		3	120	66
 1% PS-DMAP	<1	–	–	–
 Polypyridine-JandaJel™	<1	–	–	–
 JandaJel™-Wang	97	1	15	85
		5	20	77

<sup>a</sup> Data from ref 151.

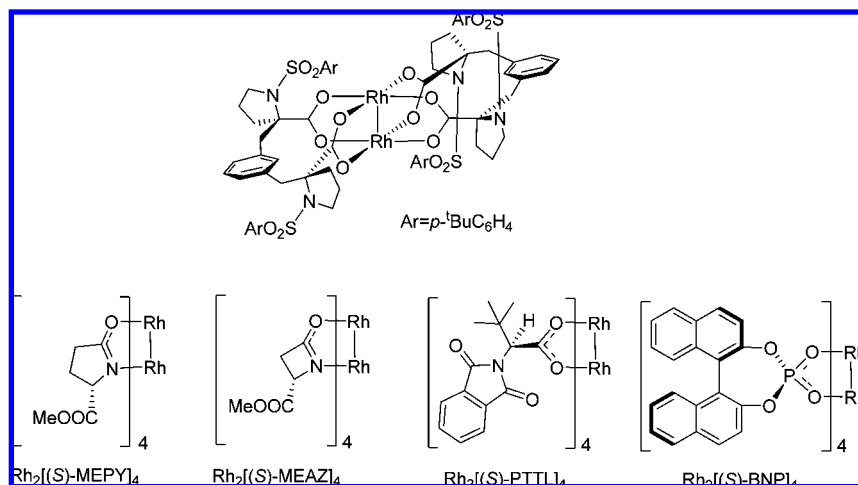


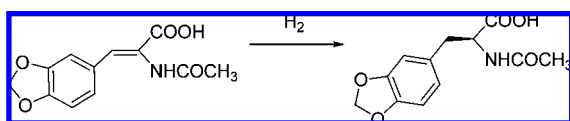
Figure 57. Dirhodium prolineate catalysts.

Table 20. Results from the Hydrogenation of (Z)-2-Acetamidocinnamic Acid with Adsorbed Catalysts<sup>a</sup>

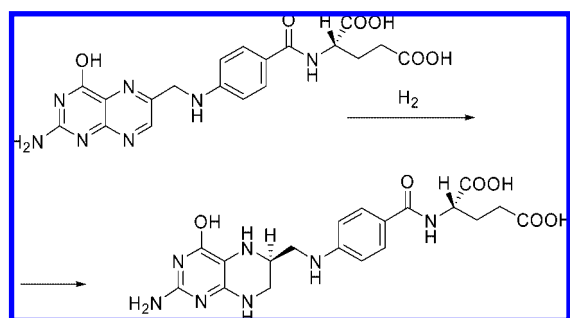
catalyst	pretreatment	% ee
[(DIOP)Rh(cod)Cl]	none	64
[(DIOP)Rh(cod)Cl] /charcoal	NaOAc	43
	Et <sub>3</sub> N	50
	Cr(OAc) <sub>3</sub> + Et <sub>3</sub> N	56
		71
[(BPPM)Rh(cod)Cl]	none	79
[(BPPM)Rh(cod)Cl] /charcoal	none	67
	NaOAc	84
	Et <sub>3</sub> N	84
	Cr(OAc) <sub>3</sub> + Et <sub>3</sub> N	87

<sup>a</sup> Data from ref 154.

Scheme 52



Scheme 53



similar to those obtained with unmodified supports (80–100% conv and 40–50% ee) with small decreases in activity and selectivity upon recovery. However, only low conversions were reached with the modified 26 Å silica, due to restricted access to the pores, as indicated by pore volume measurements.

These results indicated that van der Waals interactions of the catalyst with the porous system of the support are strong enough to retain the catalyst in aqueous hydrogenation and the catalyst was not improved by the use of a potential internal tether. In general, these systems seem to be limited to hydrogenation reactions in water, probably due to the low solubility of the catalytic complexes in this solvent.

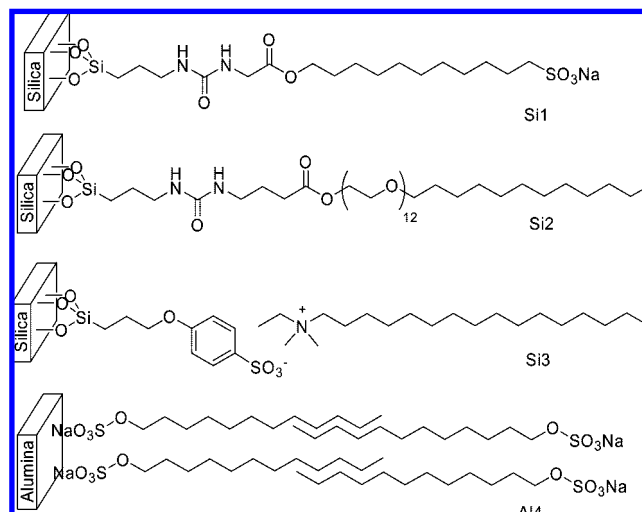


Figure 58. Hydrophobic supports.

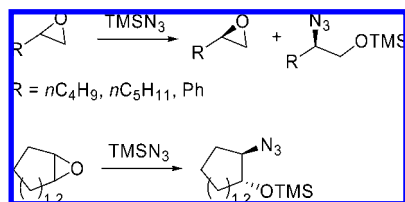
Table 21. Results Obtained from the Hydrogenation of Methyl (Z)-2-Acetamidocinnamate with Surfactants in Solution and in Heterogeneous Phase<sup>a</sup>

surfactant (S/Rh)	cycle	% ee	<i>t</i> <sub>1/2</sub> (min)
none	1	78	90
SDS (50:1)	1	94	3.5
SDS (20:1)	1	94	6
Si1 (20:1)	1	78	17
	6	74	7
Si2 (20:1)	1	93	24
	2	96	62
Al4 (20:1)	1	90	7.5
Si3 (20:1)	1	92	11
	10	94	40

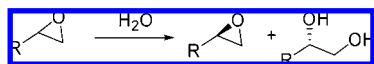
<sup>a</sup> Data from ref 157.

Cationic chiral salen–Mn (III) complex was supported by impregnation from CH<sub>2</sub>Cl<sub>2</sub> solution inside Al-, Ga-, and Fe-substituted mesoporous silicates (MS).<sup>160</sup> Analytical and spectroscopic studies showed the integrity of the complex and a 3–5 wt % loading. TG-DTA allowed the authors to conclude the presence of chloride; therefore the complex was not immobilized by electrostatic interaction with the anionic support. On the basis of IR spectra, a strong interaction between the complex and the silanol groups of the host was suggested. Siliceous nanoporous materials had a weaker interaction than Al-containing forms.<sup>161</sup> Catalysts were tested in the epoxidation of 1,2-dihydronaphthalene with sodium

Scheme 54



Scheme 55



hypochlorite (Scheme 10). To this end, Al-MS catalyst was previously washed with  $CH_2Cl_2$  until a content of 1.3% wt. The similar activity and enantioselectivity in both homogeneous and heterogeneous phases indicated the free access of reactants to the catalytic sites into the solid. Catalyst reuse was not studied.

Dioos and Jacobs used salen-Cr(III) complexes, impregnated on silica, as heterogeneous catalysts for the asymmetric ring opening of epoxides<sup>162</sup> (Scheme 54). Due to the solubility of the complex, impregnation was carried out from ether and reactions were conducted in hexane.

The kinetic resolution of terminal epoxides (1,2-epoxyhexane and 1,2-epoxyheptane) resulted in very high enantioselectivities (>97% ee) at conversions of about 50%. However, lower selectivities were obtained with other substrates, like styrene, cyclohexene, and cyclopentene oxides. Diastereomeric excesses of 80–90%, at conversions from 48% to 65%, were reached in the kinetic resolution of (+) and (–)-limonene-1,2-epoxide.

Catalyst recycling was studied in the opening of 1,2-epoxyhexane for 10 consecutive runs. During these experiments 1,2-epoxyhexane was obtained with an enantiomeric excess ranging from 82% to 93% ee, whereas ee values for the azido trimethylsilyl ether varied from 60% to 71%. Conversion was also maintained, although longer times were needed, in particular in the last two batches. Leaching was high in the first three reactions (0.59%, 1.83%, and 1.08%), then was very low and increased again in the last two runs (0.30% and 1.22%), which was assumed to be due to mechanical attrition of the support. However the leached complex could not justify the observed activity.

In an effort to reduce leaching, a dimeric salen-Cr catalyst (Figure 59) was impregnated on silica from THF solution.<sup>163</sup> Reactions in hexane led to high ee in the kinetic resolution of terminal epoxides (Scheme 54) (up to 98% ee for 1,2-epoxyhexane) at a conversion of 55%. Recycling experiments showed an overall leaching amounting 1% after 10 runs, whereas enantioselectivities were excellent in 12 runs.

Because of abrasive effects in batch experiments, the silica material was fragmented significantly, which made difficult the quantitative recovery of the material. To reduce this

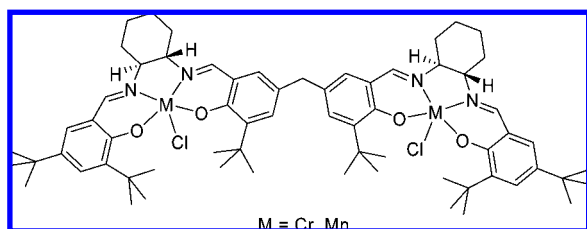


Figure 59. Dimeric salen-based complex.

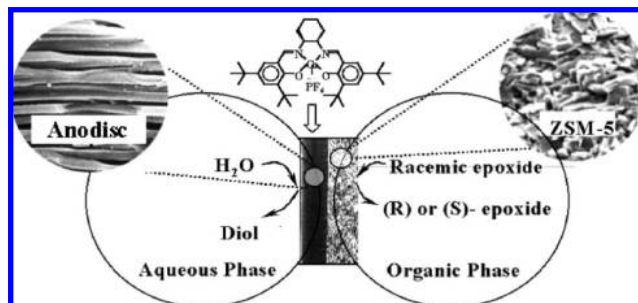


Figure 60. Schematic view of a membrane reactor with impregnated (salen)Co catalyst. Reprinted with permission of Springer, ref 164.

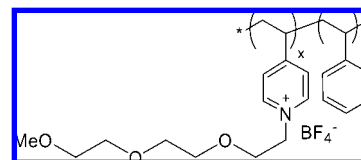


Figure 61. PEG-ylated cationic polymer.

effect, a continuous flow reactor was tested. With a similar amount of catalyst, leaching of 14.5% was observed for a TON of 180 with the monomeric catalyst, whereas leaching was limited to 3.7% with the dimeric catalyst.

Salen-Co(III) complexes were impregnated at the interface between the macroporous matrix and the ZSM-5 film layer of a membrane reactor and used in the hydrolytic kinetic resolution of several epoxides<sup>164</sup> (Figure 60).

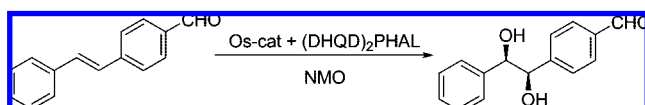
Racemic epichlorohydrine, 1,2-epoxybutane, and styrene oxide were efficiently hydrolyzed (Scheme 55) by (salen)-CoOAc with very high enantioselectivity (up to 98% ee). After the reaction,  $AcO^-$  was dissociated, and the catalyst was not active when reused. (Salen)CoPF<sub>6</sub> and BF<sub>4</sub> complexes were more active and recoverable without any loss of activity. Thus (salen)CoPF<sub>6</sub> in the membrane exhibited high optical purity of product (up to 99.8% ee) during repeated reuse, but prolonged reaction time was needed as the number of recycles increased. The same catalyst was used in a continuous-type membrane reactor. The organic phase, containing the epoxide, was circulated along the side of the ZSM-5 layer, and the aqueous phase was countercurrent circulated along the porous alumina side. Because of the insolubility of the complex in water, the catalyst was entrapped at the interface between layers. The hydrophilic diol diffused into the aqueous phase through the macropores, whereas the unreacted enantiomerically enriched epoxide remained in the organic phase. Terminal epoxides were efficiently hydrolyzed with this system. Epoxide yields were in the range of 38–45%, and enantioselectivities were very high both in the epoxide (up to 98–99% ee) and in the diol (up to 98% ee).

Osmium tetroxide was immobilized<sup>165</sup> onto a PEG-ylated cationic polymer (Figure 61) by shaking a suspension of OsO<sub>4</sub> and the polymer in acetonitrile/water = 9:1 (0.19 mmol of OsO<sub>4</sub>/g). The wide variety of possible complex-support interactions (electrostatic, coordinative, van der Waals, entrapment) makes it difficult to classify this example. Authors proposed that immobilization was due to the interaction between ions and induced dipoles of OsO<sub>4</sub> in the same manner as ionic liquids.

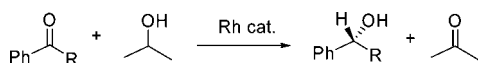
The resin was used for asymmetric dihydroxylation of *trans*-stilbene-4-carboxaldehyde using (DHQD)<sub>2</sub>PHAL ligand (Scheme 56). Reaction took place in 3 h with a 99% conv.



Scheme 56



Scheme 57



and 96% ee. Catalyst was reused four times with the same enantioselectivity but decreased activity; in the fifth reaction, 12 h was needed to reach the same conversion. When recovered catalyst was reused without additional chiral ligand after the first use, 88% ee was obtained, which indicated that a significant amount of chiral ligand was immobilized in the form of an osmium–ligand complex. A small amount of Os, from 3% to 5%, was found in the filtrates. The catalyst was successfully used with other alkenes (styrene, 4-methoxystyrene, *trans*-stilbene, and methyl *trans*-cinnamate) with isolated yields  $\geq 88\%$  and enantioselectivities  $\geq 88\%$  ee.

We can conclude that physisorptive methods involve the formation of weak support–catalyst interactions, and hence the stability of the catalysts greatly depends on the catalytic reaction conditions. Low solubility of the complex in the reaction medium seems to be the crucial point to prevent leaching.

## 4.2. Immobilization by Hydrogen Bonding with the Support

Inorganic supports that present different types of OH groups have been used to immobilize several types of catalysts taking advantage of the possible formation of hydrogen bonds.

The first successful example was reported by P. Gamez et al.<sup>166</sup> in the reduction of pro-chiral ketones using the 2:1 complexes of (*S,S*)-1,2-diphenylethylenediamine with  $[\text{Rh}(\text{C}_6\text{H}_{10})\text{Cl}]_2$ . The complex was adsorbed onto different supports and used in the hydride transfer reduction of the ketones (Scheme 57) using a continuous flow reaction.

The results obtained in the reduction of methyl 2-phenyl-2-oxoacetate ( $\text{R} = \text{CO}_2\text{Me}$ ) were strongly dependent on the nature of the support, so with neutral alumina, diamine was eluted and only a stoichiometric amount of substrate was reduced. Better diamine adsorption was observed on silica, but conversion was dependent on the particle size; with 15–40  $\mu\text{m}$ , conversion was 28%, whereas with 35–70  $\mu\text{m}$ , conversion reached 90% at a flow rate of 2  $\text{mL h}^{-1}$ , which represented a TON = 300, much higher than the TON = 20 obtained in the homogeneous phase. The same catalyst was tested in the reduction of other pro-chiral ketones (Scheme 57), and the results were similar to or better than those obtained under homogeneous conditions (Table 22).

It was proposed that the silica support was forming hydrogen bonds with the nitrogen atoms of the chiral ligand. This interaction seemed to be strong enough because the decrease of both ee and conversion observed after the reduction of 300 mmol of methyl 2-phenyl-2-oxoacetate per mmol of Rh was due to a destruction of the catalytic complex rather than a simple problem of elution.

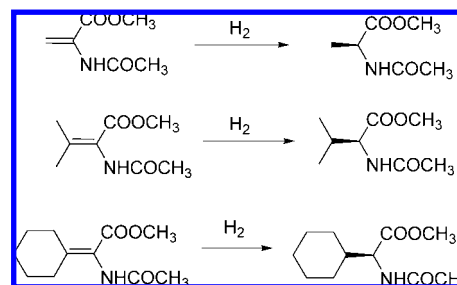
More recently, immobilization was designed to be carried out by hydrogen-bond formation between support and a suitable counterion of the catalytic complex, instead of the chiral ligand.

**Table 22. Comparison of Homogeneous and Heterogeneous Catalysts in the Continuous Flow Reduction of Pro-chiral Ketones<sup>a</sup>**

R	solvent	homogeneous (batch)		heterogeneous (flow)	
		conversion %	ee %	conversion %	ee %
$\text{CH}_3$	<i>i</i> PrOH	80	65	80	61
$\text{COOMe}$	<i>i</i> PrOH	100	$\geq 99$		
$\text{COOMe}$	<i>i</i> PrOH/heptane (1:1)			90	$\geq 99$
$\text{CF}_3$	<i>i</i> PrOH/heptane (1:1)	100	16	100	21

<sup>a</sup> Data from ref 166.

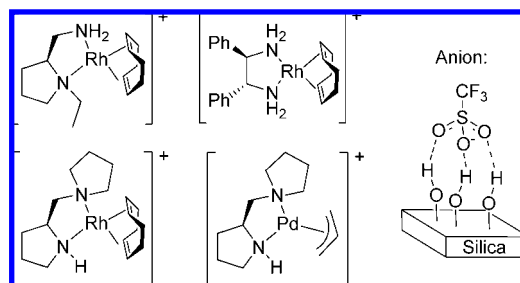
Scheme 58



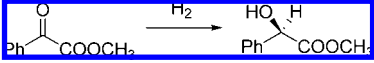
Using this approach,  $[(\text{MeDuPhos})\text{Rh}(\text{cod})]\text{OTf}$  was immobilized on MCM-41, a solid support with a large and well-defined pore structure.<sup>167</sup> A solution of the complex in  $\text{CH}_2\text{Cl}_2$ , rapidly decolorized upon addition of the solid. The role of triflate was made clear when compared with other counterions. Although the role of hydrogen bonding could not be confirmed by IR due to the low loading (0.9 wt % Rh), broadening of the signals in  $^{31}\text{P}$  and  $^{19}\text{F}$  NMR spectra indicated that the triflate counterion strongly interacted with the surface.

The catalyst proved to be highly active and selective in the hydrogenation of several enamides (Scheme 58) at room temperature in hexane, with results ( $>99\%$  conversion, 98–99% ee) better than those in solution. Leaching of active species was not observed, and the catalyst was recovered by decantation leaving the solid with a small amount of solvent. The reaction was repeated four times without loss of conversion or selectivity.

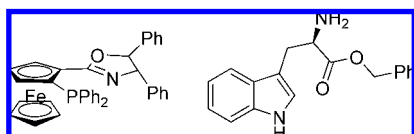
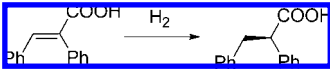
By the same approach, complexes of chiral diamines with Rh(I) and Pd(II) (Figure 62) were immobilized on a series of commercially available silicas<sup>168</sup> (Davidson 923, 634, and 654) having a narrow pore size distribution. The average diameter of the pores was 3.8, 6.0, and 25 nm, respectively, with surface areas of 700, 500, and 300  $\text{m}^2/\text{g}$ . Chiral catalysts were presumably immobilized through H-bonds between the triflate counterion and the silanol groups of silica surface.



**Figure 62.** Supported  $[(\text{AEP})\text{Rh}(\text{cod})]\text{OTf}$ ,  $[(\text{DED})\text{Rh}(\text{cod})]\text{OTf}$ ,  $[(\text{PMP})\text{Rh}(\text{cod})]\text{OTf}$ , and  $[(\text{PMP})\text{Pd}(\text{allyl})]\text{OTf}$ .

**Table 23. Asymmetric Hydrogenation of Methyl 2-Oxo-2-phenylacetate with Immobilized Catalysts<sup>a</sup>**


catalyst	support	pore size (nm)	<i>t</i> (h)	conversion (%)	ee (%)
[(AEP)Rh(cod)]OTf	none		2	62	0
	silica	3.8	2	93	77
		6.0	2	94	61
[(DED)Rh(cod)] OTf	none		2	70	0
	silica	3.8	2	98	79
		6.0	1	75	73
25		2	83	4	
[(PMP)Rh(cod)] OTf	none		0.5	46	53
	silica	3.8	2	96	94
		6.0	2	92	78
25		2	87	59	
[(PMP)Pd(allyl)] OTf	none		0.5	96	55
	MCM-41	3.0	2	99	67
	reuse		2	100	66

<sup>a</sup> Data from ref 168.**Figure 63.** Phosphinoxazoline (Phox) and tryptophane derivative (Trypt) used as chiral ligands.**Table 24. Results Obtained from the Hydrogenation of (*E*)-2-Phenylcinnamic Acid with Homogeneous and Heterogeneous Catalysts<sup>a</sup>**


ligand	homogenous			heterogenous		
	conv. %	select. %	ee %	conv. %	select. %	ee %
Phox	65	70	73	85	62	88
reuse				79	67	91
Trypt	88	59	69	81	47	69
AEP	86	84	83	90	84	97
DED	64	84	66	70	91	90

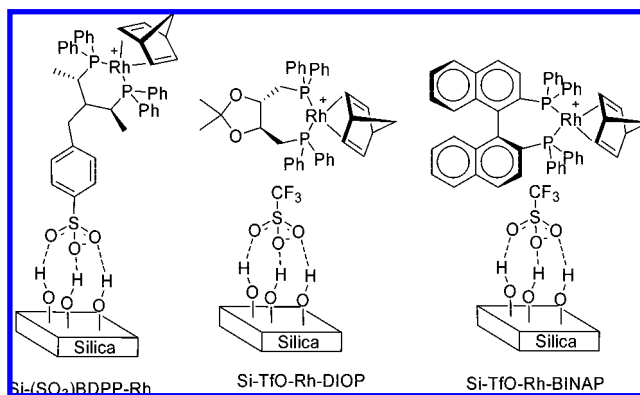
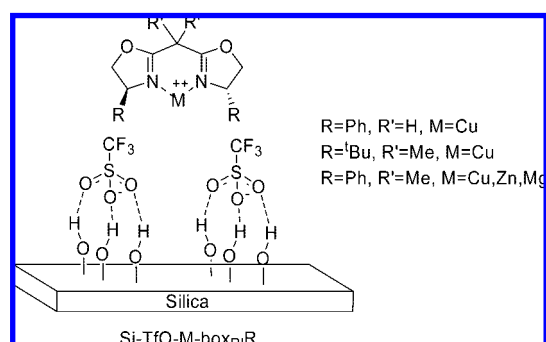
<sup>a</sup> Data from ref 169.

Homogeneous and heterogeneous catalysts were compared in the enantioselective hydrogenation of methyl 2-oxo-2-phenylacetate, and the results are summarized in Table 23.

The results clearly showed the influence of the spatial restrictions imposed by the support on enantioselectivity. This influence declined as the pore diameter of the silica support increased from 3.8 to 6 and 25 nm. Although [(PMP)-Rh(cod)]OTf and [(PMP)Pd(allyl)]OTf exhibited noticeable enantioselectivity in solution, these values were significantly increased upon immobilization. This noncovalent immobilization did not lead to leaching when catalysts were recycled.

By the same strategy, the Rh complexes of two new ligands, a phosphinoxazoline and a tryptophane derivative (Figure 63), [(AEP)Rh(cod)]OTf and [(DED)Rh(cod)]OTf (Figure 62), were immobilized onto the surface of MCM-41 silica.<sup>169</sup> The presence of the chiral catalyst was demonstrated by elemental analysis and, when possible, by <sup>31</sup>P-CP-MAS NMR. The catalysts were used in the hydrogenation of (*E*)-2-phenylcinnamic acid (Table 24).

The results showed a marked increase in enantiomeric excess once the catalyst is anchored onto the mesoporous

**Figure 64.** Two strategies to form hydrogen bonds between catalytic complex and support.**Figure 65.** [Box-metal]OTf catalysts immobilized by hydrogen bonds.

material, in agreement with a confinement effect. The recycling test showed the stability of the catalyst, despite the rather weak bonding to the solid support.

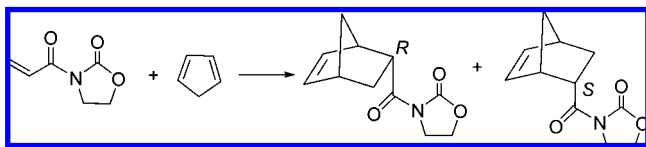
The strategy of using triflate as the counterion with [(DIOP)Rh(nbd)]OTf and [(BINAP)Rh(nbd)]OTf was compared with the modification of the chiral ligand with a sulfonate moiety (Figure 64) by Bianchini et al.<sup>170</sup> Catalysts were incorporated (1 wt % metal loading) on activated Grace Davidson 62 silica by impregnation from anhydrous CH<sub>2</sub>Cl<sub>2</sub>. Complex was not leached with CH<sub>2</sub>Cl<sub>2</sub> but it was leached by MeOH and EtOH, showing the rather weak support-catalyst interaction. Some NMR experiments with the ligands supported via triflate hydrogen bond to silica indicated that triflate anion is bonded to the support.

Homogeneous (in MeOH) and heterogeneous (in *n*-heptane) hydrogenations were compared with all the catalysts and three different alkenes. With Si-(SO<sub>3</sub>)BDPP-Rh and Si-TfO-Rh-BINAP results were similar in both phases, although the immobilized catalysts were more active in the hydrogenation of ethyl (*E*)-3-methylcinnamate (up to 20% ee). Regarding enantioselectivity, 53% ee was obtained with Si-(SO<sub>3</sub>)BDPP-Rh in dimethyl itaconate hydrogenation and 30% ee in methyl 2-acetamidoacrylate hydrogenation. With Si-TfO-Rh-DIOP, enantioselectivity decreased upon immobilization, which may be due to the interaction of the oxygen atoms of the ligand with the surface. Leaching of metal was less than 1 ppm after three runs, and recovered catalysts showed the same activity and selectivity.

Hydrogen bond supported bis(oxazoline) based complexes with different cations (Figure 65) were used as catalysts in Lewis acid promoted reactions.

In the hetero-Diels-Alder reaction between ethyl (*E*)-2-oxopent-3-enoate and ethyl vinyl ether (Scheme 16),<sup>171</sup> Si-TfO-Cu-box<sub>H</sub>Ph showed a behavior, both in activity and

Scheme 59



enantioselectivity, similar to that observed in solution. A maximum of 42% ee was obtained at  $-60\text{ }^{\circ}\text{C}$ , and the catalyst was reused four times. However Si-TfO-Cu-box<sub>Me</sub><sup>t</sup>Bu was much less efficient than the homogeneous counterpart, 41% ee obtained at  $-78\text{ }^{\circ}\text{C}$  vs 95% ee in solution. These results are probably due to a partial loss of chiral ligand, a consequence of the lower stability of the Cu-box<sub>Me</sub><sup>t</sup>Bu complex.

The immobilized complexes were tested as catalysts in the Diels–Alder reaction between 3-acryloyl-oxazolidin-2-one and cyclopentadiene<sup>171</sup> (Scheme 59).

Catalyst Cu-box<sub>Me</sub><sup>t</sup>Bu showed activity and enantioselectivity (57% ee) similar to those observed in homogeneous phase. However, a reversal of the major *endo* enantiomer obtained with catalyst Cu-box<sub>H</sub>Ph, with regard to the homogeneous phase reaction, was noted. Whereas in solution 20% ee of the *S* enantiomer was obtained, 33% ee of the *R* enantiomer was obtained with the supported catalyst at  $-30\text{ }^{\circ}\text{C}$ .

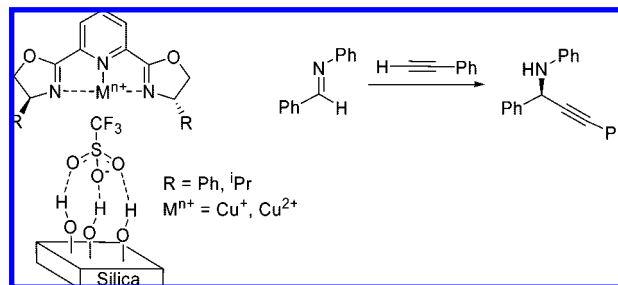
Later on, these results were revisited by Li and co-workers<sup>172</sup> using copper catalysts, together with analogous Zn and Mg catalysts (Figure 65). Results obtained with Cu-box<sub>Me</sub><sup>t</sup>Bu were much better than those reported earlier, with enantioselectivities in the range of 85–93% ee at rt. Activity and recoverability were improved by using toluene as reaction solvent and 3 Å MS as water scavenger, allowing three uses with the same activity (98%, 92%, and 83% conversion) and enantioselectivity (91% ee in the three runs).

The reversal in enantioselectivity with Cu-box<sub>H</sub>Ph was confirmed and even enhanced (up to 46% ee of the *R* enantiomer) with the analogous Cu-box<sub>Me</sub>Ph in toluene. The same effect was also observed with Zn-box<sub>Me</sub>Ph and Mg-box<sub>Me</sub>Ph catalysts, with a reversal in the case of the Mg catalyst from 60% ee (*S*) in solution to 30% ee (*R*) with the heterogeneous catalyst. This effect was ascribed to a change in the coordinating ability of the anion. It was observed that the substitution of triflate by a less coordinating anion, SbF<sub>6</sub><sup>−</sup> or ClO<sub>4</sub><sup>−</sup>, produces the same reversal in solution due to a change in the geometry, from octahedral with the coordinating anion to tetrahedral with the noncoordinating one. The hydrogen bonds between silanols and triflates might be responsible for this change in coordinating character on the solid support. This explanation however cannot be applied to the copper catalyst, because the reversal is not observed in solution and the conformational preferences are completely different from the other two metals. The possibility of a surface effect of a steric nature has not been invoked in this case.

The same strategy was used to immobilize pyridinebis-(oxazoline)–copper complexes on silica gel.<sup>173</sup> The solids were used as catalysts in the asymmetric synthesis of propargylamines via direct addition of terminal alkynes to imines (Scheme 60). Complex was adsorbed from a dichloromethane solution until color disappeared from the solution (theoretical loading, 2.8% copper).

With the Phpybox-Cu(OTf) complex, the homogeneous reaction was conducted in refluxing toluene to yield 100%

Scheme 60



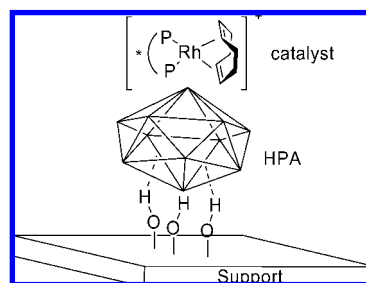
conv and 51% ee. The immobilized catalyst gave similar results (97% conv, 47.5% ee). Results using the <sup>t</sup>Prpybox-Cu(OTf) were disappointing because the enantioselectivity was low with both homogeneous (33% ee) and heterogeneous (25% ee) catalysts, although the solid catalyst was more active and reusable with the same results.

With Phpybox-Cu(OTf)<sub>2</sub>, the activity increased from homogeneous (32% conv, 83.5% ee) to solid (52% conv, 83.5% ee) catalyst, although Cu leaching led to a decrease of activity upon recovery (29% conv., 81.5% ee). The use of toluene instead of CH<sub>2</sub>Cl<sub>2</sub> reduced leaching (in agreement with previous results<sup>172</sup>). In fact, the use of this solvent improved catalyst recovery (100% conv in two runs) although with lower enantioselectivity (56% and 68% ee).

Heteropolyacids (HPAs) constitute a family of strong acids; therefore their corresponding anions are weakly basic and can be used as weakly coordinating counterions for cationic catalysts. These heteropolyacids can be immobilized<sup>174</sup> by weak, normally hydrogen bond, interactions with suitable inorganic supports, so that the combination of these two strategies leads to a new family of solid-supported chiral catalysts (Figure 66).

Because the nonimmobilized heteropolyacids normally give rise to soluble catalysts, immobilization is due to the interaction of the support with the counterion, and in this regard, this strategy is closely related to the immobilization by hydrogen-bond interaction of triflate counterions with surface silanols.

Pioneering work in this field was carried out by Augustine et al.,<sup>175–177</sup> who used phosphotungstic acid (PTA) over different supports. [(DiPAMP)Rh(cod)]/PTA/K10 montmorillonite catalyst was used in the hydrogenation of methyl 2-acetamidoacrylate (Scheme 13). In the first use, the reaction was slower and less enantioselective than in solution, but the recovered catalyst was far more active and enantioselective, and these results were maintained during 15 cycles. Several other supports were tested (carbon, alumina, and lanthana), and the best results were reached with alumina (Table 25).



**Figure 66.** Schematic representation of supported HPA–Rh–(diphosphine) complexes.

**Table 25. Results from the Hydrogenation of Methyl 2-Acetamidoacrylate with [(DiPAMP)Rh(cod)]/PTA Catalysts<sup>a</sup>**

support	cycle	rate <sup>b</sup>	ee %
homogeneous	1	0.25	76
	K10	1	0.18
	3	1.26	94
alumina	1	0.32	90
	3	1.67	93

<sup>a</sup> Data from ref 175. <sup>b</sup> Given as mol of H<sub>2</sub> (mol of Rh)<sup>-1</sup> min<sup>-1</sup>.

**Table 26. Results from the Hydrogenation of Methyl 2-Acetamidoacrylate with [(Ligand)Rh(cod)]/PTA/Alumina Catalysts<sup>a</sup>**

ligand	cycle	immobilized		homogenous	
		rate <sup>b</sup>	ee %	rate <sup>b</sup>	ee %
Prophos	1	2.0	68	0.26	60
	3	2.6	63		
MeDuPhos	1	1.8	83	3.3	96
	3	4.4	95		
BPPM	1	3.75	21	7.4	84
	3	8.15	87		

<sup>a</sup> Data from ref 175. <sup>b</sup> Given in mol of H<sub>2</sub> (mol of Rh)<sup>-1</sup> min<sup>-1</sup>.

The strategy was also efficient for other ligands (Table 26).

More recently some chiral catalysts immobilized using this approach have been tested in the hydrogenation of dimethyl itaconate. A comparison of [(MeDuPhos)Rh(cod)]BF<sub>4</sub> with [(MeDuPhos)Rh(cod)]/PTA/charcoal and [(MeDuPhos)Rh(cod)]/PTA/alumina showed a higher activity for the homogeneous catalyst with higher TOF (23 000 h<sup>-1</sup> vs 6600 h<sup>-1</sup> and 1100 h<sup>-1</sup>, respectively). With all the catalysts, TON was around 10 000 and 96% ee was obtained. One advantage of these heterogeneous catalysts was that they could be reused several times, leading to high cumulative TON without leaching of Rh. While the homogeneous catalyst was more active in the first run, when the substrate was fully hydrogenated and a second amount of alkene was added to the reaction mixture, no further reaction was observed, in contrast with the activity of the supported catalysts, showing their higher stability.

A similar behavior was observed with Rh–BDPP catalysts; again the homogeneous catalyst was more active but less stable. Enantioselectivity was also higher with the immobilized system, in particular at high TON. Some experiments showed that the lower activity of the immobilized catalysts was related to diffusion control.

In an attempt to determine the nature of the HPA–metal interaction, several substrates were hydrogenated using chiral and nonchiral complexes anchored to alumina by the commercially available Keggin HPAs, phosphotungstic acid (PTA), phosphomolybdic acid (PMA), silicotungstic acid (STA), and silicomolybdic acid (SMA).<sup>177</sup> The use of different supports in the hydrogenation of methyl 2-acetamidoacrylate with [(DIPAMP)Rh(cod)] showed a different influence of pressure and temperature. In general, higher TOF and enantioselectivity were obtained with PMA, although the best TOF was reached with STA at 40 °C and 30 psig.

In the hydrogenation of dimethyl itaconate promoted by [(MeDuPhos)Rh(cod)], the best results were again obtained using PTA (TOF 1050 h<sup>-1</sup>, 97% ee). Whereas enantioselectivity was less influenced by the nature of the HPA, with the lowest value (88% ee) obtained using SMA, reaction rate suffered from more significant changes and TOF decreased

**Table 27. HPA Effect on the Hydrogenation of Dimethyl Itaconate Catalyzed by [(BINAP)Ru]HPA/Alumina<sup>a</sup>**

HPA	run	reaction rate (mmol H <sub>2</sub> min <sup>-1</sup> )	ee %
PTA	1	0.028	85
	5	0.034	72
	11	0.035	68
STA	1	0.052	84
	4	0.036	85
	7	0.032	83
SMA	1	0.047	86
	4	0.056	90
	6	0.048	94

<sup>a</sup> Data from ref 177.

**Table 28. Hydrogenation of Dimethyl Itaconate with [(MeDuPhos)Rh(cod)]X Catalysts<sup>a</sup>**

catalyst	X	solvent	H <sub>2</sub> pressure (bar)	T (°C)	TOF (h <sup>-1</sup> )	ee %
homogenous	BF <sub>4</sub>	MeOH	3.3	20	30 000	96
	BF <sub>4</sub>	<sup>t</sup> PrOH	3.3	20	32 000	95
	Cl	MeOH	3.3	20	1 200	92
heterogenous	BF <sub>4</sub>	<sup>t</sup> PrOH	3.3	20	2 000	97
	Cl	<sup>t</sup> PrOH	3.3	20	1 400	97
	BF <sub>4</sub>	<sup>t</sup> PrOH	6.6	50	17 000	96
	Cl	<sup>t</sup> PrOH	6.6	50	13 000	97

<sup>a</sup> Data from ref 178.

to only 95 h<sup>-1</sup> using STA. The catalyst [(BINAP)Ru]HPA/alumina was also tested in the same reaction (Table 27). The PTA immobilized catalyst was the least active and enantioselective, recovered with the same activity but reduced asymmetric induction. With STA, enantioselectivity was stable upon recycling, but activity decreased. It seems that the best HPA for this reaction is SMA, with activity and enantioselectivity reasonably stable upon recovery. From these results, it was clear that the nature of HPA influenced both activity and selectivity in a way more important than expected by a simple change of counterion.

By the same immobilization approach, [(MeDuPhos)Rh(cod)]X/PTA/ $\gamma$ -alumina (X = Cl, BF<sub>4</sub>) catalysts were obtained by reaction of the chiral ligand with the corresponding immobilized Rh precursor. These immobilized catalysts were compared with the corresponding homogeneous [(MeDuPhos)Rh(cod)]X catalysts in the hydrogenation of dimethyl itaconate (Table 28).<sup>178</sup> Immobilized systems were less active but gave rise to similar enantioselectivity. It is important to note that, under comparable conditions, differences between homogeneous catalysts were larger than those observed between the immobilized systems. Authors speculated that immobilization on the HPA influenced the Rh–Cl bond, given that a shift toward less coordinating ability, similar to that of BF<sub>4</sub>, would explain this result. It was shown that leaching could be minimized, provided optimized parameters (substrate concentration, solvent, reaction temperature) were used.

Zsigmond et al. also used this approach to immobilize homogeneous chiral catalysts. In a first report, rhodium complexes were immobilized by a “ship-in-a-bottle” method (see section 5.2) and through PTA immobilized on NaY zeolite.<sup>179</sup> FT-IR spectra of the homogeneous and supported catalysts showed the same characteristic bands, but quite disturbed in the case of the heteropolyacid-immobilized catalyst. Unfortunately, the supported catalysts were compared in nonenantioselective reactions.

The chiral Rh–*N*-<sup>t</sup>Bu-prolinamide catalysts were tested in the enantioselective hydrogenation of the (*E*)-2-methyl-

**Table 29. Results Obtained from the Hydrogenation of (Z)-2-Acetamidocinnamic Acid and the Methyl Ester with Homogeneous and PTA-Immobilized Chiral Catalysts<sup>a</sup>**

catalyst	conversion %	TOF (h <sup>-1</sup> )	ee %
Substrate (Z)-2-Acetamidocinnamic Acid			
Rh-BDPP	30	180	99
Rh-BDPP/PTA/alumina	55	1250	89
Rh-diMeBDPP	90	540	96
Rh-diMeBDPP/PTA/alumina	70	1800	96
Rh-MeOBDPP	75	450	96
Rh-MeOBDPP/PTA/alumina	80	2000	99
Substrate Methyl (Z)-2-Acetamidocinnamate			
Rh-BDPP	5	30	96
Rh-BDPP/PTA/alumina	8	200	89
Rh-diMeBDPP	32	194	95
Rh-diMeBDPP/PTA/alumina	25	600	95
Rh-MeOBDPP	40	120	98
Rh-MeOBDPP/PTA/alumina	45	562	99

<sup>a</sup> Data from refs 180 and 181.**Table 30. Effect of Temperature on the Hydrogenation of Dimethyl Itaconate in scCO<sub>2</sub> at 10 MPa<sup>b</sup>**

T (°C)	conversion %	ee %
40	10	5
60	66	63
80	63	42
100	61	32

<sup>a</sup> CO<sub>2</sub> flow rate = 1.0 mL min<sup>-1</sup>; substrate (2.5 M solution in *i*-PrOH) flow rate = 0.25 mL min<sup>-1</sup>; H<sub>2</sub>/substrate ratio = 4:1 dosed at 5 MPa overpressure. <sup>b</sup> Data from ref 182.

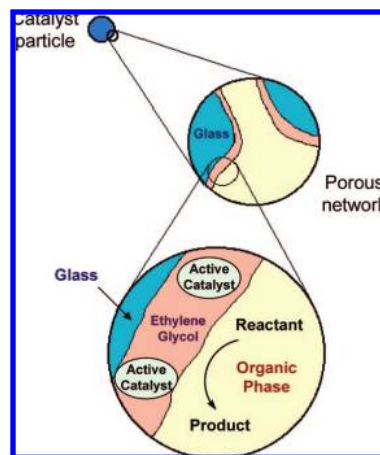
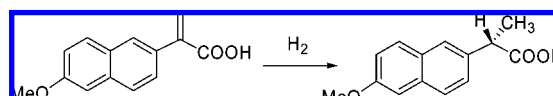
pent-2-enoic acid. Total conversions were obtained in 1 h with the homogeneous and both immobilized catalysts; however enantioselectivity increased from the homogeneous (13% ee) to the NaY encapsulated (17% ee) and mainly with the HPA/NaY catalyst (31% ee). Recovery of the immobilized systems was not studied.

Better results were obtained<sup>180,181</sup> with chiral diphosphines in the hydrogenation of (Z)-2-acetamidocinnamic acid (Scheme 1) and its methyl ester (Scheme 13). Results obtained (Table 29) showed a higher activity of the supported catalysts with a closely similar enantioselectivity. The increase of ligand basicity, by the introduction of two methyl groups and especially a methoxy group in the aromatic rings<sup>181</sup> noticeably improved both activity and enantioselectivity. Immobilized catalysts were used in three consecutive runs with the same activity and the same enantioselectivity.

Looking for a technically more attractive and greener enantioselective hydrogenation system, Poliakoff and co-workers<sup>182</sup> tested the continuous hydrogenation of dimethyl itaconate in scCO<sub>2</sub> using [(BDPP)Rh(nbd)]BF<sub>4</sub>/PTA/alumina as a catalyst. Conversion was relatively unaffected by changes in the total pressure of the system; however higher enantioselectivities were obtained at 10 MPa. Enantioselectivity is strongly influenced by temperature (Table 30), with the lowest value observed at low reaction temperature and moderate enantioselectivity obtained at 60 °C.

Under optimal conditions conversion is stable over a period of 8 h, with a total metal leaching <1 ppm. However when a similar ICP-MS analysis was conducted on the product stream from a reaction carried out at 100 °C, Rh (7.16 ppm) and W (1 ppm) were detected, indicating the lower stability of the immobilization under those conditions.

Sheldon and co-workers compared this methodology with cationic exchange in the case of [(MonoPhos)<sub>2</sub>Rh(cod)]<sup>+</sup> complex for hydrogenation of methyl 2-acetamidoacrylate.<sup>90</sup>

**Figure 67.** Schematic representation of SAP catalysts.**Scheme 61**

The effect of solvent was important, with ethyl acetate as the most efficient one, reaching TOF of 2300 h<sup>-1</sup>, higher than the values obtained with exchanged catalysts, and 97% ee with a recoverable catalyst. This system was also better when Rh leaching was considered, showing the strong interaction between complex and support.

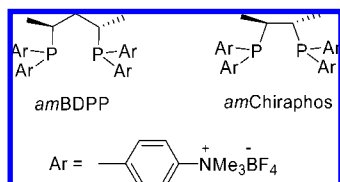
As can be seen, the formation of hydrogen bonds between support and anion (triflate or HPA) is a suitable method of immobilization for ionic complexes. Recoverability is highly influenced by the reaction solvent, although high stability has been reported in several examples.

### 4.3. Supported Liquid Phases

One original solution for the immobilization of homogeneous catalysts is the use of supported liquid phases (SLP). This approach was originally used for reactions in the gas phase. More recently glass bead technology<sup>183</sup> and related approaches have been used in many transition metal catalyzed reactions. In this context, the technique of supported aqueous phase (SAP) uses the hydrophilic nature of a surface to adhere a layer of water polar solvent in which a hydrophilic catalyst can be anchored. The catalyst retains the mobility in the solvent phase, which has a large surface area (Figure 67).

This approach was used in the asymmetric synthesis of naproxen by hydrogenation of 2-(6'-methoxy-2'-naphthyl)acrylic acid (Scheme 61) catalyzed by Ru-BINAP-4SO<sub>3</sub>Na (Figure 37).<sup>184</sup> An aqueous solution of the catalyst was adsorbed on a controlled pore glass (CPG-240) to yield a solid containing 1.9 wt % H<sub>2</sub>O and (1.2–2.5) × 10<sup>-5</sup> mol of Ru g<sup>-1</sup>. In the homogeneous phase in MeOH, the reaction reached about 90% ee, a result similar to that obtained with BINAP. With a biphasic system of AcOEt/H<sub>2</sub>O = 1:1, the enantioselectivity was near 80% ee, but the reaction was 350 times slower, which was due to the low interfacial surface, although aqueous catalyst was reused with the same results.

The SAP catalyst was 50 times more active than the biphasic system, and no leaching of ruthenium was observed. Enantioselectivity reached 70% ee, a value representing the



**Figure 68.** Tetraalkylammonium-modified diphosphine ligands.

intrinsic limit in water, and similar values were reached with the catalyst recovered by simple filtration.

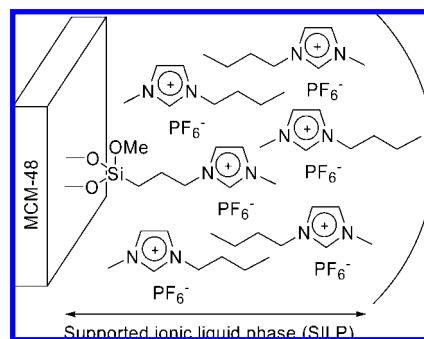
The low enantioselectivity was shown to be due to the hydrolytic cleavage of a Ru–Cl bond. In order to avoid this problem, water was substituted by ethylene glycol supported on CPG-240 and a mixture of cyclohexane/chloroform = 1:1 was used as the organic phase.<sup>185</sup> Up to 96% ee was obtained with an initial TOF only one-third of that of the homogeneous reaction and no leaching of Ru, leading to a recovered catalyst with almost the same performance.<sup>186</sup> In a liquid mixture of ethylene glycol/(cyclohexane/chloroform 1:1), the catalysts led to <2% conversion, due to the limited interfacial area; however complete conversion was reached when CPG-240 was added, demonstrating that the components of the heterogeneous system self-assembled and were more stable than they were separately.<sup>185,186</sup>

In these papers, water solubility of the catalysts was achieved by the incorporation of sulfonic groups on the ligand. Tóth et al. used chiral ligands bearing ammonium groups for catalysis with aqueous phase supported on CPG-350<sup>187</sup> (Figure 68).

A Pt catalyst with the modified BDPP ligand was used in the hydroformylation of styrene, but activity with the SAP was lower than that in organic solvents, and enantioselectivity was only 10% ee. The [(amBPPD)Rh(cod)]BF<sub>4</sub> complex in SAP was tested in the hydrogenation of (*Z*)-2-benzamido-cinnamic acid in AcOEt/benzene (1:1). Enantioselectivity (16% ee) was similar to that obtained in the organic phase (23% ee) but lower than the 50% ee reached with the biphasic aqueous/organic system. Higher enantioselectivity was obtained with the Chiraphos derivative (55.1% ee with SAP vs 65.0% ee with the biphasic system). In general, the SAP systems were less active than the homogeneous one and more active than the analogous biphasic system. Unlike other SAP examples, some deactivation and Rh leaching were observed upon recycling, and extensive oxidation of the phosphine was detected in the recovered catalyst.

Success of this kind of strategy depends on the correct choice of the solvents involved in the biphasic system, as well as the correct volume ratio between catalyst phase and reaction phase.

Supported ionic liquid phases (SILP) constitute a new kind of supported liquid phase with a high potential in enantioselective supported catalysis. Following this strategy, a solution of the dimeric salen–Cr(III) (Figure 59) in [bmim][PF<sub>6</sub>] was immobilized on silica and used in the asymmetric ring opening of epoxides<sup>188</sup> (Scheme 54). Compared with the impregnated system,<sup>163</sup> the SILP had some advantages, so in the reaction of 1,2-epoxyhexane, TOF increases from 1.9 to 11.5 h<sup>-1</sup> and enantioselectivity from 66% ee to 87% ee. Similar improvements were observed for the reaction of epoxy cyclohexane with enantioselectivity increasing from 65% ee to 75% ee, leaching being similar in both cases (about 3.1% over four runs). As it happened with impregnated catalyst, silica was deteriorated by stirring and continuous flow reaction was shown to yield excellent



**Figure 69.** Supported ionic liquid phase on a modified silica support.

**Table 31. Results Obtained from the Epoxidation of Several Alkenes Promoted by Salen–Mn in a Supported Ionic Liquid Phase<sup>a</sup>**

Alkene	Catalyst	conversion %	ee %
	homogeneous	>99	48
	SILP	50	41
	homogeneous	>99	50
	SILP	99	99
	homogeneous	96	80
	SILP	95	92
	(2 <sup>nd</sup> run)	93	90
	(3 <sup>rd</sup> run)	93	91

<sup>a</sup> Data from ref 189.

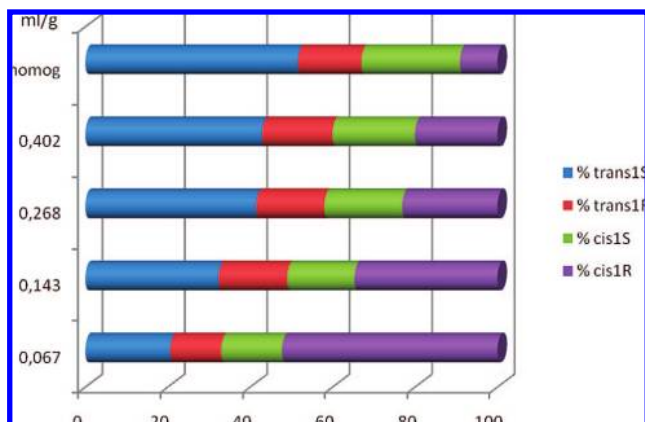
stability and selectivity over the time. After three consecutive runs accumulative TON of 314 and overall leaching of 0.7% were observed.

In an attempt to increase the affinity between the ionic liquid and the support, MCM-48 was modified by grafting to the surface 1-methyl-3-(3-trimethoxysilylpropyl) imidazolium hexafluorophosphate (Figure 69).<sup>189</sup> Over this MCM-48–imidazolium PF<sub>6</sub> (0.68 mmol/g), a solution of salen–Mn(III) in [bmim][PF<sub>6</sub>] was supported, and the catalyst was tested in the epoxidation of several alkenes with *m*CPBA.

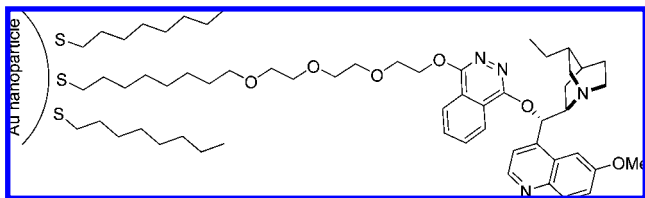
Except in the epoxidation of styrene, the immobilized system showed similar or even increased enantioselectivity compared with the homogeneous system (Table 31). This effect is remarkable in particular for  $\alpha$ -methylstyrene, with 99% ee obtained with the SILP system vs 50% ee in the liquid phase. These results were tentatively explained by a spatial effect caused by the well-defined 3D topological structure of the support, limiting the free rotation of the reaction intermediates. Due to the use of dichloromethane, a part of the reaction could take place in solution.

Recycling was carried out by evaporation of dichloromethane, washing with hexane, and filtration of the catalyst. No leaching of Mn(III) or ionic liquid (IL) was observed. Recycling was studied for epoxidation of 1-phenylcyclohexene, with no decrease in activity or selectivity for at least three runs.

The same strategy has been recently described for the cyclopropanation reactions using Box–copper catalysts.<sup>190</sup> In this work, [bmim][PF<sub>6</sub>] was supported on different solids (clays, graphite, Y zeolite, silica, and hydrotalcite). With decreasing amounts of IL, the thickness of the IL film was reduced, in the search of surface confinement effects similar



**Figure 70.** Effect of ionic liquid phase thickness on selectivity results of cyclopropanation reaction between styrene and ethyl diazoacetate.



**Figure 71.** DHQD derivative supported on gold nanoparticles.

to those described for the electrostatic exchange of the same Box-copper complexes in clays.<sup>43,44</sup> Only when a small amount of IL was supported on clays (laponite, bentonite, K10 montmorillonite) were the confinement effects observed (Figure 70), pointing to a strong interaction of the catalytic complex with the charged surface of the clay. Other lamellar solids, such as graphite or hydrotalcite, did not exhibit this effect, the catalytic results being identical to those obtained in homogeneous IL phase.

Supported liquid phases have shown until now limited applicability, with the crucial decision in the choice of solvents. Effects on activity and enantioselectivity, not only on recoverability, have been also described, but they are at the moment not fully understood.

#### 4.4. Nanoparticles as Supports for Chiral Catalysts

Nanoparticles can be used as supports for catalysts if a spacer bearing a suitable group is introduced in the complex, usually the chiral ligand. Given that the exact nature of the Au-S bond is still a matter of controversy,<sup>191–193</sup> this strategy may be considered to be on the border between covalent and noncovalent immobilization. Despite this, we have decided to include this approach in order to offer of a more complete view of “nonclassical” methods for immobilization of chiral catalysts.

First reports described the union of chiral ligands to gold nanoparticles through spacers bearing thiolate groups on one of the ends. Li et al.<sup>194</sup> immobilized dihydroquinidine (DHQD) ligands by the phase-exchange methodology on nanoparticles containing octanethiolates with a diameter of 2.5 nm (Figure 71).

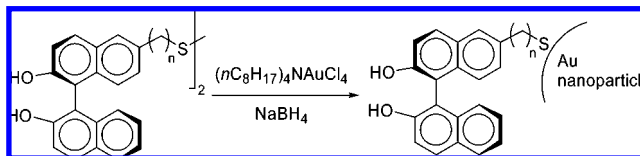
The ligand was used in the asymmetric dihydroxylation of alkenes, and the results are gathered in Table 32. Enantioselectivity was slightly lower than that in solution. Colloids were isolated by gel permeation chromatography, and both yield and enantioselectivity decreased upon recov-

**Table 32. Results Obtained in the Dihydroxylation Reaction Using DHQD Supported on Gold Nanoparticles<sup>a</sup>**

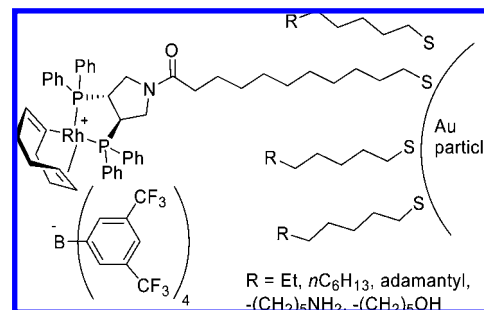
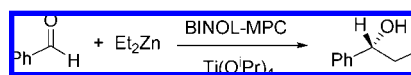
Alkene	Run	% yield	% ee
Ph-CH=CH-Me	1	81	90
	2	79	88
	3	72	79
Ph-CH=CH-COOMe	1	78	84
Ph-CH=CH-Ph	1	83	88

<sup>a</sup> Data from ref 194.

**Scheme 62**



**Scheme 63**



**Figure 72.** Example of diphosphine-Rh complex supported on gold nanoparticles.

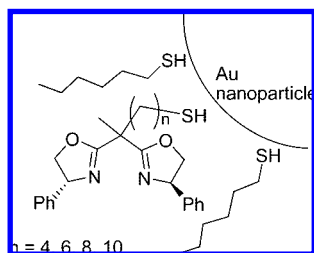
ery, which was probably due to desorption of alkene thiolates from the colloids, due to the oxidation to disulfides.

Despite these problems, the approach has two important features: the structure of the monolayer is well ordered, and it is possible to control the environment and density of molecules on the surface. Furthermore preparation allows wide flexibility in tailoring both the size and the chemical functionality of the particles.

Monolayer-protected Au clusters (MPCs) of nanometric size were prepared by treatment of a toluene solution of  $(n\text{-C}_8\text{H}_{17})_4\text{N}^+\text{AuCl}_4^-$  with disulfide bearing two (*R*)-BINOL moieties and  $\text{NaBH}_4$ . Transmission electron microscopy (TEM) and dynamic light scattering (DLS) showed the existence of swollen BINOLate MPCs (Scheme 62).<sup>195</sup>

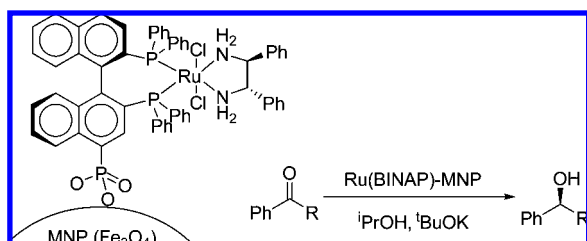
MPCs were tested in the catalytic alkylation of benzaldehyde with diethylzinc (Scheme 63). With 10% MPC, yields higher than 90% were obtained; the highest enantioselectivity (86% ee) was obtained with  $n = 5$ , a value slightly lower than the 90% obtained with BINOL. The supported ligand with  $n = 5$  was recovered by treatment with 1 N HCl and reused with more  $\text{Ti}(\text{iPrO})_4$  with a 92% yield and 68% ee. BINOL leaching was not observed.

Chiral diphosphines were also immobilized by reaction of gold particles with the corresponding disulfides (Figure 72).<sup>196</sup> The rhodium complex was used in the hydrogenation of methyl (*Z*)-2-acetamidocinnamate (Scheme 13). In the first



**Figure 73.** Bis(oxazoline) ligands with different spacers supported on gold nanoparticles.

**Scheme 64**



reaction, 98% yield and 92% ee were obtained (homogeneous, 99% yield and 93% ee), but upon recovery, activity decreased despite the absence of leaching.

In an effort to improve the catalyst, smaller gold nanoparticles (diameter between  $2.3$  and  $3.5 \pm 0.6$  nm) were prepared with several thiol groups bearing apolar and polar ends, and chiral ligand was incorporated by thiolate exchange (Figure 72). The catalyst-bearing thiolates remained statistically distributed on the surface; furthermore the S–Au bonds proved to be stable up to  $150$  °C and under the reaction conditions. The nature of the thiolate chain influenced the reaction results, and the best results were obtained with the nonpolar chains, even in reactions carried out in dichloromethane (>99 yield, 93% ee; homogeneous >99% yield, 93% ee) and in EtOH (91% yield, 88% ee; homogeneous 61% yield, 88% ee). Polar colloids proved to be less active and enantioselective. Recovery was carried out by treatment with cycloocta-1,5-diene to restore the original catalyst and filtration with a centrifugal filter (molecular size cutoff of 50 kD). Enantioselectivity was constant after three recycling steps, but conversion decreased to 74% in the fourth reaction.

Ono et al.<sup>197</sup> prepared nanosized gold particles stabilized by hexanethiol partially substituted with a thiol bearing a bis(oxazoline) ligand complexed with  $\text{Cu}(\text{OTf})_2$  (Figure 73). These nanoparticles were used as catalysts in the ene reaction between 2-phenylpropene and ethyl glyoxylate (Scheme 17).

Catalyst with  $n = 4$  was the most active (99% yield, 86% ee) due to the minimized aggregation in  $\text{CH}_2\text{Cl}_2$ , so that the system behaved as an almost homogeneous catalyst. Nanoparticles underwent dense aggregation when diluted in hexane, so that they could be separated by filtration. The optimal catalyst showed also better recoverability, with constant enantioselectivity and slight decreases in activity (94%, 90%, 87%, and 80% yield) in successive reuses.

In order to make separation easier, chiral catalysts have been also immobilized on magnetic nanoparticles (MNPs). One example is the immobilization of a modified Ru(BINAP) on MNPs of  $\text{Fe}_3\text{O}_4$  by ultrasonication (Scheme 64).<sup>198</sup> Slight aggregation was observed by TEM. Magnetic particles synthesized by thermal decomposition (MNP1) or coprecipitation (MNP2) were compared in the hydrogenation of aromatic ketones (Scheme 64).

Both  $\text{cat}^+$ -MNPs catalyzed the reduction of several ketones with complete conversion and enantioselectivities from 86% to 98% ee, similar to those obtained with the same catalyst in homogeneous phase. Catalysts were easily separated using an external magnet. Catalyst on MNP1 was used for six cycles with the same enantioselectivity (from 98% to 96.8% ee) and a decrease in activity in the fifth run (92% conv) and even more in the sixth (35% conv). Catalyst on MNP2 was used 14 times without decrease in conversion and selectivity; conversion noticeably dropped in the 15th reaction.

The use of nanoparticles as supports for enantioselective catalysts is a field still scarcely explored and conclusions about the general applicability cannot be drawn.

## 5. Entrapment Methods

In the entrapment methods, the objective is to keep the catalytic complex enclosed inside the structure of the support without the need for an additional support–complex interaction. For this purpose, the size of the complex must be larger than the pore mouth of the solid during the catalytic process. We can distinguish two main methods: entrapment into a flexible polymer or entrapment into a rigid inorganic matrix. Both the requirements and the limitations of the method are clearly influenced by the type of support, and the discussion has been separated.

### 5.1. Entrapment into Flexible Matrixes

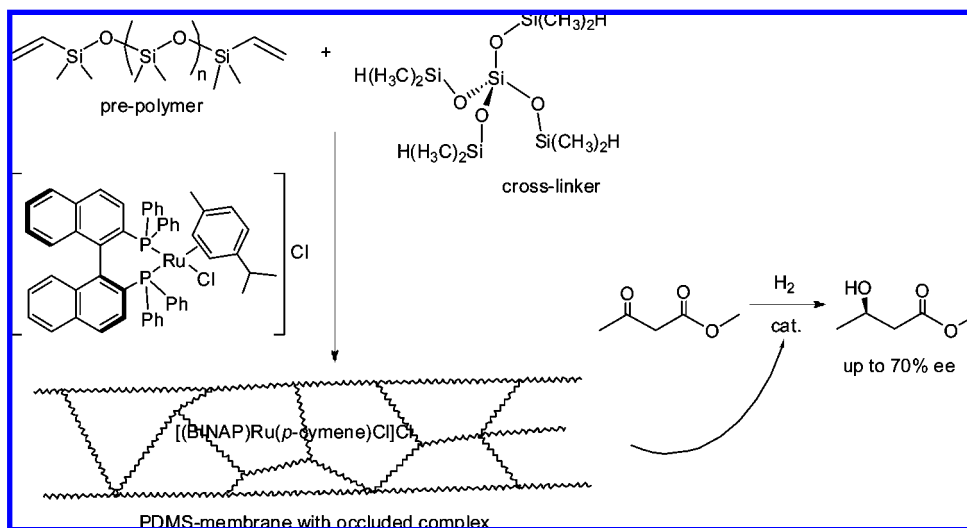
The first example of this kind of immobilization was described by Jacobs and co-workers.<sup>199,200</sup> The complex,  $[(\text{BINAP})\text{Ru}(p\text{-cymene})\text{Cl}]\text{Cl}$ , was immersed in a mixture of a dimethylsilicone prepolymer and a tetrasilane cross-linker in a Petri dish. After curing at  $150$  °C for 1 h, a silicone membrane (PDMS) of 0.2 mm thickness was formed containing the catalytic complex (Scheme 65). This membrane was used as catalyst for the hydrogenation of methyl acetylacetate at 6 MPa in different solvents: water, ethylene glycol, PEG, and glycerol. Leaching was not detected in any of them, and the results were in the range of 61–70% ee and  $0.09$ – $0.17$   $\text{min}^{-1}$  TOF in the three alcohols.

In a subsequent work by the same group,<sup>201</sup> *p*-toluenesulfonic acid was simultaneously entrapped into the PDMS membrane with  $[(\text{BINAP})\text{-Ru}(p\text{-cymene})\text{Cl}]$ . The effect of the acid in the homogeneous phase was dramatic both to accelerate the reaction and to improve enantioselectivity from 61% to 96% ee in ethylene glycol. This effect was not observed with the entrapped catalyst unless the acid was also included in the membrane in sufficient amount but not too much given that an excess of acid reduced the cross-linking degree of the membrane and some leaching of acid was detected. Results of  $41.6$   $\text{h}^{-1}$  TOF with 92% ee were obtained with a reusable catalyst, although the recovery results were not reported.

The same type of PDMS membrane was used to immobilize  $[(\text{MeDuPhos})\text{Rh}(\text{cod})]\text{OTf}$  (Figure 74) in the same way.<sup>202</sup> The catalytic activity in the hydrogenation of methyl acetylacetate was significantly lower than that in solution, irrespective of the solvent used (methanol or ethylene glycol), and enantioselectivity was also reduced from 99% to 90–93% ee. However, the catalyst was fully recoverable once, and leaching was not detected in any case. The same immobilized catalyst was later used in the hydrogenation of methyl 2-acetamidoacrylate (Scheme 13).<sup>203</sup> The experimental procedure was changed, from using a complete



## Scheme 65

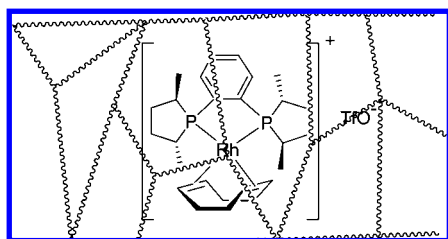


membrane between two porous stainless steel disks to the addition of the membrane cut into pieces to the reaction medium. Under those conditions extensive leaching was detected with a strong effect of solvent (31% in methanol, 52% in dichloromethane, <1% in water or heptane) that depends both on the solubility of the complex and on the swelling degree of the membrane. Again catalytic activity was significantly lower than that in homogeneous phase, and enantioselectivity up to 96.7% ee was obtained.

The same [(MeDuPhos)Rh(cod)]OTf complex was occluded into poly(vinyl alcohol) (PVA) films,<sup>204</sup> formed either by physical (hydrogen bonding) or by chemical (malate formation) cross-linking. A careful comparative study of leaching in different solvents with both types of films and the previously described PDMS membrane was described. The leaching degree was similar with both PVA films and always higher than in the case of PDMS, with the only exception of xylene. Despite this result, the hydrogenation of methyl 2-acetamidoacrylate was carried out in water, with catalytic performance very similar to that obtained with PDMS.

At the same time as for immobilization of hydrogenation catalysts, PDMS membranes were described to immobilize Jacobsen's catalyst (Figure 75) for alkene epoxidation.<sup>199,200</sup> Epoxidation reactions were carried out in a countercurrent reactor, with separate streams of alkene dissolved in heptane and oxidant (NaOCl) in aqueous solution. Enantioselectivities were moderate (52% ee with styrene, 18% ee with *trans*- $\beta$ -methylstyrene) but similar to those obtained in solution. Reuse of the membranes was carried out after washing with acetone and drying, reaching the same results of activity and selectivity, with only 1% leaching detected.

This low leaching degree contrasts with results reported in a subsequent paper<sup>205</sup> in which leaching for Jacobsen's



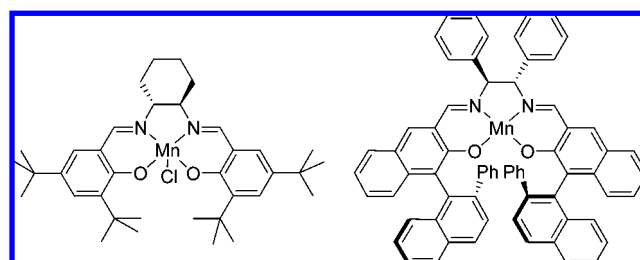
**Figure 74.** [(MeDuPhos)Rh(cod)]OTf occluded in a PDMS membrane.

catalysts ranging from 12% in heptane to 100% in chlorobenzene were described. A new dimeric complex was developed (Figure 59, M = Mn) in an attempt to reduce the leaching degree, thanks to the larger size of the catalyst. The results were only partially successful, as the leaching was reduced (56% maximum in chlorobenzene) but not completely eliminated.

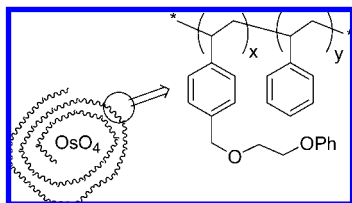
The leaching problem was later revisited,<sup>206</sup> and data for the bulkier Katsuki's catalyst (Figure 75) were given, ranging from 2.7% in heptane to 65.9% in chloroform. The important reduction of leaching degree under reaction conditions was ascribed to the change in configuration of the catalytic complex from the planar form to a pyramidalized shape upon activation due to the formation of the Mn-oxo species.

Other authors have reported the occlusion of Jacobsen's catalyst into modified PDMS membranes to perform the epoxidation of different alkenes.<sup>207,208</sup> Despite using a chiral complex, the reactions were not enantioselective and the role of the membrane was the modulation of the results and the applicability of different oxidants depending on the hydrophilic/hydrophobic character.

Another methodology to entrap catalysts into flexible matrices is microencapsulation. The idea of microcapsules (MC), formed by linear polymers to coat and isolate substances until they are needed to act, is imported from medicine and pharmacy fields.<sup>209</sup> The first example of use of a microencapsulated catalyst in enantioselective reactions was described by Kobayashi and co-workers in 1999.<sup>210</sup> The support was a linear copolymer of acrylonitrile-butadiene-styrene (ABS) and OsO<sub>4</sub> was encapsulated by cooling a THF solution of support and osmium species, with final hardening of the capsules with methanol. This nonchiral catalyst was tried in the asymmetric dihydroxylation of alkenes by addition of (DHQD)<sub>2</sub>PHAL as a chiral ligand in the reaction



**Figure 75.** Jacobsen's and Katsuki's (salen)Mn complexes.



**Figure 76.** Phenoxyethoxymethyl–polystyrene (PEM) support.

medium. Catalyst was recovered by filtration after reaction, whereas the chiral ligand was recovered (>90%) by extraction. In this way, five consecutive reactions of *trans*- $\beta$ -methylstyrene hydroxylation with *N*-methylmorpholine *N*-oxide gave 88%, 75%, 97%, 81%, and 88% yield with 84%, 95%, 94%, 96%, and 95% ee.

Potassium hexacyanoferrate ( $K_3Fe(CN)_6$ ) was used as an oxidant in a subsequent work.<sup>211</sup> Results were highly dependent on the polymer nature, with polystyrene and poly(acrylonitrile–styrene) unsuitable, whereas ABS polymer was highly efficient but with recovery poorer than in the previous paper. This was ascribed to the hydrophilic character of the polymer, leading to a partial dissolution in the water/<sup>t</sup>BuOH reaction medium. A new support (phenoxyethoxymethyl–polystyrene, PEM, Figure 76) was prepared and reaction medium was changed to water/acetone in order to optimize recovery. Enantioselectivities in the range of 76–99% ee were obtained with different alkenes.

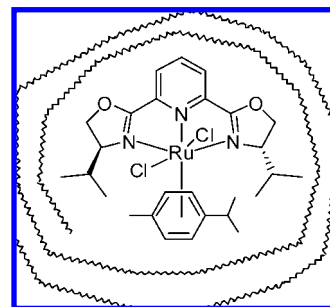
A further improvement on this methodology allows the use of water alone as reaction solvent, but it requires the addition of a surfactant.<sup>212</sup> The nature and amount of the surfactant have a great influence on the results, regarding both performance and recoverability. The optimal results were obtained with nonionic surfactants, in particular with Triton X405 (isooctylphenyl-capped polyethylene glycol), reaching 75% ee with 82–86% yield in three consecutive runs of styrene dihydroxylation. Different alkenes were also dihydroxylated with enantioselectivities in the range of 55–92% ee.

Microcapsules need to be formed by flexible polymers, and linear ones are generally used. However, the same authors described the possibility of preparing microcapsules with cross-linked polymers, keeping a low cross-linking degree to ensure the flexibility of the support. In such case, simple polystyrene with only 1% divinylbenzene cross-linker led to similar results<sup>213</sup> to those obtained with linear functionalized polymers in aqueous reaction medium with Triton X405 surfactant: five consecutive runs of styrene dihydroxylation with 78–86% yield, 72–78% ee, and no detectable Os leaching.

Polysulfone–OsO<sub>4</sub> microcapsules were recently described as efficient catalysts for asymmetric dihydroxylation of *trans*-stilbene with *N*-methylmorpholine *N*-oxide,<sup>214</sup> leading to 97% ee in five consecutive runs and also excellent results with other substrates.

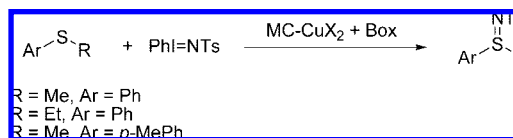
In none of those papers is the recycling of the whole chiral complex described, probably due to its labile character, origin of the leaching problems detected with other types of solid catalysts. In fact, most papers describe the addition of methanol or ethanol at the end of the reaction to harden again the microcapsules, indicating that probably the catalytic reaction takes place in homogeneous phase, where the chiral complex is formed, whereas after reaction completion the Os catalyst is encapsulated again to be filtered.

In fact, the reversibility of the process was assumed in the work describing the microencapsulation of <sup>i</sup>PrPybox-



**Figure 77.** Encapsulated <sup>i</sup>PrPybox–RuCl<sub>2</sub> complex.

#### Scheme 66



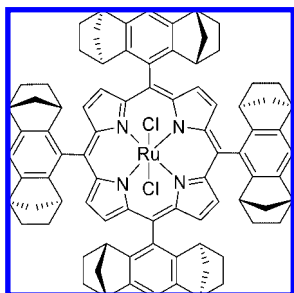
RuCl<sub>2</sub> into polystyrene capsules (Figure 77).<sup>215</sup> In such case the benchmark cyclopropanation reaction between styrene and ethyl diazoacetate (Scheme 5) was carried out in CH<sub>2</sub>Cl<sub>2</sub>, where the encapsulated catalyst was completely soluble, and the reaction took place in homogeneous phase. However, the addition of a nonpolar solvent (hexane or cyclohexane) led to the reformation of the capsules, which were filtered-off, washed, and reused. Up to three recycles were possible, without loss of catalytic activity and enantioselectivity, under the best conditions.

The microencapsulation method was used by Kantam et al. to immobilize Cu(acac)<sub>2</sub> in polystyrene, which was subsequently modified with <sup>t</sup>BuBox and PhBox ligands and used as catalyst in enantioselective sulfimidation reactions (Scheme 66).<sup>216</sup> A Box/Cu ratio = 2 was necessary to obtain a significant enantioselectivity, which was low (up to 23% ee) in all the cases. In a more recent work by the same group,<sup>217</sup> poly(*N*-vinyl pyrrolidone) was used as a support for Cu(OAc)<sub>2</sub>. In this case, encapsulation was not the only immobilization mechanism, as some coordination between Cu and support was detected by different spectroscopic techniques. Moderate enantioselectivity was obtained with <sup>t</sup>BuBox: 50% ee for methyl phenyl sulfide, 60% ee for ethyl phenyl sulfide, 68% ee for methyl *p*-tolyl sulfide. Again an excess (2:1 ratio) of chiral ligand was necessary to achieve this enantioselectivity level, and ligand was lost upon recycling, in agreement with the low formation constant of the <sup>t</sup>BuBox–Cu complex described by our group.<sup>42</sup>

As a general conclusion on the entrapment into flexible supports, we can say that leaching is the main problem, related to the swelling behavior of the polymer in the presence of the reaction solvent and the corresponding solubility of the complex in the same solvent. In the case of microcapsules, the immobilization may be considered reversible, the catalyst being released to the solution under reaction conditions and encapsulated again by change of solvent.

## 5.2. Entrapment into Rigid Supports

The problems related to the use of flexible matrixes might be solved by using rigid supports to entrap the chiral catalyst. Because the catalyst must be retained, the pore opening must be smaller than the molecular catalyst size. Some authors have tried to build the support around the preformed complex, always taking into account that the catalyst must be stable under the conditions of support preparation.



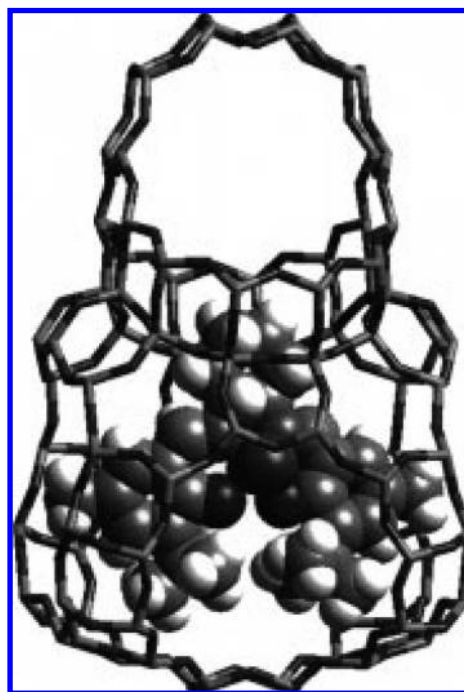
**Figure 78.** Ru–porphyrin complex entrapped in silica.

One example of this strategy was described by Gelman et al.<sup>218</sup> [(BINAP)Ru(*p*-cymene)Cl]Cl, [(DIOP)Rh(cod)Cl], and [(BPPM)Rh(cod)Cl] complexes were physically entrapped into porous silica prepared by sol–gel method from Si(OEt)<sub>4</sub>, either directly or by prehydrolysis of the silane in acidic medium (required for Rh complexes). We can speculate the existence of three species in the final amorphous solid: inaccessible internal species, accessible internal species, and external molecules. Molecules of the first type would not participate in the catalytic process, whereas external molecules would be leached to the solution. Despite the thorough washing of the solid with CH<sub>2</sub>Cl<sub>2</sub>, hydrogenation reactions of itaconic acid in THF led to substantial leaching, showing that an important part of the complex remained on the external surface. The lack of leaching in aqueous reactions may be ascribed to the low solubility of the complexes in water.

A similar procedure was used to entrap a chiral Ru–porphyrin complex (Figure 78).<sup>219</sup> As in the precedent case, the nature of the solid was not studied. The epoxidation of alkenes (styrene as benchmark) with 2,6-dichloropyridine *N*-oxide was much slower than that in solution, showing important diffusion restrictions, although with similar enantioselectivity (70% ee). In the recycling, catalytic activity diminished in three successive runs, with final total deactivation. This phenomenon is also observed in solution due to the formation of Ru–CO complex. For this type of problem, site isolation in a solid matrix has no positive effect. In any case, it is remarkable that in one single reaction a TON > 10 000 was obtained. As in the previous case, leaching was observed (30% in benzene), but the activity of the remaining complex was not described.

Jacobsen's catalyst was entrapped in alumina, prepared by a nonhydrolytic route consisting of the reaction of AlCl<sub>3</sub> with diisopropyl ether.<sup>220</sup> The resulting hybrid material showed lower porosity (0.09 vs 0.18 mL/g) and surface area (31 vs 100 m<sup>2</sup>/g) than the analogous pure alumina material. The solid catalyst was more active and stable than the homogeneous counterpart with several oxidants, *m*-CPBA and 70% H<sub>2</sub>O<sub>2</sub> being the most significant cases, and recycling was possible. However, no results of enantioselectivity were described.

In these limited number of examples using amorphous solids, the accessibility to the entrapped catalytic sites was not controlled by the structure of the matrix. In order to assess access to the catalyst, a crystalline solid with a regular pore system is necessary. In this regard, zeolites with supercages in their structure were considered as the best alternative. The immobilization strategy would be the introduction of portions of the catalyst, small enough to enter through the pore aperture, and formation of the complex inside the supercages. Because the complex would be larger than the pore aperture,



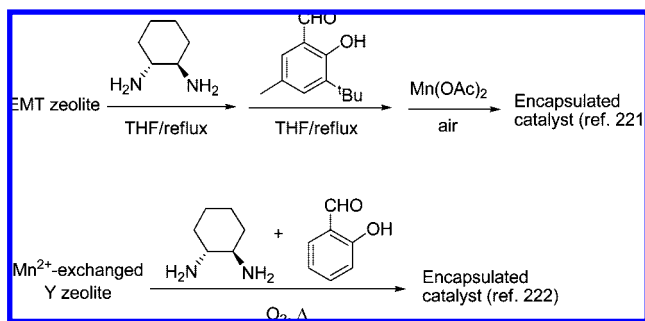
**Figure 79.** View of the molecular fit of Mn(salen) in EMT (Cerius2 software). Reprinted by permission of the Royal Society of Chemistry, ref 221.

it would be retained inside the pore system. This is the method called “ship-in-a-bottle” synthesis. At least four points should be stressed when this methodology is applied: (i) the real complex–matrix interaction, because many examples deal with cationic complexes and anionic supports; (ii) the formation of the whole ligand or complex, mainly in cases where two identical functional groups must be formed and spectroscopic techniques cannot give reliable information; (iii) the presence of uncomplexed metal, which may act as a nonchiral catalytic species; (iv) the suitability of the support cages to host not only the catalytic complex but, more importantly, the reaction intermediate and the corresponding transition state.

The first examples reported in the literature of application of this methodology to chiral complexes were devoted to (salen)Mn complexes. Ogunwumi and Bein<sup>221</sup> used EMT zeolite as support. This zeolite presents hypercages with three 12-ring windows (0.69 nm × 0.74 nm) and two circular windows (0.74 nm Ø). It was estimated that Jacobsen's complex would not fit inside those hypercages, and a reduced ligand with methyl groups in the 4-position of the salicylaldehyde moieties was considered (Figure 79).

The immobilized complex was prepared by sequential adsorption of chiral 1,2-diaminocyclohexane and 6-*tert*-butyl-4-methylsalicylaldehyde in the zeolite, reaction under reflux, complexation with Mn(OAc)<sub>2</sub> and simultaneous oxidation in air, and final Soxhlet extraction (Scheme 67). The reduced void volume of the obtained solid was evidence for the occlusion of the catalytic complex. The immobilized complex was tested in the epoxidation of different alkenes with aqueous NaOCl, showing activities and selectivities to epoxide much lower than those in solution. It was proposed that a significant portion of the immobilized complex did not take part in the reaction due to diffusion restrictions. Another possible explanation for this effect might be the presence of free Mn in the solid, although this possibility was not explored. The use of an axial ligand increased both

Scheme 67



activity and enantioselectivity, up to 88% ee in the case of (*Z*)- $\beta$ -methylstyrene. Another evidence for the true inclusion of the complex was the lack of activity with bulkier substrates (cholesterol) or oxidants (iodosylbenzene). This catalyst was not recoverable, in agreement with our own findings.<sup>53</sup>

An analogous strategy was followed by Corma and co-workers.<sup>222</sup> The use of Y zeolite as support precluded the use of Jacobsen's complex, and unsubstituted salicylaldehyde was used in the synthesis of (salen)Mn complex. In this case, Mn was first exchanged in the zeolite, with subsequent reaction with salicylaldehyde and chiral 1,2-diaminocyclohexane. Similar conclusions (reduced activity and selectivity, restrictions to bulkier oxidants) were obtained.

The same group explored the preparation of (salen)Cr with different bulkiness entrapped into Y and EMT zeolites.<sup>223</sup> The preparation method included Cr<sup>3+</sup> exchange of the zeolite, reaction with the salicylaldehyde under reflux, reaction with the chiral diamine, and finally Soxhlet extraction. Very low enantioselectivities were obtained in the ring opening of epoxides with trimethylsilyl azide. This problem, also detected in the case of the same complex exchanged in K10 montmorillonite, was ascribed to the bimolecular character of the catalysis, impossible for the heterogeneous catalysts due to the site isolation phenomenon.

In the both preceding cases, the use of cationic (salen)M<sup>III</sup> complexes made doubtful the total elimination of external complex by Soxhlet extraction. This is not the case for the (salen)Co<sup>II</sup> complex entrapment.<sup>224</sup> The use of ultrastable Y zeolite (USY), with a more developed porosity, allowed the formation of the complex by the "flexible ligand" method. It considers that the free ligand is flexible enough to enter the pore aperture, but once the complex is formed, the forced conformation prevents it from exiting. In this case, the ligand was introduced by sublimation on Co-exchanged USY. Unfortunately, the immobilized catalyst showed almost no enantioselectivity in the reduction of acetophenone with NaBH<sub>4</sub>.

Another entrapped neutral complex was (salen)Pd<sup>II</sup>.<sup>225</sup> Jacobsen's ligand was used for both Y and EMT zeolites by the "flexible ligand" method, and in disagreement with previous estimations,<sup>222</sup> it was considered that the complex was formed inside the hypercages at 230 °C in a sealed ampule. In contrast with previous works, in this case the formation of acidic sites in the zeolite, with protons coming from the phenolic groups of the ligand, was considered, and a final exchange with Na<sup>+</sup> was carried out. The encapsulated complexes were tested in the enantioselective hydrogenation of 3-methylcyclohex-2-enone, but the asymmetric induction was always very low (up to 7% ee).

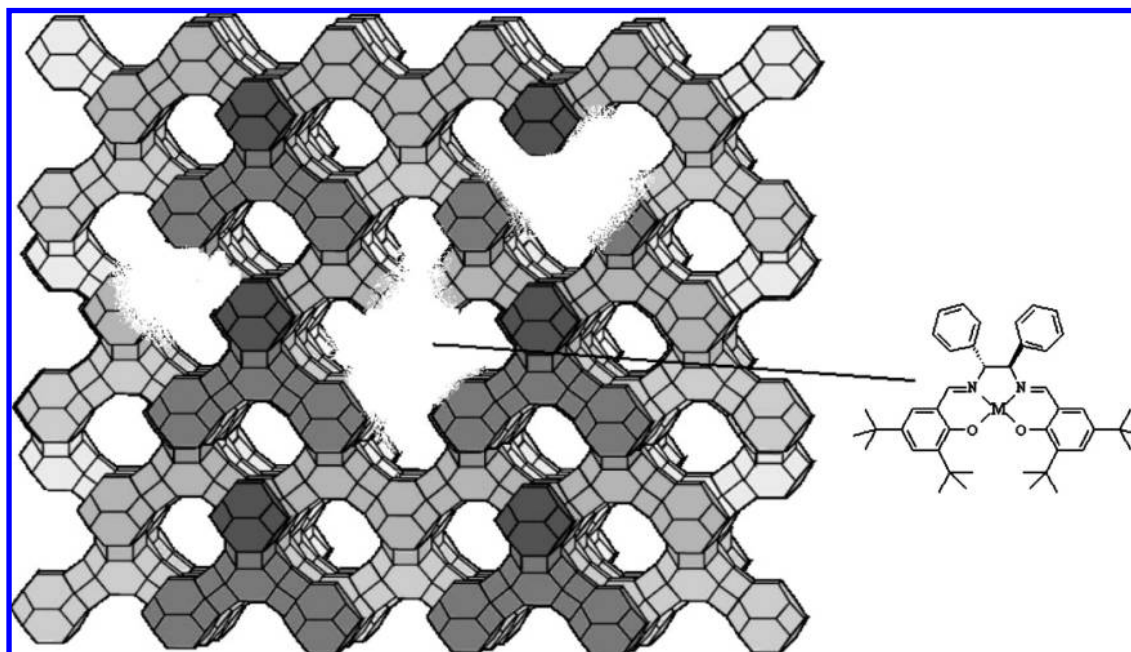
The main problem with the "ship-in-a-bottle" methodology is the use of zeolite structures with too small pore systems,

which might lead to incomplete assembly of the complexes. One alternative was proposed by Hölderich and co-workers, who prepared dealuminated faujasites by a combination of SiCl<sub>4</sub> treatment and steaming.<sup>226</sup> The elimination of most of the framework Al, only partially substituted by Si, generates mesopores, which according to the authors are completely surrounded by micropores, assuring the retention of the complex by a ship-in-a-bottle mechanism (Figure 80). However manganese is included in the zeolite by cationic exchange, and the charge is maintained in the final (salen)-Mn<sup>III</sup> complex, in such a way that an electrostatic interaction cannot be precluded. The immobilized catalysts were tested in the epoxidation of (*R*)-limonene (Scheme 23) with oxygen/pivalaldehyde and *N*-methylimidazole as an axial ligand. High pressure of O<sub>2</sub> was necessary to obtain moderate to high epoxide selectivities (32–70%) with moderate diastereoselectivities (32–55% ee).

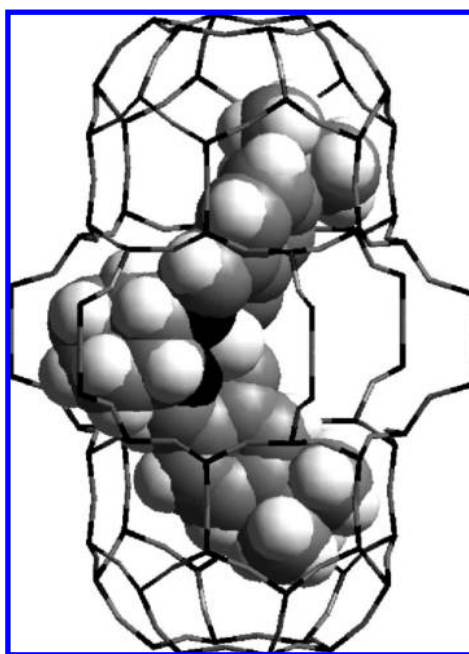
The same system was used to immobilize different (salen)M complexes (M = Mn, V, Fe, Cr, Co, Rh, or Ir), and the resulting solids were tested in the epoxidation of (*R*)-limonene and  $\alpha$ -pinene with the system O<sub>2</sub>/pivalaldehyde (Scheme 23).<sup>227,228</sup> Selectivity results for (*R*)-limonene epoxidation did not improve with the rest of tested complexes, although reuse of catalyst was proven. In the case of  $\alpha$ -pinene, results of conversion, epoxide selectivity, and diastereoselectivity were highly dependent on the metal and ligand nature, as well as the homogeneous or heterogeneous character of the catalyst. The best results were obtained with the (salen)Co complex shown in Figure 80, reaching total conversion, 96% epoxide selectivity, and 91% de, slightly better results than those obtained with the homogeneous counterpart. Both Mn- and Co-supported catalysts reached very high TON per batch, on the order of 1500–2500.

Alternatively, Gbery et al. proposed the construction of the zeolite structure around the preformed complex, taking advantage of the layered structure of MCM-22 zeolite.<sup>229</sup> Its larger pore size (0.71 nm  $\times$  1.82 nm) makes this zeolite suitable to accommodate the large Jacobsen's complex (Figure 81). The complex was adsorbed on the layered precursor and the final zeolite was assembled by heating at 280 °C. Finally the external species, together with the possible broken complex, were exchanged with Na<sup>+</sup>. The immobilized complex showed enhanced catalytic activity and enantioselectivity (91% ee vs 51% ee in solution) in the epoxidation of  $\alpha$ -methylstyrene with Clorox bleach. The heterogeneous character of the reaction was checked by filtration experiments, and the internal situation of the complex was inferred from the low activity in the epoxidation of cyclooctene, related to the difficulty to enter the 0.4 nm  $\times$  0.54 nm pore opening. As in previous cases, recycling was not described.

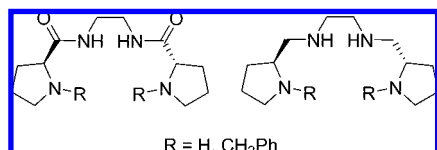
The real situation of the occluded complex molecules, their accessibility, and their participation in the catalytic process has been deeply studied by the group of García and Sabater. The effect of the zeolite matrix was first detected by the high stability of occluded (salen)Mn<sup>II</sup> against oxidation, in contrast with the behavior in solution.<sup>230</sup> An experimental proof of the chiral nature of the complex was the selective quench of the excited state of the complex by (*S*)-2-butanol and not by the *R* enantiomer. This study was only possible on the solid catalyst due to the instability of the Mn<sup>II</sup> complex in solution. The combination of different techniques allowed the detection of different nonchiral (salen)Mn species in two subsequent papers.<sup>231,232</sup> Cyclic voltammetry showed peaks



**Figure 80.** Model of (salen)Mn complex entrapped in mesopores of dealuminated faujasite. Reprinted with permission of Elsevier, ref 227.

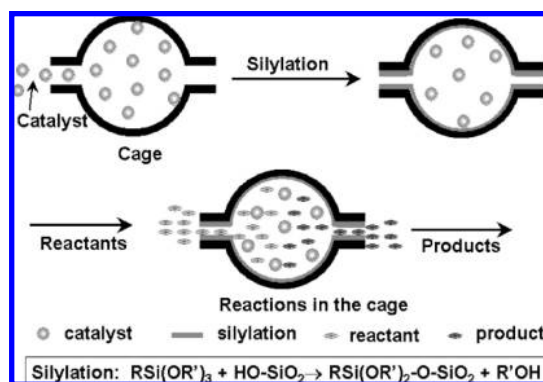


**Figure 81.** Structure of Jacobsen's catalyst minimized in an MCM-22 supercage calculated using Cerius<sup>2</sup> and the crystallographic parameters. Reprinted with permission of Springer, ref 229.



**Figure 82.** Tetradentate ligands used for encapsulated Mn complexes.

corresponding to  $\text{Mn}^{2+}$  and  $\text{Mn}^{3+}$  oxidation states, the former belonging mainly to uncomplexed  $\text{Mn}^{2+}$  easily exchanged by  $\text{Na}^+$ , as noted also by other authors. The combination of XPS and EPR experiments demonstrated that only 15–20% of the starting  $\text{Mn}^{2+}$  in Y zeolite was oxidized to  $\text{Mn}^{3+}$  and hence complexed with salen ligand and that portion was more



**Figure 83.** Schematic description of entrapping homogeneous catalyst within the cage of mesoporous silicas. Reprinted with permission of the Royal Society of Chemistry, ref 239.

abundant in the external part of the pore system of the zeolite. In view of that, the authors concluded that “in the case of transition metal complexes encapsulated within zeolites, the catalytic behavior could be due to a minor fraction of the total population residing in the outermost layers”.

Another attempt to demonstrate the effect of the zeolite matrix was carried out by Hölderich and co-workers.<sup>233</sup> Molecular dynamics simulation of (salen)Co<sup>II</sup> complex inside the cage of a purely siliceous zeolite was performed. Conformational restrictions were observed from calculations, accounting for the lower activity of the encapsulated complex due to blocking of the substrate approach trajectory. However, the enantioselectivities of the homogeneous and immobilized catalysts were as low as 8% ee, involving an energy difference less than  $0.1 \text{ kcal mol}^{-1}$ , and it is dubious that any molecular modeling method, especially one based on a general purpose force field, was able to correctly describe such tiny energy differences.

Encapsulation of Mn complexes with tetradentate ligands (Figure 82) were described by Iglesias and co-workers.<sup>234</sup> Complexes were prepared from Mn-exchanged Y zeolite by the “flexible ligand” method, and together with the occlusion phenomenon, an additional complex–zeolite electrostatic

**Table 33. Effect of Cobalt Density on the Catalytic Performance of (Salen)Co Complex in SBA-16 (Solid) and in Solution<sup>a</sup>**

cobalt per cage	solid			solution		
	conversion (%)	TOF (h <sup>-1</sup> )	diol, ee%	conversion (%)	TOF (h <sup>-1</sup> )	diol, ee%
1.2	8	27	93	49	115	98
1.9	30	100	94	50	149	98
3.4	49	163	98	49	228	98
4.9	50	167	98			

<sup>a</sup>Data from ref 241.

interaction was proposed. Elimination of external and non-complexed cationic species was carried out by Na<sup>+</sup> exchange, and additional stabilization with *N*-methylmorpholine *N*-oxide was used in the reaction medium. The enantioselective oxidation of alkyl aryl sulfides with NaOCl was tested (Scheme 29). Whereas the heterogeneous catalyst was less active and enantioselective with methyl phenyl sulfide (up to 19% ee), the activity was much higher in the case of 2-ethylbutyl phenyl sulfide, which is rather surprising taking into account the branched nature of this sulfide. Although similar levels of enantioselectivity (up to 21% ee) were obtained, it was better than that in solution (<5% ee), and the catalyst was recoverable four times.

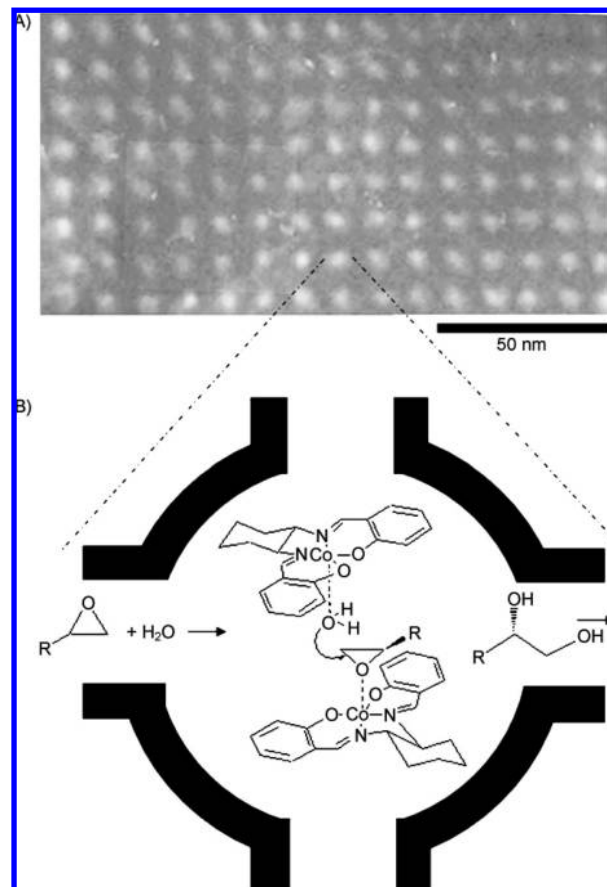
The same authors compared these encapsulated complexes with the analogous grafted catalysts.<sup>235</sup> In all cases, enantioselectivity was low, but the encapsulated catalysts showed lower activity and selectivity for sulfoxide.

Smaller complexes were encapsulated by Zsigmond and co-workers. [(Prolinamide)Rh(cod)]<sup>+</sup> and [(*N*-*Bu*-prolinamide)Rh(cod)]<sup>+</sup> complexes were formed in Rh-exchanged Y zeolite.<sup>236</sup> External species were eliminated only by washing with CH<sub>2</sub>Cl<sub>2</sub>, not by Na exchange. The lack of distortion in IR spectrum was ascribed to the small size of the complex, in comparison with the supercages of zeolite. Enantioselective hydrogenation of methyl (*Z*)-2-acetamidocinnamate (Scheme 13) was only briefly described, reporting an improvement of enantioselectivity (20% ee) from the almost null value in solution. In a subsequent paper,<sup>237</sup> the same authors compared the performance of these solids with other catalysts prepared in the outer surface of zeolite. The lower activity was considered evidence of the encapsulation, and also low enantioselectivity (17% ee) was reported for the hydrogenation of (*E*)-2-methyl-hept-2-enoic acid.

As can be seen from the preceding results, the “ship-in-a-bottle” methodology seems to be very limited with regard to complex size, due to the restrictions imposed by the microporous character of zeolites. Moreover, the construction of the complex inside the solid left some shadows on the real amount of complex, the presence of external or non-complexed species, and the accessibility to the catalytic sites.

One attempt to overcome those limitations was the use of pillared clays as the support.<sup>238</sup> In that case, the starting clay, the nature of the pillars, and their distribution would condition the porosity of the solid. However, the encapsulation of (salen)Mn complexes was not successful, as shown by the rather poor results of chemo- and enantioselectivity obtained in the epoxidation of styrene. Moreover, the nature of the catalyst–support interaction (simple occlusion or electrostatic) was not clear.

A breakthrough in this field has recently been described by Li and co-workers.<sup>239</sup> These authors reported a new strategy that might be called “closing-the-bottle-neck” (Figure 83). In this case, a mesoporous crystalline silica (SBA-16) was used as a support, with pores large enough to allow the complex to enter in the adsorption process. A subsequent



**Figure 84.** (A) TEM image of the (100) projection of cubic SBA-16 (*Im3m*) and (B) schematic representation of the (salen)Co catalyst trapped in the isolated nanocage of mesoporous materials. Reprinted with permission of John Wiley and Sons, ref 241.

treatment with an alkylsilane reduces the pore aperture to a value small enough to entrap the complex but able to admit the diffusion of reagents and products. One additional advantage of this methodology is the possibility of tailoring both the porosity of the raw support and the size of the silane for a given complex.

In this paper, two examples were reported, (salen)Co with Jacobsen’s ligand and Rh–TsDPEN (TsDPEN = *N*-(*p*-toluenesulfonyl)-1,2-diphenylethylenediamine). In the first case, the optimal size of the silane was determined by adsorption of the complex on SBA-16 modified with methyl, propyl, benzyl, octyl, and dodecyl silanes. Only C<sub>8</sub> and C<sub>12</sub> silanes were able to prevent the adsorption of (salen)Co, but C<sub>12</sub> blocked completely the porosity. The suitability of this strategy was demonstrated in the asymmetric ring opening of epoxides. Whereas the nonmodified support was unable to retain the complex, C<sub>8</sub>-modified SBA-16 led to excellent results in the opening of epoxides (Scheme 55), epichlorhydrin, and propylene oxide retaining both activity and enantioselectivity for 12 and 13 runs, respectively. As an example

51% yield (20 h) with 95% ee was obtained in the first run with propylene oxide, and 46% yield (28 h) with 97% ee in the 13th run. In order to retain the smaller Rh complex, diphenylsilane was necessary as modifier. This complex was used in the enantioselective transfer hydrogenation of acetophenone with HCOONa, with excellent results in six runs, >99% conversion (5 h) with 93% ee in the first run and 99% conversion (19 h) with 92% ee in the sixth run.

The same group described an alternative approach, the “classical ship-in-a-bottle” synthesis.<sup>240</sup> In this case, the modification of the SBA-16 support with phenylsilane was previous to the complex entrapment, carried out by salen ligand adsorption and final reaction with Co(OAc)<sub>2</sub>. Different SBA-16 supports were used with different porosity properties. In the case of SBA-16 with small pores, the as-synthesized material was able to occlude the complex, whereas silanization hampered the entrance of salen ligand. In case of SBA-16 with larger pores, silanization was not sufficient to retain the complex. Excellent results were obtained in the hydrolytic kinetic resolution of epoxides. As an example, propylene oxide was hydrolyzed with 50% conversion and 96% ee, and the catalyst was recovered and reused for 10 cycles with similar results.

One important advantage of this method is the possibility to accommodate two molecules of complex in the same cage of the support. This is of crucial importance in reactions with a cooperative activation effect, as happens with the hydrolytic kinetic resolution of epoxides. The same group has demonstrated that this effect, difficult or even impossible in most heterogeneous catalysts due to site isolation, is not only possible but greatly enhanced with the “closing-the-bottle-neck” strategy.<sup>241</sup> Catalysts with different average Co content were prepared, and their catalytic performance was compared. The effective concentration of complex was calculated, taking into account the void volume of the support, and the conditions were reproduced in solution (Table 33). As can be seen, at low Co loading the results are much better in solution, given that in the solid the catalyst molecules are unable to find each other due to the closing of the pores connecting the hypercages. When the average number of cobalt per cage in the solid is higher than 2, results in homogeneous and heterogeneous phase are more similar, due to the cooperative effect in both cases (Figure 84).

This effect is much more interesting in the case of reactions with very low catalyst amount. When the substrate/catalyst ratio (S/C) was increased to 4000:1, the result obtained with the heterogeneous catalyst was better (49% conversion, TOF 163 h<sup>-1</sup>, 98% ee diol) than that obtained in solution (34% conversion, TOF 113 h<sup>-1</sup>, 98% ee diol). The difference was even much more significant when S/C was increased to 12 000:1, 50% conversion, TOF 250 h<sup>-1</sup>, 98% ee diol vs 7% conversion, TOF 35 h<sup>-1</sup>, 89% ee diol in solution. The dilution in homogeneous phase, and therefore the elimination of the cooperative effect, is responsible for this worsening of the results, whereas in the solid the effect is maintained due to the confinement of the catalyst inside the supercages of the support. The same tendency was observed for other epoxides, such as styrene oxide or phenyl glycidyl ether.

As a general conclusion, it seems that the only really efficient entrapment method requires the use of rigid supports with tuneable large hypercages connected through medium size pore apertures. However, this system has been only recently described, and it must still show general applicability to different catalytic systems.

## 6. Concluding Remarks

An overview of these results shows that noncovalent immobilization strategies allow, in most cases, the preparation of supported enantioselective catalysts in a way simpler than covalent bonding of the chiral ligand, mainly when no modifications of the chiral ligand are needed to establish the support–catalyst interaction. Stability against leaching and deactivation is highly dependent on the catalytic reaction and can be avoided or at least minimized by careful selection of the reaction conditions, the immobilization method, the support, and the catalytic complex. It seems clear that some of the catalysts described in this review are quite stable and efficient, which together with the simple preparation methodology make them an interesting alternative.

In some cases, the immobilized catalysts are able to improve or even completely change the stereochemical course of the reaction in which they are used. Although the origin of these effects is still a matter of debate, in most cases the influence of the support seems to be the reason and more extensive studies are needed in order to take advantage of these effects in a rational manner.

## 7. Acknowledgments

We are indebted to all the co-workers, postdoctoral fellows, and students who have been working in our laboratory on this subject over the last 12 years, whose names appear as coauthors in the cited papers. The financial support of C.I.C.Y.T. (Project CTQ2005-08016 and Consolider Ingenio 2010 CSD2006-0003) is greatly acknowledged.

## 8. References

- (1) *Comprehensive Asymmetric Catalysis*; Jacobsen, E. N.; Pfaltz, A.; Yamamoto, H., Eds.; Springer-Verlag: Berlin, 1999.
- (2) Blaser H.-U.; Schmidt E. In *Asymmetric Catalysis on Industrial Scale*; Blaser, H.-U., Schmidt, E., Eds.; Wiley-VCH: Weinheim, Germany, 2004; pp 1–19.
- (3) Blaser, H.-U.; Pugin, B.; Spindler, F. *J. Mol. Catal. A* **2005**, *231*, 1.
- (4) Blaser, H.-U. *Chem. Commun.* **2003**, 293.
- (5) *Chiral Catalysts Immobilization and Recycling*; De Vos, D. E., Vankelecom I. F. J., Jacobs, P. A., Eds.; Wiley-VCH: Weinheim, Germany, 2000.
- (6) Baleizão, C.; Garcia, H. *Chem. Rev.* **2006**, *106*, 3987.
- (7) Rechavi, D.; Lemaire, M. *Chem. Rev.* **2002**, *102*, 3467.
- (8) Fraile, J. M.; García, J. I.; Mayoral, J. A. *Coord. Chem. Rev.* **2008**, *252*, 624.
- (9) Severeys, A.; De Vos, D. E.; Jacobs, P. A. *Top. Catal.* **2002**, *19*, 125.
- (10) Kobayashi, S.; Sugiura, M. *Adv. Synth. Catal.* **2006**, *348*, 1496.
- (11) Saluzzo, C.; Lemaire, M. *Adv. Synth. Catal.* **2002**, *344*, 915.
- (12) Barbaro, P. *Chem.—Eur. J.* **2006**, *12*, 5666.
- (13) Xia, Q. H.; Ge, H. Q.; Ye, C. P.; Liu, Z. M.; Su, K. X. *Chem. Rev.* **2005**, *105*, 1603.
- (14) Leadbeater, N. E.; Marco, M. *Chem. Rev.* **2002**, *102*, 3217.
- (15) Mastroianni, P.; Nobile, C. F. *Coord. Chem. Rev.* **2004**, *248*, 377.
- (16) Diosa, B. M. L.; Vankelecom, I. F. J.; Jacobs, P. A. *Adv. Synth. Catal.* **2006**, *348*, 1413.
- (17) Song, C. E.; Lee, S.-G. *Chem. Rev.* **2002**, *102*, 3495.
- (18) Li, C. *Catal. Rev.—Sci. Eng.* **2004**, *46*, 419.
- (19) Song, C. E.; Kim, D. H.; Choi, D. S. *Eur. J. Inorg. Chem.* **2006**, 2927.
- (20) Li, C.; Zhang, H.; Jiang, D.; Yang, Q. *Chem. Commun.* **2007**, 547.
- (21) Fan, Q. H.; Li, Y. M.; Chan, A. S. C. *Chem. Rev.* **2002**, *102*, 3385.
- (22) McMorn, P.; Hutchings, G. J. *Chem. Soc. Rev.* **2004**, *33*, 108.
- (23) Heitbaum, M.; Glorius, F.; Escher, I. *Angew. Chem., Int. Ed.* **2006**, *45*, 4732.
- (24) Studer, M.; Blaser, H.-U.; Exner, C. *Adv. Synth. Catal.* **2003**, *345*, 45.
- (25) Mazzei, M.; Marconi, W.; Riocci, M. *J. Mol. Catal.* **1980**, *9*, 381.
- (26) Shimazu, S.; Ro, K.; Sento, T.; Ichikuni, N.; Uematsu, T. *J. Mol. Catal. A* **1996**, *107*, 297.
- (27) Sento, T.; Shimazu, S.; Ichikuni, N.; Uematsu, T. *J. Mol. Catal. A* **1999**, *137*, 263.

- (28) Sento, T.; Shimazu, S.; Ichikuni, N.; Uematsu, T. *Chem. Lett.* **1998**, 1191.
- (29) Margalef-Català, R.; Claver, C.; Salagre, P.; Fernández, E. *Tetrahedron: Asymmetry* **2000**, *11*, 1469.
- (30) Segarra, A. M.; Guerrero, R.; Claver, C.; Fernandez, E. *Chem. Commun.* **2001**, 1808.
- (31) Segarra, A. M.; Guirado, F.; Claver, C.; Fernandez, E. *Tetrahedron: Asymmetry* **2003**, *14*, 1611.
- (32) Segarra, A. M.; Guerrero, R.; Claver, C.; Fernandez, E. *Chem.—Eur. J.* **2003**, *9*, 191.
- (33) Fraile, J. M.; García, J. I.; Martínez-Merino, V.; Mayoral, J. A.; Salvatella, L. *J. Am. Chem. Soc.* **2001**, *123*, 7616.
- (34) Fraile, J. M.; García, J. I.; Mayoral, J. A.; Tarnai, T. *Tetrahedron: Asymmetry* **1997**, *8*, 2089.
- (35) Alonso, P. J.; Fraile, J. M.; García, J. I.; Martínez, J. I.; Mayoral, J. A.; Sánchez, M. C. *Langmuir* **2000**, *16*, 5607.
- (36) Fraile, J. M.; García, J. I.; Mayoral, J. A.; Tarnai, T. *J. Mol. Catal. A* **1999**, *144*, 85.
- (37) Fraile, J. M.; García, J. I.; Gil, M. J.; Martínez-Merino, V.; Mayoral, J. A.; Salvatella, L. *Chem.—Eur. J.* **2004**, *10*, 758.
- (38) Fraile, J. M.; García, J. I.; Mayoral, J. A.; Tarnai, T. *Tetrahedron: Asymmetry* **1998**, *9*, 3997.
- (39) Fraile, J. M.; García, J. I.; Mayoral, J. A.; Tarnai, T.; Harmer, M. A. *J. Catal.* **1999**, *186*, 214.
- (40) Fernández, M. J.; Fraile, J. M.; García, J. I.; Mayoral, J. A.; Burguete, M. I.; García-Verdugo, E.; Luis, S. V.; Harmer, M. A. *Top. Catal.* **2000**, *13*, 303.
- (41) Fraile, J. M.; García, J. I.; Herrerías, C. I.; Mayoral, J. A.; Harmer, M. A. *J. Catal.* **2004**, *221*, 532.
- (42) Fraile, J. M.; García, J. I.; Herrerías, C. I.; Mayoral, J. A.; Reiser, O.; Socuellamos, A.; Werner, H. *Chem.—Eur. J.* **2004**, *10*, 2997.
- (43) Fernández, A. I.; Fraile, J. M.; García, J. I.; Herrerías, C. I.; Mayoral, J. A.; Salvatella, L. *Chem. Commun.* **2001**, 2, 165.
- (44) Fraile, J. M.; García, J. I.; Harmer, M. A.; Herrerías, C. I.; Mayoral, J. A.; Reiser, O.; Werner, H. *J. Mater. Chem.* **2002**, *12*, 3290.
- (45) Cornejo, A.; Fraile, J. M.; García, J. I.; Gil, M. J.; Herrerías, C. I.; Legarreta, G.; Martínez-Merino, V.; Mayoral, J. A. *J. Mol. Catal. A* **2003**, *196*, 101.
- (46) Fraile, J. M.; García, J. I.; Jiménez-Osés, G.; Mayoral, J. A.; Roldán, M. *Organometallics* **2008**, *27*, 2246.
- (47) García, J. I.; Jiménez-Osés, G.; Martínez-Merino, V.; Mayoral, J. A.; Pires, E.; Villalba, I. *Chem.—Eur. J.* **2007**, *13*, 4064.
- (48) Fraile, J. M.; García, J. I.; Mayoral, J. A.; Roldán, M. *Org. Lett.* **2007**, *9*, 731.
- (49) Fraile, J. M.; García, J. I.; Lafuente, G.; Mayoral, J. A.; Salvatella, L. *Arkivoc* **2004**, 67.
- (50) Fraile, J. M.; García, J. I.; Harmer, M. A.; Herrerías, C. I.; Mayoral, J. A. *J. Mol. Catal. A* **2001**, *165*, 211.
- (51) Fraile, J. M.; Pérez, I.; Mayoral, J. A.; Reiser, O. *Adv. Synth. Catal.* **2006**, *348*, 1680.
- (52) Fraile, J. M.; Pérez, I.; Mayoral, J. A. *J. Catal.* **2007**, *252*, 303.
- (53) Fraile, J. M.; García, J. I.; Massam, J.; Mayoral, J. A. *J. Mol. Catal. A* **1998**, *136*, 47.
- (54) Kureshy, R. I.; Khan, N. H.; Abdi, S. H. R.; Ahmad, I.; Singh, S.; Jasra, R. V. *Catal. Lett.* **2003**, *91*, 207.
- (55) Kureshy, R. I.; Khan, N. H.; Abdi, S. H. R.; Ahmad, I.; Singh, S.; Jasra, R. V. *J. Catal.* **2004**, *221*, 234.
- (56) Mori, K.; Oshiba, M.; Hara, T.; Mizugaki, T.; Ebitani, K.; Kaneda, K. *Tetrahedron Lett.* **2005**, *46*, 4283.
- (57) Selke, R. *J. Mol. Catal.* **1986**, *37*, 227.
- (58) Selke, R.; Häupke, K.; Krause, H. W. *J. Mol. Catal.* **1989**, *56*, 315.
- (59) Brunner, H.; Bielmeier, E.; Wiehl, J. *J. Organometal. Chem.* **1990**, *384*, 223.
- (60) Barbaro, P.; Bianchini, C.; Giambastiani, G.; Oberhauser, W.; Bonzi, L. M.; Rossi, F.; Dal Santo, V. *Dalton Trans.* **2004**, 1783.
- (61) Tóth, I.; Hanson, B. E.; Davis, M. E. *J. Organomet. Chem.* **1990**, *397*, 109.
- (62) Tóth, I.; Hanson, B. E. *J. Mol. Catal.* **1992**, *71*, 365.
- (63) Zhang, H.; Zhang, Y.; Li, C. *Tetrahedron: Asymmetry* **2005**, *16*, 2417.
- (64) Lloret, J.; Estevan, F.; Bieger, K.; Villanueva, C.; Ubeda, M. A. *Organometallics* **2007**, *26*, 4145.
- (65) Langham, C.; Piaggio, P.; Bethell, D.; Lee, D. F.; McMorn, P.; Page, P. C. B.; Willock, D. J.; Sly, C.; Hancock, F. E.; King, F.; Hutchings, G. J. *Chem. Commun.* **1998**, 1601.
- (66) Langham, C.; Taylor, S.; Bethell, D.; McMorn, P.; Page, P. C. B.; Willock, D. J.; Sly, C.; Hancock, F. E.; King, F.; Hutchings, G. J. *J. Chem. Soc., Perkin Trans. 2* **1999**, 1043.
- (67) Langham, C.; Bethell, D.; Lee, D. E.; McMorn, P.; Page, P. C. B.; Willock, D. J.; Sly, C.; Hancock, F. E.; King, F.; Hutchings, G. J. *Appl. Catal., A* **1999**, *182*, 85.
- (68) Taylor, S.; Gullick, J.; McMorn, P.; Bethell, D.; Page, P. C. B.; Hancock, F. E.; King, F.; Hutchings, G. J. *J. Chem. Soc., Perkin Trans. 2* **2001**, 1714.
- (69) Taylor, S.; Gullick, J.; McMorn, P.; Bethell, D.; Page, P. C. B.; Hancock, F. E.; King, F.; Hutchings, G. J. *J. Chem. Soc., Perkin Trans. 2* **2001**, 1724.
- (70) Gullick, J.; Taylor, S.; McMorn, P.; Bethell, D.; Bulman-Page, P. C.; Hancock, F. E.; King, F.; Hutchings, G. J. *J. Mol. Catal. A* **2002**, *182*, 571.
- (71) Taylor, S.; Gullick, J.; McMorn, P.; Bethell, D.; Page, P. C. B.; Hancock, F. E.; Hutchings, G. J. *Top. Catal.* **2003**, *24*, 43.
- (72) Gullick, J.; Ryan, D.; McMorn, P.; Bethell, D.; King, F.; Hancock, F.; Hutchings, G. *New J. Chem.* **2004**, *28*, 1470.
- (73) Ryan, D.; McMorn, P.; Bethell, D.; Hutchings, G. *Org. Biomol. Chem.* **2004**, *2*, 3566.
- (74) Traa, Y.; Murphy, D. M.; Farley, R. D.; Hutchings, G. J. *Phys. Chem. Chem. Phys.* **2001**, *3*, 1073.
- (75) Gullick, J.; Taylor, S.; Ryan, D.; McMorn, P.; Coogan, M.; Bethell, D.; Page, P. C. B.; Hancock, F. E.; King, F.; Hutchings, G. J. *Chem. Commun.* **2003**, 2808.
- (76) Taylor, S.; Gullick, J.; Galea, N.; McMorn, P.; Bethell, D.; Page, P. C. B.; Hancock, F. E.; King, F.; Willock, D. J.; Hutchings, G. J. *Top. Catal.* **2003**, *25*, 81.
- (77) Wan, Y.; McMorn, P.; Hancock, F. E.; Hutchings, G. J. *Catal. Lett.* **2003**, *91*, 145.
- (78) Caplan, N. A.; Hancock, F. E.; Page, P. C. B.; Hutchings, G. J. *Angew. Chem., Int. Ed.* **2004**, *43*, 1685.
- (79) Piaggio, P.; McMorn, P.; Langham, C.; Bethell, D.; Bulman-Page, P. C.; Hancock, F. E.; Hutchings, G. J. *New J. Chem.* **1998**, 1167.
- (80) Piaggio, P.; Langham, C.; McMorn, P.; Bethell, D.; Bulman-Page, P. C.; Hancock, F. E.; Sly, C.; Hutchings, G. J. *J. Chem. Soc., Perkin Trans. 2* **2000**, 143.
- (81) Piaggio, P.; McMorn, P.; Murphy, D.; Bethell, D.; Bulman-Page, P. C.; Hancock, F. E.; Sly, C.; Kerton, O. J.; Hutchings, G. J. *J. Chem. Soc., Perkin Trans. 2* **2000**, 2008.
- (82) Kim, G. J.; Kim, S. H. *Catal. Lett.* **1999**, *57*, 139.
- (83) Kim, G. J.; Shin, J. H. *Catal. Lett.* **1999**, *63*, 83.
- (84) Wagner, H. H.; Hausmann, H.; Hölderich, W. F. *J. Catal.* **2001**, *203*, 150.
- (85) Crosman, A.; Hoelderich, W. F. *J. Catal.* **2005**, *232*, 43.
- (86) Crosman, A.; Hoelderich, W. F. *Catal. Today* **2007**, *121*, 130.
- (87) Simons, C.; Hanefeld, U.; Arends, I. W. C. E.; Sheldon, R. A.; Maschmeyer, T. *Chem.—Eur. J.* **2004**, *10*, 5829.
- (88) Hems, W. P.; McMorn, P.; Riddell, S.; Watson, S.; Hancock, F. E.; Hutchings, G. J. *Org. Biomol. Chem.* **2005**, *3*, 1547.
- (89) Simons, C.; Hanefeld, U.; Arends, I. W. C. E.; Minnaard, A. J.; Maschmeyer, T.; Sheldon, R. A. *Chem. Commun.* **2004**, 2830.
- (90) Simons, C.; Hanefeld, U.; Arends, I. W. C. E.; Maschmeyer, T.; Sheldon, R. A. *J. Catal.* **2006**, *239*, 212.
- (91) Selke, R.; Capka, M. *J. Mol. Catal.* **1990**, *63*, 319.
- (92) Carpentier, J.-F.; Agbossou, F.; Mortreux, A. *Tetrahedron: Asymmetry* **1995**, *6*, 39.
- (93) Xiang, S.; Zhang, Y.; Xin, Q.; Li, C. *Chem. Commun.* **2002**, 2696.
- (94) Zhang, H.; Xiang, S.; Li, C. *Chem. Commun.* **2005**, 1209.
- (95) Zhang, H.; Xiang, S.; Xiao, J.; Li, C. *J. Mol. Catal. A* **2005**, *238*, 175.
- (96) Zhang, H.; Li, C. *Tetrahedron* **2006**, *62*, 6640.
- (97) Zhang, H.; Zhang, Y.; Li, C. *J. Catal.* **2006**, *238*, 369.
- (98) Domínguez, I.; Fornés, V.; Sabater, M. J. *J. Catal.* **2004**, *228*, 92.
- (99) Hultman, H. M.; de Lang, M.; Nowotny, M.; Arends, I. W. C. E.; Hanefeld, U.; Sheldon, R. A.; Maschmeyer, T. *J. Catal.* **2003**, *217*, 264.
- (100) Hultman, H. M.; de Lang, M.; Arends, I. W. C. E.; Hanefeld, U.; Sheldon, R. A.; Maschmeyer, T. *J. Catal.* **2003**, *217*, 275.
- (101) Tas, D.; Jeanmart, D.; Parton, R. F.; Jacobs, P. A. *Stud. Surf. Sci. Catal.* **1997**, *108*, 493.
- (102) Köckritz, A.; Bischoff, S.; Morawsky, V.; Prüsse, U.; Vorlop, K.-D. *J. Mol. Catal. A* **2002**, *180*, 231.
- (103) Lücke, B.; Köckritz, A.; Vorlop, K.-D.; Bischoff, S.; Kant, M. *Top. Catal.* **2004**, *29*, 111.
- (104) Bhattacharjee, S.; Anderson, J. A. *Chem. Commun.* **2004**, 554.
- (105) Bhattacharjee, S.; Anderson, J. A. *Catal. Lett.* **2004**, *95*, 119.
- (106) Bhattacharjee, S.; Dines, T. J.; Anderson, J. A. *J. Catal.* **2004**, *225*, 398.
- (107) Bhattacharjee, S.; Anderson, J. A. *Adv. Synth. Catal.* **2006**, *348*, 151.
- (108) Choudary, B. M.; Ramani, T.; Maheswaran, H.; Prashant, L.; Ranganath, K. V. S.; Kumar, K. V. *Adv. Synth. Catal.* **2006**, *348*, 493.
- (109) Kantam, M. L.; Ramani, T.; Chakrapani, L.; Choudary, B. M. *J. Mol. Catal. A* **2007**, *274*, 11.
- (110) Choudary, B. M.; Chowdari, N. S.; Kantam, M. L.; Raghavan, K. V. *J. Am. Chem. Soc.* **2001**, *123*, 9220.
- (111) Choudary, B. M.; Chowdari, N. S.; Jyothi, K.; Kantam, M. L. *J. Am. Chem. Soc.* **2002**, *124*, 5341.
- (112) Choudary, B. M.; Chowdari, N. S.; Madhi, S.; Kantam, M. L. *J. Org. Chem.* **2003**, *68*, 1736.



- (113) Dehury, S. K.; Hariharakrishnan, V. S. *Tetrahedron Lett.* **2007**, *48*, 2493.
- (114) Choudary, B. M.; Chowdari, N. S.; Jyothi, K.; Kantam, M. L. *J. Mol. Catal. A* **2003**, *196*, 151.
- (115) Kantam, M. L.; Prakash, B. V.; Bharathi, B.; Reddy, Ch. V. *J. Mol. Catal. A* **2005**, *226*, 119.
- (116) Fraile, J. M.; García, J. I.; Mayoral, J. A.; Royo, A. J. *Tetrahedron: Asymmetry* **1996**, *7*, 2263.
- (117) Gerstberger, G.; Palm, C.; Anwander, R. *Chem.—Eur. J.* **1999**, *5*, 997.
- (118) Gerstberger, G.; Anwander, R. *Microporous Mesoporous Mater.* **2001**, *44*, 303.
- (119) Fraile, J. M.; García, J. I.; Lázaro, B.; Mayoral, J. A. *Chem. Commun.* **1998**, 1807.
- (120) Iwamoto, M.; Tanaka, Y.; Hirosumi, J.; Kita, N. *Chem. Lett.* **2001**, 226.
- (121) Iwamoto, M.; Tanaka, Y.; Hirosumi, J.; Kita, N.; Triwahyono, S. *Microporous Mesoporous Mater.* **2001**, *48*, 271.
- (122) Meunier, D.; Piechaczyk, A.; de Mallmann, A.; Basset, J. M. *Angew. Chem., Int. Ed.* **1999**, *38*, 3540.
- (123) Meunier, D.; de Mallmann, A.; Basset, J. M. *Top. Catal.* **2003**, *23*, 183.
- (124) Kim, G. J.; Shin, J. H. *Catal. Lett.* **1999**, *63*, 83.
- (125) Kim, J. H.; Kim, G. J. *Catal. Lett.* **2004**, *92*, 123.
- (126) Tada, M.; Taniike, T.; Kantam, L. M.; Iwasawa, Y. *Chem. Commun.* **2004**, 2542.
- (127) Tada, M.; Kojima, N.; Izumi, Y.; Taniike, T.; Iwasawa, Y. *J. Phys. Chem. B* **2005**, *109*, 9905.
- (128) Silva, A. R.; Freire, C.; de Castro, B. *Carbon* **2004**, *42*, 3027.
- (129) Silva, A. R.; Budarin, V.; Clark, J. H.; de Castro, B.; Freire, C. *Carbon* **2005**, *43*, 2096.
- (130) Barnard, C. F.; Rouzaud, J.; Stevenson, S. H. *Org. Proc. Res. Dev.* **2005**, *9*, 164.
- (131) Choudary, B. M.; Pal, U.; Kantam, M. L.; Ranganath, K. V. S.; Sreedhar, B. *Adv. Synth. Catal.* **2006**, *348*, 1038.
- (132) Wu, C. D.; Hu, A.; Zhang, L.; Lin, W. B. *J. Am. Chem. Soc.* **2005**, *127*, 8940.
- (133) Cho, S. H.; Ma, B. Q.; Nguyen, S. T.; Hupp, J. T.; Albrecht-Schmitt, T. E. *Chem. Commun.* **2006**, 2563.
- (134) Cho, S. H.; Gadzikwa, T.; Ashfari, M.; Nguyen, S. T.; Hupp, J. T. *Eur. J. Inorg. Chem.* **2007**, 4863.
- (135) Ding, K.; Wang, Z.; Wang, X.; Liang, Y.; Wang, X. *Chem.—Eur. J.* **2006**, *12*, 5188.
- (136) Takizawa, S.; Somei, H.; Jayaprakash, D.; Sasai, H. *Angew. Chem., Int. Ed.* **2003**, *115*, 5889.
- (137) Guo, H.; Wang, X.; Ding, K. *Tetrahedron Lett.* **2004**, *45*, 2009.
- (138) Wang, X.; Wang, X.; Guo, H.; Wang, Z.; Ding, K. *Chem.—Eur. J.* **2005**, *11*, 4078.
- (139) Wang, X.; Shi, L.; Li, M.; Ding, K. *Angew. Chem., Int. Ed.* **2005**, *44*, 6362.
- (140) Liang, Y.; Jing, Q.; Li, X.; Shi, L.; Ding, K. *J. Am. Chem. Soc.* **2005**, *127*, 7694.
- (141) Shi, L.; Wang, X.; Sandoval, C. A.; Li, M.; Qi, Q.; Li, Z.; Ding, K. *Angew. Chem., Int. Ed.* **2006**, *45*, 4108.
- (142) Zhou, X. G.; Yu, X. Q.; Huang, J. S.; Li, S. G.; Li, L. S.; Che, C. M. *Chem. Commun.* **1999**, 1789.
- (143) Zhang, J. L.; Liu, Y. L.; Che, C. M. *Chem. Commun.* **2002**, 2906.
- (144) Dioos, B. M. L.; Geurts, W. A.; Jacobs, P. A. *Catal. Lett.* **2004**, *97*, 125.
- (145) Kureshy, R. I.; Ahmad, I.; Khan, N. U. H.; Abdi, S. H. R.; Singh, S.; Pandia, P. H.; Jasra, R. V. *J. Catal.* **2005**, *235*, 28.
- (146) Yang, J. W.; Han, H. Y.; Roh, E. J.; Lee, S. G.; Song, C. E. *Org. Lett.* **2002**, *4*, 4685.
- (147) Jo, C. H.; Han, S. H.; Yang, J. W.; Roh, E. J.; Shina, U. S.; Song, C. E. *Chem. Commun.* **2003**, 1312.
- (148) Kim, K. J.; Choi, H. Y.; Hwang, S. H.; Park, Y. S.; Kwueon, E. K.; Choi, D. S.; Song, C. E. *Chem. Commun.* **2005**, 3337.
- (149) Nagashima, T.; Davies, H. M. L. *Org. Lett.* **2002**, *4*, 1989.
- (150) Davies, H. M. L.; Walji, A. M. *Org. Lett.* **2003**, *5*, 479.
- (151) Davies, H. M. L.; Walji, A. M.; Nagashima, T. *J. Am. Chem. Soc.* **2004**, *126*, 4271.
- (152) Davies, H. M. L.; Walji, A. M. *Org. Lett.* **2005**, *7*, 2941.
- (153) Syukri, S.; Sun, W.; Kuhn, F. E. *Tetrahedron Lett.* **2007**, *48*, 1613.
- (154) Inoue, M.; Ohta, K.; Ishizuka, N.; Enomoto, S. *Chem. Pharm. Bull.* **1983**, *31*, 3371.
- (155) Ishizuka, N.; Togashi, M.; Inoue, M.; Enomoto, S. *Chem. Pharm. Bull.* **1987**, *35*, 1686.
- (156) Brunner, H.; Bublak, P.; Helget, M. *Chem. Ber.* **1997**, *130*, 55.
- (157) Flach, H. N.; Grassert, I.; Oehme, G.; Capka, M. *Colloid Polym. Sci.* **1996**, *274*, 261.
- (158) Jamis, J.; Anderson, J. R.; Dickson, R. S.; Campi, E. M.; Jackson, W. R. *J. Organomet. Chem.* **2000**, *603*, 80.
- (159) Jamis, J.; Anderson, J. R.; Dickson, R. S.; Campi, E. M.; Jackson, W. R. *J. Organomet. Chem.* **2001**, *627*, 37.
- (160) Frunza, L.; Kosslick, H.; Landmesser, H.; Höft, E.; Fricke, R. *J. Mol. Catal. A* **1997**, *123*, 179.
- (161) Frunza, L.; Zgura, I.; Nicolaie, I.; Dittmar, A.; Kosslick, H.; Fricke, R. *J. Optoelectron. Adv. Mater.* **2005**, *7*, 2141.
- (162) Dioos, B. M. L.; Jacobs, P. A. *Tetrahedron Lett.* **2003**, *44*, 8815.
- (163) Dioos, B. M. L.; Jacobs, P. A. *Appl. Catal., A* **2005**, *282*, 181.
- (164) Chois, D.; Kim, G. J. *Catal. Lett.* **2004**, *92*, 35.
- (165) Lee, B. S.; Mahajan, S.; Janda, K. D. *Tetrahedron Lett.* **2005**, *46*, 4491.
- (166) Gamez, P.; Fache, F.; Lemaire, M. *Bull. Soc. Chim. Fr.* **1994**, *131*, 600.
- (167) De Rege, F. M.; Morita, D. K.; Ott, K. C.; Tumas, W.; Broene, R. D. *Chem. Commun.* **2000**, 1797.
- (168) Raja, R.; Thomas, J. M.; Jones, M. D.; Johnson, B. F. G.; Vaughan, D. E. W. *J. Am. Chem. Soc.* **2003**, *125*, 14982.
- (169) Rouzaud, J.; Jones, M. D.; Raja, R.; Johnson, B. F. G.; Thomas, J. M.; Duer, M. J. *Helv. Chim. Acta* **2003**, *86*, 1753.
- (170) Bianchini, C.; Barbaro, P.; Dal Santo, V.; Gobetto, R.; Meli, A.; Oberhauser, W.; Psaro, R.; Vizza, F. *Adv. Synth. Catal.* **2001**, *343*, 41.
- (171) O'Leary, P.; Krosveld, N. P.; De Jong, K. P.; van Koten, G.; Gebbink, R. *Tetrahedron Lett.* **2004**, *45*, 3177.
- (172) Wang, H.; Liu, X.; Xia, H.; Liu, P.; Gao, J.; Ying, P.; Xiao, J.; Li, C. *Tetrahedron* **2006**, *62*, 1025.
- (173) McDonagh, C.; Conghaile, P. O.; Klein Gebbink, R. J. M.; O'Leary, P. *Tetrahedron Lett.* **2007**, *48*, 4387.
- (174) Izumi, Y.; Hasebe, R.; Urabe, K. *J. Catal.* **1983**, *84*, 402.
- (175) Augustine, R.; Tanielyan, S.; Anderson, S.; Yang, H. *Chem. Commun.* **1999**, 1257.
- (176) Augustine, R. L.; Goel, P.; Mahata, N.; Reyes, C.; Tanielyan, S. K. *J. Mol. Catal. A* **2004**, *216*, 189.
- (177) Augustine, R. L.; Tanielyan, S. K.; Mahata, N.; Gao, Y.; Zsigmond, A.; Yang, H. *Appl. Catal., A* **2003**, *256*, 69.
- (178) Brandts, J. A. M.; Berben, P. H. *Org. Proc. Res. Dev.* **2003**, *7*, 393.
- (179) Zsigmond, Á.; Bogár, K.; Notheisz, F. *J. Catal.* **2003**, *213*, 103.
- (180) Zsigmond, Á.; Balatoni, I.; Notheisz, F.; Hegedüs, C.; Bakos, J. *Catal. Lett.* **2005**, *195*, 521.
- (181) Zsigmond, Á.; Undrala, S.; Notheisz, F.; Szöllösy, Á.; Bakos, J. *Appl. Catal., A* **2006**, *303*, 29.
- (182) Stephenson, P.; Licence, P.; Ross, S. K.; Poliakov, M. *Green Chem.* **2004**, *6*, 521.
- (183) Anson, M. S.; Leese, M. P.; Tonks, L.; Williams, J. M. J. *J. Chem. Soc., Dalton Trans.* **1998**, 3529.
- (184) Wan, K. T.; Davis, M. E. *J. Catal.* **1994**, *148*, 1.
- (185) Wan, K. T.; Davis, M. E. *Nature* **1994**, *370*, 449.
- (186) Wan, K. T.; Davis, M. E. *J. Catal.* **1995**, *152*, 25.
- (187) Tóth, I.; Guo, I.; Hanson, B. E. *J. Mol. Catal. A* **1997**, *116*, 217.
- (188) Dioos, B. M. L.; Jacobs, P. A. *J. Catal.* **2006**, *243*, 217.
- (189) Lou, L.-L.; Yu, K.; Ding, F.; Zhou, W.; Peng, X.; Liu, S. *Tetrahedron Lett.* **2006**, *47*, 6513.
- (190) Castillo, M. R.; Fousse, L.; Fraile, J. M.; García, J. I.; Mayoral, J. A. *Chem.—Eur. J.* **2007**, *13*, 287.
- (191) Whetten, R. L.; Price, R. C. *Science* **2007**, *318*, 407.
- (192) Jadzinsky, P. D.; Calero, G.; Ackerson, C. J.; Bushnell, D. A.; Kornberg, R. D. *Science* **2007**, *318*, 430.
- (193) Hasan, M.; Bethell, D.; Brust, M. *J. Am. Chem. Soc.* **2002**, *124*, 1132.
- (194) Li, H.; Luk, Y. Y.; Mrksich, M. *Langmuir* **1999**, *15*, 4957.
- (195) Marubayashi, K.; Takizawa, S.; Kawakusu, T.; Arai, T.; Sasai, H. *Org. Lett.* **2003**, *5*, 4409.
- (196) Belsler, R.; Stöhr, M.; Pfaltz, A. *J. Am. Chem. Soc.* **2005**, *127*, 8720.
- (197) Ono, T.; Kanomasa, S.; Tanaka, J. *Tetrahedron Lett.* **2005**, *46*, 7623.
- (198) Hu, A.; Yee, G. T.; Lin, W. *J. Am. Chem. Soc.* **2005**, *127*, 12486.
- (199) Vankelecom, I. F. J.; Tas, D.; Parton, R. F.; Van de Vyver, V.; Jacobs, P. A. *Angew. Chem., Int. Ed.* **1996**, *35*, 1346.
- (200) Parton, R. F.; Vankelecom, I. F. J.; Tas, D.; Janssen, K. B. M.; Knops-Gerrits, P.-P.; Jacobs, P. A. *J. Mol. Catal. A* **1996**, *113*, 283.
- (201) Tas, D.; Thoelen, C.; Vankelecom, I. F. J.; Jacobs, P. A. *Chem. Commun.* **1997**, 2323.
- (202) Vankelecom, I.; Wolfson, A.; Geresh, S.; Landau, M.; Gottlieb, M.; Herskowitz, M. *Chem. Commun.* **1999**, 2407.
- (203) Wolfson, A.; Janssens, S.; Vankelecom, I.; Geresh, S.; Gottlieb, M.; Herskowitz, M. *Chem. Commun.* **2002**, 388.
- (204) Wolfson, A.; Geresh, S.; Gottlieb, M.; Herskowitz, M. *Tetrahedron: Asymmetry* **2002**, *13*, 465.
- (205) Janssen, K. B. M.; Laquiere, I.; Dehaen, W.; Parton, R. F.; Vankelecom, I. F. J.; Jacobs, P. A. *Tetrahedron: Asymmetry* **1997**, *8*, 3481.
- (206) Vankelecom, I. F. J.; Jacobs, P. A. *Catal. Today* **2000**, *56*, 147.
- (207) Guedes, D. F. C.; MacLeod, T. C. O.; Gotardo, M. C. A. F.; Schiavon, M. A.; Yoshida, I. V. P.; Ciuffi, K. J.; Assis, M. D. *Appl. Catal., A* **2005**, *296*, 120.

- (208) Mac Leod, T. C. O.; Barros, V. P.; Faria, A. L.; Schiavon, M. A.; Yoshida, I. V. P.; Queiroz, M. E. C.; Assis, M. D. *J. Mol. Catal. A* **2007**, *273*, 259.
- (209) Microencapsulated chiral and non-chiral catalysts are reviewed in Kobayashi, S.; Akiyama, R. *Chem. Commun.* **2003**, 449.
- (210) Kobayashi, S.; Endo, M.; Nagayama, S. *J. Am. Chem. Soc.* **1999**, *121*, 11229.
- (211) Kobayashi, S.; Ishida, T.; Akiyama, R. *Org. Lett.* **2001**, *3*, 2649.
- (212) Ishida, T.; Akiyama, R.; Kobayashi, S. *Adv. Synth. Catal.* **2003**, *345*, 576.
- (213) Ishida, T.; Akiyama, R.; Kobayashi, S. *Adv. Synth. Catal.* **2005**, *347*, 1189.
- (214) Reddy, S. M.; Srinivasulu, M.; Reddy, Y. V.; Narasimhulu, M.; Venkateswarlu, Y. *Tetrahedron Lett.* **2006**, *47*, 5285.
- (215) Cornejo, A.; Fraile, J. M.; Garcia, J. I.; Gil, M. J.; Martinez-Merino, V.; Mayoral, J. A. *Tetrahedron* **2005**, *61*, 12107.
- (216) Kantam, M. L.; Kavita, B.; Neeraja, V.; Haritha, Y.; Chaudhuri, M. K.; Dehury, S. K. *Adv. Synth. Catal.* **2005**, *347*, 641.
- (217) Kantam, M. L.; Chakravarti, R.; Neehima, B.; Arundhati, R.; Sreedhar, B. *Appl. Catal., A* **2007**, *333*, 136.
- (218) Gelman, F.; Avnir, D.; Schumann, H.; Blum, J. *J. Mol. Catal. A* **1999**, *146*, 123.
- (219) Zhang, R.; Yu, W.-Y.; Wong, K.-Y.; Che, C.-M. *J. Org. Chem.* **2001**, *66*, 8145.
- (220) Mac Leod, T. C. O.; Guedes, D. F. C.; Lelo, M. R.; Rocha, R. A.; Caetano, B. L.; Ciuffi, K. J.; Assis, M. D. *J. Mol. Catal. A* **2006**, *259*, 319.
- (221) Ogunwumi, S. B.; Bein, T. *Chem. Commun.* **1997**, 901.
- (222) Sabater, M. J.; Corma, A.; Doménech, A.; Fornés, V.; García, H. *Chem. Commun.* **1997**, 1285.
- (223) Gigante, B.; Corma, A.; García, H.; Sabater, M. J. *Catal. Lett.* **2000**, *68*, 113.
- (224) Kahlen, W.; Wagner, H. H.; Hölderich, W. F. *Catal. Lett.* **1998**, *54*, 85.
- (225) Ernst, S.; Fuchs, E.; Yang, X. *Microporous Mesoporous Mater.* **2000**, *35–36*, 137.
- (226) Heinrichs, C.; Hölderich, W. F. *Catal. Lett.* **1999**, *58*, 75.
- (227) Schuster, C.; Hölderich, W. F. *Catal. Today* **2000**, *60*, 193.
- (228) Schuster, C.; Möllmann, E.; Tompos, A.; Hölderich, W. F. *Catal. Lett.* **2001**, *74*, 69.
- (229) Gbery, G.; Zsigmond, A., Jr. *Catal. Lett.* **2001**, *74*, 77.
- (230) Sabater, M. J.; Garcia, S.; Alvaro, M.; Garcia, H.; Scaiano, J. C. *J. Am. Chem. Soc.* **1998**, *120*, 8521.
- (231) Doménech, A.; Formentin, P.; García, H.; Sabater, M. J. *Eur. J. Inorg. Chem.* **2000**, 1339.
- (232) Doménech, A.; Formentin, P.; Garcia, H.; Sabater, M. J. *J. Phys. Chem. B* **2002**, *106*, 574.
- (233) Mollmann, E.; Tomlinson, P.; Holderich, W. F. *J. Mol. Catal. A* **2003**, *206*, 253.
- (234) Alcón, M. J.; Corma, A.; Iglesias, M.; Sánchez, F. *J. Mol. Catal. A* **2002**, *178*, 253.
- (235) Alcón, M. J.; Corma, A.; Iglesias, M.; Sánchez, F. *J. Mol. Catal. A* **2003**, *194*, 137.
- (236) Zsigmond, A.; Bogár, K.; Notheisz, F. *Catal. Lett.* **2002**, *83*, 55.
- (237) Zsigmond, A.; Bogár, K.; Notheisz, F. *J. Catal.* **2003**, *213*, 103.
- (238) Das, P.; Kuzniarska-Biernacka, I.; Silva, A. R.; Carvalho, A. P.; Pires, J.; Freire, C. *J. Mol. Catal. A* **2006**, *248*, 135.
- (239) Yang, H.; Li, J.; Yang, J.; Liu, Z.; Yang, Q.; Li, C. *Chem. Commun.* **2007**, 1086.
- (240) Yang, H.; Zhang, L.; Su, W.; Yang, Q.; Li, C. *J. Catal.* **2007**, *248*, 204.
- (241) Yang, H.; Zhang, L.; Zhong, L.; Yang, Q.; Li, C. *Angew. Chem., Int. Ed.* **2007**, *46*, 6861.

CR800363Y